United States Environmental Protection Agency
Office of Enforcement and Compliance Assurance
Office of Criminal Enforcement, Forensics and Training

NEICVP1060E02

TECHNICAL REPORT

Characterization of Lead in Soils

Pilsen Neighborhood
Chicago, Illinois

NEIC Project No.: VP1060

February 2015

Authors:

Steven D. Machemer, Ph.D.
Theresa J. Hosick, M.S.
National Enforcement Investigations Center

Michael J. Pribil, M.S.
U.S. Geological Survey

Steven D. Machemer, Ph.D.,
Lead Author / Principle Analytical Chemist

Prepared for:

EPA Region 5
77 West Jackson Boulevard, N-19R
Chicago, Illinois 60604

Jeffery D. Cahill, Project Manager

Authorized for Release by:

Diane L. Sipe, Laboratory Branch Chief

NATIONAL ENFORCEMENT INVESTIGATIONS CENTER
P.O. Box 25227
Building 25, Denver Federal Center
Denver, Colorado 80225

CONTENTS

Any use of trade, product, or firm names is for descriptive purposes only and does not imply endorsement by the U.S. Government.

TABLES

FIGURES

FIGURES--continued

FIGURES--continued

FIGURES--continued

The Contents pages show all of the sections contained in this report and provides a clear indication of the end of this report.

EXECUTIVE SUMMARY

INTRODUCTION

In July 2013, the U.S. Environmental Protection Agency's (EPA) Region 5 requested that the EPA's National Enforcement Investigations Center (NEIC) characterize lead (Pb)-bearing particulate matter in soils with elevated Pb levels in the Pilsen neighborhood of Chicago, Illinois, to discern the possible sources of the Pb present. An interim report (NEIC, 2014) completed in March 2014 presented analytical results of soils collected along an alley and a railroad spur adjacent to the H. Kramer Brass and Bronze Foundry (H. Kramer) (**Figures 1-2**). In addition to the data presented in the interim report and EPA (2014a) pertaining to the alley and railroad soils, this follow-up report (NEICVP1060E02) presents analytical results and interpretation of additional soil samples collected from residential properties in the vicinity of the alley and railroad spur (**Figure 3**). Potential responsible parties (PRPs) for elevated levels of Pb in these residential soils included Century Smelting & Refining (Century), H. Kramer, Loewenthal Metals Corporation (Loewenthal), National Lead/Southern White Lead Works (NL), Tire Grading Company (Tire Grading), and Midwest Generation Fisk Station (Fisk) (EPA, 2014a and b). Of these PRPs, only H. Kramer is still in operation. Additional details of these facilities were presented in EPA (2014a and b).

Century was a small-scale producer of babbit and solder products; H. Kramer continues to manufacture brass and bronze products; Loewenthal produced babbit and solder products and conducted aluminum (Al), antimonial Pb, battery Pb, and zinc (Zn) smelting; NL manufactured white Pb paint, babbit, and solder products and conducted secondary Pb and tin (Sn) smelting; Tire Grading was a tire service company; Fisk generated electricity by burning coal which produces fly ash (EPA, 2014a and b). Babbits are alloys of Sn that may include copper (Cu), antimony (Sb), and/or Pb with negligible Zn and are used as anti-friction linings for bearings (Calvert, 2004; ASTM, 2014). Battery Pb used for battery grids in Pb-acid batteries may consist of 1 to 3 weight % Sb (Prengaman, 1995). Other potential sources of elevated lead in the soil of the Pilsen area included vehicle exhaust from the historical use of leaded gasoline, leaded paint historically used on homes and buildings, and historical Pb processing and manufacturing in the area.

NEIC previously reported analytical results for total suspended particulate (TSP) matter collected on glass fiber filters at ambient air monitoring sites at two different locations in the Pilsen neighborhood and for baghouse dust from H. Kramer (NEIC, 2011a, 2012). One of these ambient air monitoring sites was located at the Perez Elementary School. Results indicated Pb-bearing particulate matter collected at both air monitoring sites originated from process emissions at H. Kramer. In April 2013, H. Kramer agreed to install upgraded emission control equipment at its Pilsen facility (EPA, 2013).

Three residential soil areas with elevated levels of Pb (receptor soils) were defined by EPA Region 5 (Canar et al., 2014; EPA 2014b) and referred to as Residential 1 (Res 1), Residential 2 (Res 2), and Residential 3 (Res 3). Res 1, Res 2, and Res 3 were located at increasing distances from the H. Kramer facility, respectively (**Figures 1 and 3**).

In addition to the three residential soil areas, analytical results and interpretation of two reference soil areas referred to as Little Italy and Harrison Park were also considered in this study (**Figure 4**). The Little Italy and Harrison Park (also known as West) soil areas were chosen by EPA Region 5 (Canar et al., 2014; EPA 2014b) to represent baseline or background soil in the Pilsen neighborhood relative to soil in the residential areas and adjacent to H. Kramer (**Figure 4**). Because the predominant wind direction in the Pilsen neighborhood was from the south and west according to National Oceanic and Atmospheric Administration (NOAA) meteorological data (1928 to 2013) (EPA, 2014a and b), the Little Italy and Harrison Park soil areas were located primarily upwind of the PRPs' facility locations and much farther away from their locations than the residential soil areas. Because of their upwind and more distant locations, Little Italy and Harrison Park soils likely experienced negligible to relatively little impact from any of the PRPs compared to the much closer residential soils. Thus, the Little Italy and Harrison Park reference soils were considered non-receptor control areas *with respect to* the PRPs considered here. Although the Little Italy soils included soil with relatively low Pb levels, suggesting a better representation of background Pb, elevated Pb levels were common in Harrison Park soils and were likely indicators of historical Pb contamination that was probably unrelated to the PRPs described above. As such, the elevated Pb in these soils provided the best available comparison to material related to historical Pb processing and manufacturing in the Pilsen area.

Characteristics of Pb contamination that distinguish potential contamination sources may be referred to as discriminators. In this study, the following discriminators were considered to distinguish potential sources of Pb contamination in the soil areas sampled: (1) relative elemental composition, texture, size, and morphology of individual particles; (2) Pb isotope ratios of bulk soils; (3) relative elemental compositions of bulk soils; (4) relative distance from potential source to receptor soil with consideration of predominant wind direction.

Initial evaluations of discriminators determined whether a potential source of Pb was *consistent with* Pb contamination in a receptor soil with respect to a given discriminator. As used throughout this report, sources of Pb that were ***consistent with*** Pb in a receptor soil could not be excluded as possible sources. Sources of Pb that were ***not consistent with*** Pb in a receptor soil were excluded.

The likelihood of a source of Pb *matching* Pb contamination in a receptor soil increased as the number of discriminators that were consistent increased. The more discriminators that were consistent with a potential source of Pb, the stronger the identification of that Pb source as a major contributor of Pb contamination in the receptor soil. When potential sources of Pb could

be excluded because at least one discriminator was inconsistent, identification became more certain of the source of Pb that was consistent with receptor soil Pb contamination. When a given discriminator was inconsistent with all other potential sources of Pb, the discriminator was unique to the source being considered and that source of Pb was identified as a major contributor of Pb to the soil.

Microscopy analysis of alley, railroad, residential, and reference soils; TSP filters; and H. Kramer baghouse dust to determine particle composition, texture, size, and morphology was conducted by NEIC using scanning electron microscopy (SEM) with energy dispersive X-ray spectrometry (EDS). The SEM analyses described in this report were conducted in accordance with the NEIC quality system, and this technique is within the scope of NEIC's ISO/IEC 17025 accreditation issued by ANSI-ASQ National Accreditation Board/FQS (Certificate No. AT-1646). Pb isotope ratio measurements of alley, railroad, residential, and reference soils; TSP filters collected at the Perez air monitoring site; and baghouse dust from H. Kramer were conducted by the U.S. Geological Survey (USGS) under contract with EPA Region 5 using multicollector inductively coupled plasma mass spectrometry (MC-ICP-MS). Pb concentrations for TSP filters were determined by the Cook County Department of Environmental Control (CCDEC) (EPA, 2011). Elemental analysis of alley, railroad, residential, and reference soils and H. Kramer baghouse dust was conducted by STAT Analysis Corporation (STAT Analysis Corp) under contract with EPA Region 5 using inductively coupled plasma mass spectrometry (ICP-MS). NEIC evaluated and applied statistical analysis to ICP-MS data generated by STAT Analysis Corp and provided interpretation of those results. Analytical results of soils were compared to each other, to results of TSP filters collected at the Perez Elementary School, to results of baghouse dust from H. Kramer, and to the metals composition of H. Kramer slag material provided by H. Kramer (2014a). Slag is produced from industrial processes such as smelting (primary or secondary). Slag is not associated with coal fly ash, leaded paint, leaded gasoline, automobile battery lead, or tire materials.

SUMMARY OF FINDINGS

Analytical results of alley, railroad, residential, and reference soils from the Pilsen neighborhood were compared to results of TSP filters, H. Kramer baghouse dust, and H. Kramer slag data, and to distance from H. Kramer in the predominant downwind direction. These comparisons allowed potential sources of Pb in these soils to be included or excluded.

Results were ***consistent with*** brass and bronze foundry materials (emissions dust or slag) as predominant sources of Pb in alley, railroad, Res 1, and Res 2 soils because of the following:

1) Micrometer-scale (1–10 μm) Zn-oxide particles found in railroad soil were similar to micrometer-scale Zn-oxide particles observed in baghouse dust from H. Kramer.

2) Relative elemental concentrations indicated similar relative abundances of Cu, Pb, and Sn in H. Kramer baghouse dust and in alley and railroad soils near H. Kramer.

3) Correlation analysis and scatterplots indicated cadmium (Cd), Cu, Sn, and Zn were co-contaminants with a predominant source of Pb in alley, railroad, Res 1, and Res 2 soil. Cu, Pb, Sn, and Zn are associated with brass and bronze production, and Cd is a common contaminant associated with Zn recovery from scrap metal.

4) The predominant morphology (angular), size (1s–100s μm), and composition of Pb-bearing particles (iron [Fe]- and silicon [Si]-oxides, multi-phase particles) in alley, railroad, Res 1, and Res 2 soils were consistent with slag material from industrial processes such as smelting.

5) The predominant relative spectral responses of Cu, Pb, and Zn (Cu, Zn > Pb) in these slag particles and the presence of Pb-bearing Cu-oxide, Sn-oxide, and Zn-oxide particles were consistent with compositions of brass and bronze foundry slag and in agreement with Zn/Pb ratios in alley, Res 1, and Res 2 soils being similar to H. Kramer slag composition.

6) Lead isotope ratios measured in particulate matter collected on TSP filters were isotopically similar to Pb isotope ratios measured in H. Kramer baghouse dust. In addition, four alley soil samples exhibited Pb isotopic compositions consistent with the TSP filters and H. Kramer baghouse dust.

7) Pb isotope ratios in alley, railroad, Res 1, and 2 soils exhibited a broad range and linear trend, suggesting mixing of a source of Pb isotopically consistent with the TSP filters and H. Kramer baghouse dust with soil containing a historical baseline Pb isotope signature. Res 1 and 2 soils generally exhibited a greater contribution from the baseline Pb isotope signature with increasing distance from the H. Kramer facility.

8) A general shift to higher $^{208}Pb/^{207}Pb$ ratios; lower Cd, Cu, Sn, and Zn concentrations; and lower (X)/Pb ratios with increased distance from H. Kramer was indicated by the relative compositions of Res 1, Res 2, and Res 3 soils. Shifts in these data with increased distance from H. Kramer were strong indicators that these soil areas were impacted by Pb from H. Kramer with diminishing Pb impact with distance from the facility.

Results were ***not consistent with*** the following as predominant sources of Pb in alley, railroad, Res 1, Res 2, Res 3, and Harrison Park soils because of the following:

9) Although correlation analysis and scatterplots indicated Res 3 soil was impacted by Pb associated with Cd, Cu, Sn, and Zn, the predominant source of Pb was ***not*** consistent with H. Kramer materials.

10) Because of minimal Pb from fly ash in ambient air dust and because a unique particle type of amorphous, alumino-silicate spheres exhibited by coal fly ash was ***not*** observed by SEM in any of the soil areas, the only PRP producing coal fly ash, Fisk, was eliminated as a dominant source of Pb in the soils.

11) Pb, Cd, Cu, Sn, and Zn collectively are ***not*** characteristic of tire dust, suggesting tire dust was ***not*** a dominant source of Pb (or Zn) in these soils. As the only PRP associated with tires, Tire Grading was eliminated as a dominant source of Pb in the soils.

12) Associations of Cd, Cu, and Sn in leaded paint are rare, and Pb-based paint particle types were ***not*** observed by SEM in any of the soil areas. Thus, non-industrial Pb from leaded paint historically used on homes and buildings in the Pilsen area was ***not*** a dominant source of Pb in alley, railroad, residential, and Harrison Park soils.

13) Pb, Cd, Cu, Sn, and Zn collectively are ***not*** characteristic of leaded gasoline emissions, and leaded fuel combustion particles types were ***not*** observed by SEM in any of the soil areas. Thus, vehicle exhaust from the historical use of leaded gasoline was ***not*** a dominant source of Pb in alley, railroad, residential soils, and Harrison Park soils.

14) Babbit, solder, antimonial Pb, and battery lead manufacturing by Century, Loewenthal, or NL were excluded as dominant sources of Pb in the soils because Sb soil concentrations were low; correlations between Sb and Pb were lacking; Sb-bearing particle types were ***not*** observed by SEM in any of the soil areas; and Pb, Cd, Cu, Sn, and Zn collectively are ***not*** characteristic of babbit, solder, antimonial Pb, or battery lead materials.

15) Loewenthal and NL were differentiated from H. Kramer as potential sources of Pb by the pattern of Pb, Cd, Cu, Sn, and Zn soil concentrations relative to distance from H. Kramer. This pattern was ***not*** consistent with Loewenthal and NL as predominant sources of Pb in alley, railroad, Res 1 and Res 2 soils.

16) The predominant morphology (angular), size (1s–100s μm), and composition of Pb-bearing (Fe- and Si-oxides, multi-phase particles) particles in Res 3 and Harrison Park soils were consistent with slag material from an industrial source (not leaded gasoline emissions or leaded paint). The predominant relative spectral responses of Cu, Pb, and Zn (Pb > Cu, Zn) in these Pb-bearing particles were ***not*** characteristic of brass and bronze foundry slag compositions. The Pb isotope ratios in two Res 3 soils suggested significant Pb in those samples was ***not*** consistent with material from H. Kramer.

LABORATORY ANALYSIS

Laboratory measurements conducted specifically for this report included SEM/EDS and MC-ICP-MS analyses. The SEM/EDS work was performed by NEIC in accordance with NEIC quality system requirements and was within the scope of NEIC's ISO/IEC 17025 accreditation issued by ANSI-ASQ National Accreditation Board/FQS (Certificate No. AT-1646). The MC-ICP-MS analyses were conducted by USGS under contract with EPA Region 5 and are presented in this report.

Existing data used in this report included elemental concentrations by ICP-MS, Pb concentrations for TSP filters, and metals composition of H. Kramer slag material (H. Kramer, 2014a). ICP-MS was conducted by STAT Analysis Corp under contract with EPA Region 5 and reported in two site assessment reports for the Pilsen area (EPA, 2014a and b). Pb concentrations for TSP filters collected at the Perez Elementary School were determined by the CCDEC (EPA, 2011). Metals composition of H. Kramer slag material was provided by H. Kramer (2014a).

NEIC used ICP-MS results generated by STAT Analysis Corp to conduct statistical analysis, to construct and evaluate scatterplots, and to provide interpretations of those results. Analytical results of soils were compared to each other, to results of the TSP filters, to results of baghouse dust from H. Kramer, and to the metals composition of H. Kramer slag material (H. Kramer, 2014a).

The microscopic examination of individual particles for relative elemental composition, texture, size, and morphology frequently reveals information about the origin of particles and the processes that formed them. For example, spherical morphology of micrometer-scale (1–10 μm), metal oxide particles indicates particle formation via condensation of metal fume produced in a high-temperature process (Schwartz et al., 1955; Buckle and Pointon, 1976; EPA, 1977; Machemer, 2004; NEIC, 2011a and b, 2012). In contrast, angular particles, tens to hundreds of micrometers in scale (10s–100s μm), are consistent with particle formation via grinding (NEIC, 2010). Particle textures such as spherical cavities are indicative vesicles, holes that form in molten material by escaping gas bubbles and typical in slag material (van Oss, 2003). Furthermore, the relative elemental composition of individual particles reflects the composition of the materials from which the particles formed. Many studies have applied individual particle analysis using SEM/EDS to the characterization of lead containing particles from such sources as automobile exhaust, mining waste, smelters, and paint (Linton et al., 1980; Post and Buseck, 1984; Heasman and Watt, 1989; Hunt et al., 1992; Mahaffy et al., 1998; Sterling et al., 1998; Sobanska et al., 1999; Machemer et al., 2007; NEIC, 2011a and b, 2012). Differences in the composition, morphology, and size of particulate materials associated with the processes of various industries and facilities may be used to discriminate sources of the material.

There are four stable isotopes of Pb: ^{204}Pb, ^{206}Pb, ^{207}Pb, and ^{208}Pb. Only ^{204}Pb is non-radiogenic, whereas ^{206}Pb, ^{207}Pb, and ^{208}Pb are daughter products formed from the radioactive decay of uranium 238 (^{238}U), ^{235}U, and thorium 232 (^{232}Th), respectively. Over time, primordial ratios of ^{204}Pb to the other three stable isotopes of Pb (baseline ratios) were altered by the radiogenic production of ^{206}Pb, ^{207}Pb, and ^{208}Pb via the different decay constants of their radiogenic sources. Thus, the isotopic composition of Pb in an ore reflects the age of the ore, and can provide insight to the geographic area from which it was mined. For example, the ratio of ^{206}Pb/^{207}Pb is 1.03 in the Broken Hill ore, an older Pb deposit in Australia (Maddaloni et al., 1998). In comparison, the ratio of ^{206}Pb/^{207}Pb is as high as 1.42 in the younger deposits of the Mississippi Valley. Another important property of Pb isotopes is that they do not fractionate during natural or anthropogenic (smelting) processes, allowing their isotopic compositions to be used as geochemical tracers (Doe, 1970; Bollhöfer and Rosman, 2001; Shiel et al., 2010). The isotopic composition of Pb in the environment reflects not just its age and geologic history, but also any anthropogenic processes that may have affected it. Pb-bearing airborne particulate matter from industrial facilities may be traced through the smelting, transport, and deposition processes. Pb isotopes have been used for Pb source discrimination in soils (Gulson et al., 1981; Rabinowitz, 1988; Erel et al., 1997; Pribil et al., 2014) and in atmospheric aerosols and dust (Flegal et al., 1989; Hopper et al., 1991; Mukai et al., 1993, 1994; Hamelin et al., 1997; Veron and Church, 1997; Neymark et al., 2008; Ewing et al., 2010).

Various industrial processes produce aerosols, including grinding, smelting, and blending. Typically, materials are blended in specific proportions to meet manufacturing specifications and minimize impurities. Consequently, specific metals in characteristic relative abundances may be associated with various industries and may be used to discriminate sources of particulate material. For example, processing of phosphate rock for fertilizers and phosphoric acid is associated with chromium (Cr), Cu, Fe, manganese (Mn), nickel (Ni), strontium (Sr), and vanadium (V) (Lee and von Lehmden, 2012). Fly ash from coal-fired power plants is comprised largely of calcium (Ca), Al, Si, Fe, Mn, titanium (Ti), and approximately 1% rare earth elements (REEs) (Davison et al., 1974; Mattigod, 2003). Pb, Zn, Cd, Sn, and Cu are associated with brass and bronze foundries (Morris, 2004; H. Kramer, 2012 and 2014b). Therefore, relative elemental abundances may be used as source discriminators in atmospheric aerosols, dusts, and soils (Friedlander, 1973; EPA, 1998; Machemer, 2007; Lee and von Lehmden, 2012). In contrast to Pb isotope ratios, elemental fractionation is often observed with processing. Industrial processing can result in enrichment of trace metals in waste material. A comparison of trace metals in fly ash to those found in coal showed increased concentrations of Al, Cr, Cu, Fe, magnesium (Mg), and Mn in the fly ash relative to coal (Lee and von Lehmden, 2012). Similarly, a comparison of brass and bronze baghouse dust collected from zinc and copper smelter operations showed a significant increase in the concentration of Zn and Cd in furnace exit fumes (Schwartz et al., 1955; DHEW, 1969; Morris, 2004; NEIC, 2012; H. Kramer, 2014b).

SAMPLE RECEIPT AND DESCRIPTION

In the fall of 2013, NEIC received 203 soil samples collected according to EPA's site assessment reports (EPA, 2014a and b). Alley and railroad soils consisted of silty, sandy, and gravelly fill materials with wood chips; cinders; and pieces of glass, brick, plastic, and slag (EPA, 2014a). Residential soils consisted of sandy and gravelly silts and clays. Trace fill materials, including wood chips and pieces of brick, plastic, and metals, were occasionally observed in assessment area soils at various depths (EPA, 2014b). Also analyzed for the current study were four TSP filters and five baghouse dust samples from H. Kramer that were collected as part of an earlier study of airborne particulate matter in the Pilsen neighborhood (NEIC, 2011a, 2012). **Figure 1** shows the location of H. Kramer in the Pilsen neighborhood and the relative locations of the alley and railroad. **Figure 2** shows the approximate collection locations of the alley and railroad soil samples. **Figure 3** shows the relative locations of soils collected within the three defined residential areas. **Figure 4** shows a broader map view, including the more distant Harrison Park and Little Italy soil areas. **Table 1** presents the soil samples and H. Kramer baghouse dust received by NEIC, sample date, sampling depth interval, sampling area, sample description, lead concentration, and a summary of laboratory examinations for each sample. In the tables and figures and elsewhere throughout this report, soil sampling areas were shown in colored text and corresponding colored data symbols for easier differentiation. Also included in **Table 1** are the TSP filters analyzed for Pb isotope ratios for this study. All samples were handled at NEIC in accordance with the NEIC operating procedure *Evidence Management*, NEICPROC/00-059R3.

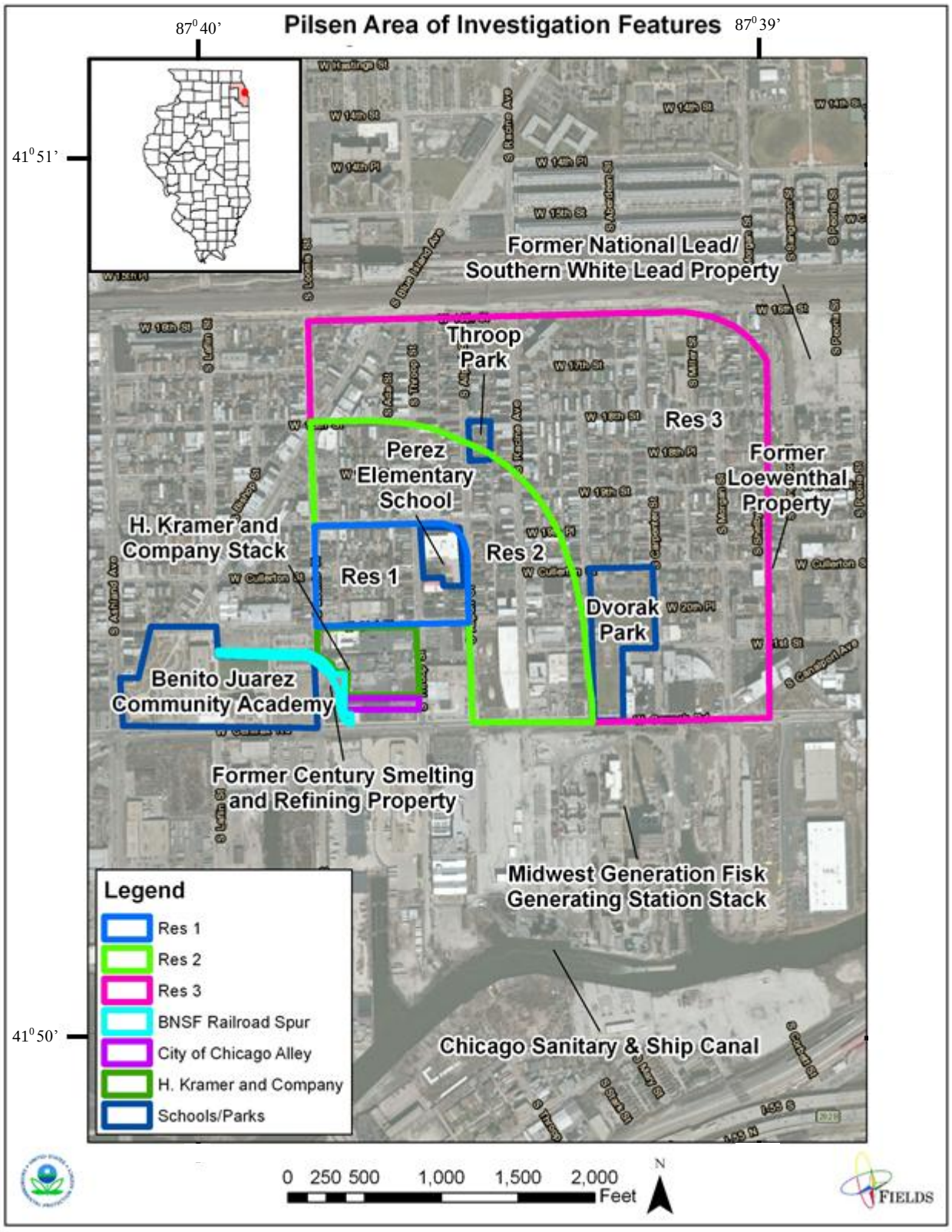

Figure 1. Location of features in the Pilsen area of investigation, Pilsen neighborhood, Chicago, Illinois. Modified from EPA (2014b).

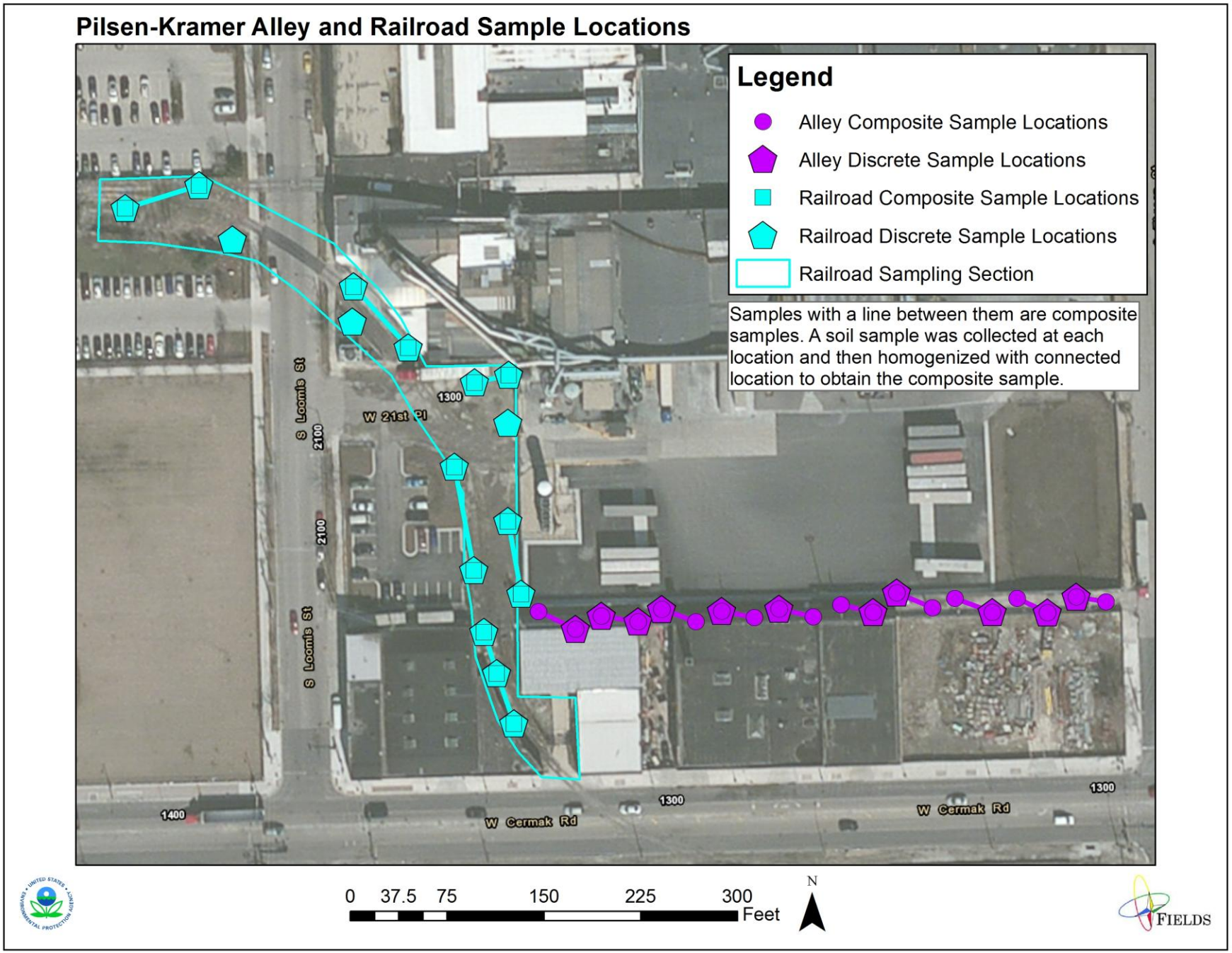

Figure 2. Alley and railroad soil sample locations, Pilsen neighborhood, Chicago, Illinois. Alley samples were numbered from west to east, and railroad soil samples were numbered from north to south. Modified from EPA (2014a).

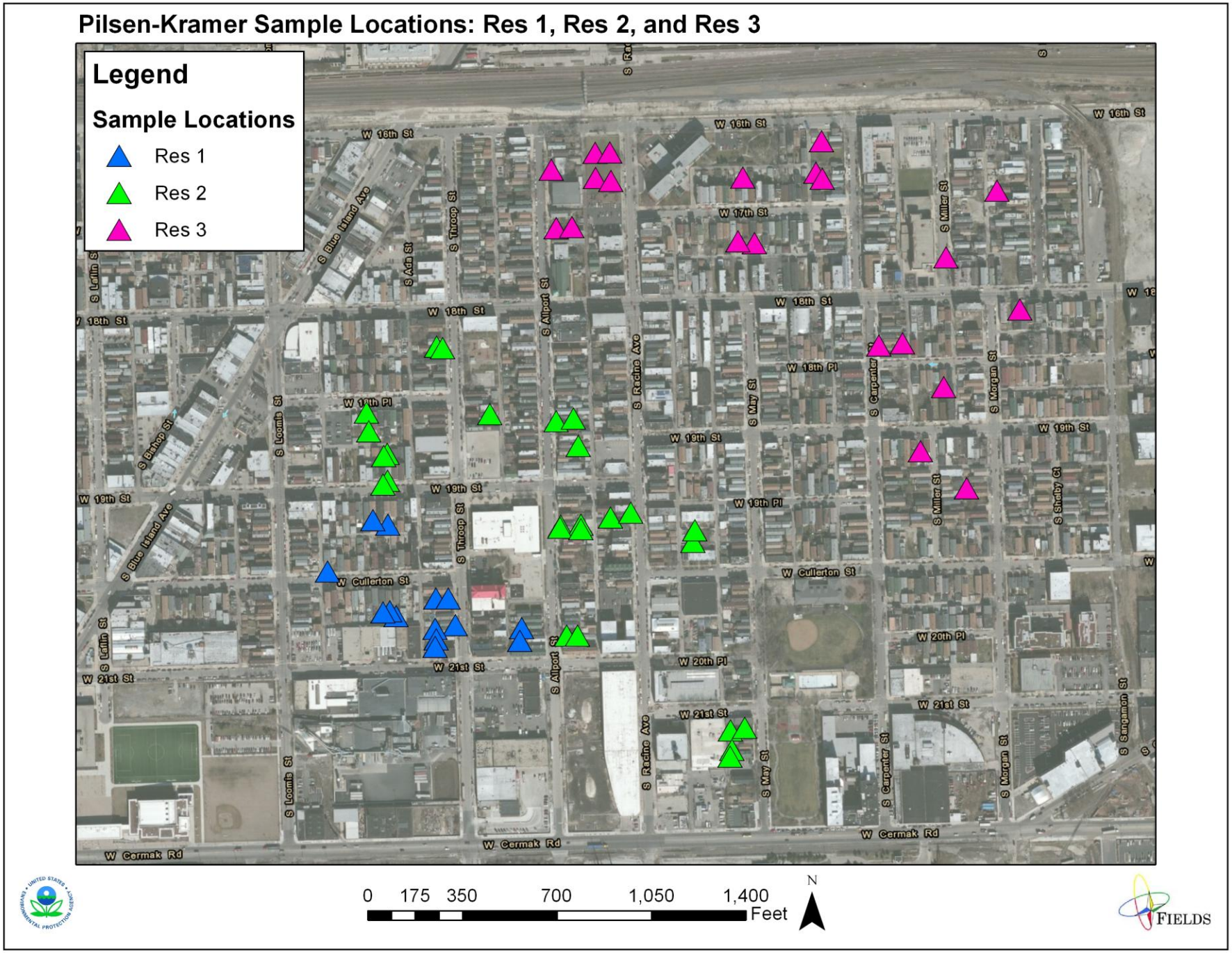

Figure 3. Res 1, Res 2, Res 3 soil sample locations, Pilsen neighborhood, Chicago, Illinois. Modified from EPA (2014b).

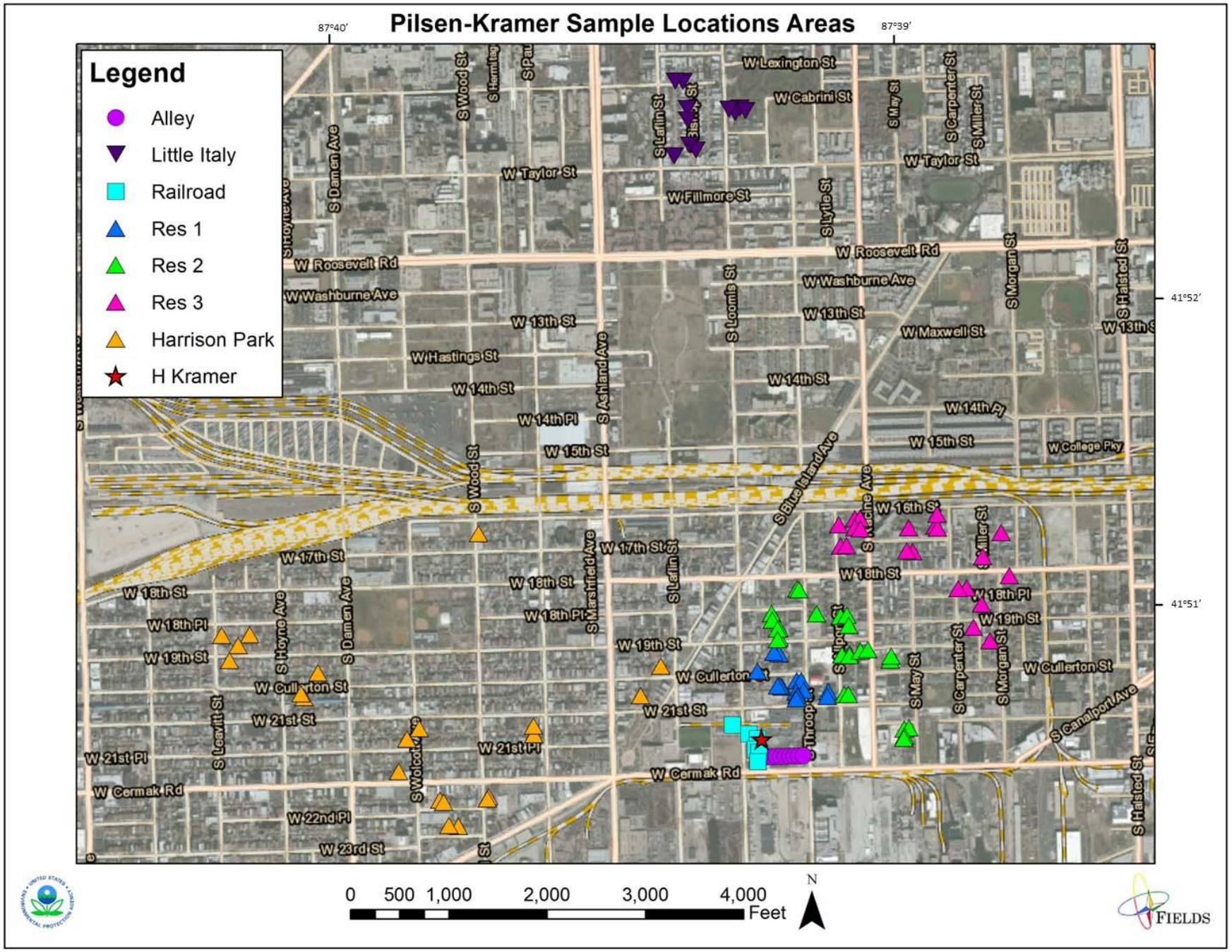

Figure 4. Wide-angle map view of the Pilsen area of investigation with soil sampling locations in reference areas, Little Italy and Harrison Park (West), Pilsen neighborhood, Chicago, Illinois. Modified from EPA (2014b).

Table 1. LIST OF SAMPLES[a]
Additional Characterization of Lead in Soils
Pilsen Neighborhood, Chicago, Illinois

Location ID	Field Sample ID	Laboratory Information Management System (LIMS) No.	Sampling Date	Depth Interval (inches)	Sampling Area	Sample Description	Lead concentration (mg/kg)[b]	Elemental Results[b]	Lead Isotope Ratio Results	SEM/EDS Results
BH1	BH 1	N105006-05	3/17/2011	n.a.[c]	H. Kramer baghouse 1	Rotary furnace	51000	Yes	Yes	(NEIC 2011)
BH2	BH 2	N105006-06	3/17/2011	n.a.[c]	H. Kramer baghouse 2	Rotary furnace	42000	Yes	Yes	(NEIC 2011)
BH4	BH 4	N105006-08	4/29/2011	n.a.[c]	H. Kramer baghouse 4	Electric induction furnace	12000	Yes	Yes	(NEIC 2011)
BH4 Duplicate	BH 4	N105006-09	4/29/2011	n.a.[c]	H. Kramer baghouse 4	Electric induction furnace	13000	Yes	Yes	No
BH5	BH 5	N105006-07	3/17/2011	n.a.[c]	H. Kramer baghouse 5	Rotary furnace	34000	Yes	Yes	(NEIC 2011)
AC01	PA-AC01(0-6)-121912	N312001-CK	12/19/2012	0–6	**Alley**	Composite soil	2700	Yes	Yes	No
AC01	PA-AC01(0-6)-121912D	N312001-CL	12/19/2012	0–6	**Alley**	Composite soil	2600	Yes	No	No
AC02	PA-AC02(0-6)-121912	N312001-CM	12/19/2012	0–6	**Alley**	Composite soil	1900	Yes	Yes	No
AC02	PA-AC02(0-6)-121912D	N312001-CN	12/19/2012	0–6	**Alley**	Composite soil	2000	Yes	No	No
AC03	PA-AC03(0-6)-121912	N312001-CO	12/19/2012	0–6	**Alley**	Composite soil	5600	Yes	Yes	No
AC03HS	PA-AC03HS(0-6)-121912	N312001-DY	12/19/2012	0–6	**Alley**	Composite soil	2600	Yes	Yes	No
AC04	PA-AC04(0-6)-121912	N312001-CP	12/19/2012	0–6	**Alley**	Composite soil	5000	Yes	Yes	No
AC05	PA-AC-05(0-6)-121912	N312001-EA	12/19/2012	0–6	**Alley**	Composite soil	3900	Yes	Yes	No
AC06	PA-AC06(0-6)-121912	N312001-CQ	12/19/2012	0–6	**Alley**	Composite soil	3000	Yes	Yes	No
AC07	PA-AC07(0-6)-121912	N312001-01	12/19/2012	0–6	**Alley**	Composite soil	940	Yes	Yes	Yes
AC08	PA-AC08(0-6)-121912	N312001-CR	12/19/2012	0–6	**Alley**	Composite soil	570	Yes	Yes	No
AC09	PA-AC09(0-6)-121912	N312001-02	12/19/2012	0–6	**Alley**	Composite soil	340	Yes	Yes	No
AC10	PA-AC10(0-6)-121912	N312001-CS	12/19/2012	0–6	**Alley**	Composite soil	63	Yes	Yes	No
AY02	PA-AY02(6-12)-121912	N312001-10	12/19/2012	6–12	Alley	Grab soil	2500	Yes	No	No
AY04	PA-AY04(6-12) -121912	N312001-07	12/19/2012	0–6	Alley	Grab soil	8700	Yes	No	No
AY05	PA-AY05(6-12)-121912	N312001-08	12/19/2012	6–12	Alley	Grab soil	8800	Yes	No	No
AY07	PA-AY07(12-24)-121912	N312001-09	12/19/2012	12–24	Alley	Grab soil	16000	Yes	No	No
AY09	PA-AY09(12-24)-121912	N312001-CT	12/19/2012	12–24	Alley	Grab soil	15000	Yes	Yes	No
AY12	PA-AY12(6-12)-121912	N312001-11	12/19/2012	6–12	Alley	Grab soil	1700	Yes	No	No
AY13	PA-AY13(12-24)-121912	N312001-06	12/19/2012	12–24	Alley	Grab soil	3200	Yes	No	No
AY16	PA-AY16(12-24)-121912	N312001-05	12/19/2012	12–24	Alley	Grab soil	2100	Yes	No	No
AY18	PA-AY18(6-12)-121912	N312001-03	12/19/2012	6–12	Alley	Grab soil	3400	Yes	No	Yes
AY19	PA-AY19(12-24)-121912	N312001-04	12/19/2012	12–24	Alley	Grab soil	1600	Yes	No	No
PA-104-01	PA-**104**-01(0-6)-050213	N312001-**94**	5/2/2013	**0–6**	**Res 2**	Front yard soil	930	Yes	Yes	No
PA-104-01	PA-104-01(6-12)-071613	N312001-AD	7/16/2013	6–12	Res 2	Front yard soil	890	Yes	No	No
PA-104-01	PA-104-01(12-24)-071613	N312001-AE	7/16/2013	12–24	Res 2	Front yard soil	500	Yes	Yes	No
PA-104-02	PA-**104**-02(0-6)-050213	N312001-**CW**	5/2/2013	**0–6**	**Res 2**	Back yard soil	1400	Yes	No	Yes
PA-105-01	PA-**105**-01(0-6)-050213	N312001-**93**	5/2/2013	**0–6**	**Res 2**	Front yard soil	640	Yes	Yes	No
PA-105-02	PA-**105**-02(0-6)-050213	N312001-**12**	5/2/2013	**0–6**	**Res 2**	Back yard soil	990	Yes	No	No

Table 1. LIST OF SAMPLES[a]
Additional Characterization of Lead in Soils
Pilsen Neighborhood, Chicago, Illinois

Location ID	Field Sample ID	Laboratory Information Management System (LIMS) No.	Sampling Date	Depth Interval (inches)	Sampling Area	Sample Description	Lead concentration (mg/kg)[b]	Elemental Results[b]	Lead Isotope Ratio Results	SEM/EDS Results
PA-122-01	PA-**122**-01(0-6)-050313	N312001-**14**	5/3/2013	**0–6**	**Res 1**	Back yard soil	1900	Yes	Yes	Yes
PA-122-01	PA-122-01(6-18)-071513	N312001-38	7/15/2013	6–18	Res 1	Back yard soil	1900	Yes	No	No
PA-122-01	PA-122-01(18-24)-071513	N312001-39	7/15/2013	18–24	Res 1	Back yard soil	470	Yes	No	No
PA-122-01	PA-122-01(18-24)-071513D	N312001-40	7/15/2013	18–24	Res 1	Back yard soil	250	Yes	No	No
PA-122-02	PA-122-02(0-12)-050313	N312001-BE	5/3/2013	0–12	Res 1	Garden soil	920	Yes	Yes	No
PA-123-01	PA-123-01(0-12)-050313	N312001-BD	5/3/2013	0–12	Res 2	Garden soil	1100	Yes	Yes	No
PA-125-01	PA-**125**-01(0-6)-050313	N312001-**CC**	5/3/2013	**0–6**	**Res 2**	Yard (west 1/2 lot)	1500	Yes	Yes	Yes
PA-125-02	PA-**125**-02(0-6)-050313	N312001-**CX**	5/3/2013	**0–6**	**Res 2**	Yard (east 1/2 lot)	1100	Yes	Yes	No
PA-125-03	PA-125-03(0-12)-050313	N312001-BC	5/3/2013	0–12	Res 2	Garden soil	700	Yes	No	No
PA-127-01	PA-**127**-01(0-6)-050313	N312001-**CY**	5/3/2013	**0–6**	**Res 1**	Back yard soil	2500	Yes	No	Yes
PA-127-01	PA-127-01(6-21)-071613	N312001-41	7/16/2013	6–21	Res 1	Back yard soil	4200	Yes	Yes	No
PA-14-01	PA-**14**-01(0-6)-050913	N312001-**51**	5/9/2013	**0–6**	**Res 2**	Back yard soil	140	Yes	No	No
PA-14-02	PA-**14**-02(0-6)-050913	N312001-**CZ**	5/9/2013	**0–6**	**Res 2**	Front yard soil	480	Yes	No	No
PA-14-03	PA-14-03(0-6)-050913	N312001-82	5/9/2013	0–6	Res 2	Drip zone soil	710	Yes	No	No
PA-141-01	PA-**141**-01(0-6)-050713	N312001-**CD**	5/7/2013	**0–6**	**Res 2**	Yard (west 1/2 lot)	860	Yes	No	No
PA-141-02	PA-**141**-02(0-6)-050713	N312001-**CI**	5/7/2013	**0–6**	**Res 2**	Yard (east 1/2 lot)	1600	Yes	No	Yes
PA-141-03	PA-141-03(0-12)-050713	N312001-BJ	5/7/2013	0–12	Res 2	Garden soil	3300	Yes	No	No
PA-163-01	PA-163-01(0-12)-050113	N312001-AZ	5/1/2013	0–12	Res 2	Garden soil	19	Yes	Yes	No
PA-163-02	PA-163-02(0-12)-050113	N312001-BA	5/1/2013	0–12	Res 2	Garden soil	130	Yes	No	No
PA-163-03	PA-163-03(0-6)-050113	N312001-80	5/1/2013	0–6	Res 2	Drip zone soil	130	Yes	No	No
PA-180-01	PA-**180**-01(0-6)-050213	N312001-**CB**	5/2/2013	**0–6**	**Res 1**	Yard (east 1/2 lot)	810	Yes	Yes	No
PA-180-02	PA-**180**-02(0-6)-050213	N312001-**CF**	5/2/2013	**0–6**	**Res 1**	Yard (west 1/2 lot)	3000	Yes	No	No
PA-183-01	PA-183-01(0-12)-050213	N312001-BB	5/2/2013	0–12	Res 1	Garden soil	1300	Yes	Yes	No
PA-186-01	PA-**186**-01(0-6)-050213	N312001-**95**	5/2/2013	**0–6**	**Res 1**	Front yard soil	360	Yes	No	No
PA-186-02	PA-**186**-02(0-6)-050213	N312001-**DA**	5/2/2013	**0–6**	**Res 1**	Back yard soil	320	Yes	Yes	No
PA-191-01	PA-**191**-01(0-6)-050213	N312001-DB	5/2/2013	**0–6**	**Res 1**	Back yard soil	2000	Yes	Yes	No
PA-191-01	PA-191-01(0-6)-050213D	N312001-DC	5/2/2013	0–6	Res 1	Back yard soil	2400	Yes	No	No
PA-193-01	PA-**193**-01(0-6)-050313	N312001-**13**	5/3/2013	**0–6**	**Res 1**	Back yard soil	580	Yes	Yes	No
PA-272-01	PA-**272**-01(0-6)-050113	N312001-**DD**	5/1/2013	**0–6**	**Res 1**	Back yard soil	2000	Yes	Yes	Yes
PA-274-01	PA-**274**-01(0-6)-050113	N312001-**DE**	5/1/2013	**0–6**	**Res 1**	Back yard soil	1900	Yes	Yes	Yes
PA-274-02	PA-274-02(0-6)-050113	N312001-DF	5/1/2013	0–6	Res 1	Drip zone soil	2000	Yes	Yes	No
PA-276-01	PA-**276**-01(0-6)-050113	N312001-**DG**	5/1/2013	**0–6**	**Res 1**	Back yard soil	2400	Yes	No	No
PA-276-01	PA-276-01(0-6)-050113D	N312001-42	5/1/2013	0–6	Res 1	Back yard – duplicate	3600	Yes	No	No
PA-276-01	PA-276-01(6-18)-071513	N312001-43	7/15/2013	6–18	Res 1	Back yard	1700	Yes	No	No

Table 1. LIST OF SAMPLES[a]
Additional Characterization of Lead in Soils
Pilsen Neighborhood, Chicago, Illinois

Location ID	Field Sample ID	Laboratory Information Management System (LIMS) No.	Sampling Date	Depth Interval (inches)	Sampling Area	Sample Description	Lead concentration (mg/kg)[b]	Elemental Results[b]	Lead Isotope Ratio Results	SEM/EDS Results
PA-276-01	PA-276-01(18-24)-071513	N312001-44	7/15/2013	18–24	Res 1	Back yard	550	Yes	No	No
PA-291-01	PA-**291**-01(0-6)-050113	N312001-**92**	5/1/2013	**0–6**	**Res 1**	Front yard soil	500	Yes	No	No
PA-291-03	PA-291-03(0-12)-050113	N312001-DH	5/1/2013	0–12	Res 2	Garden soil	34	Yes	Yes	No
PA-304-01	PA-**304**-01(0-6)-050913	N312001-**DI**	5/9/2013	**0–6**	**Res 2**	Back yard soil	58	Yes	Yes	No
PA-349-01	PA-**349**-01(0-6)-050713	N312001-**DJ**	5/7/2013	**0–6**	**Res 2**	Front yard soil	890	Yes	Yes	No
PA-349-02	PA-349-02(0-12)-050713	N312001-BH	5/7/2013	0–12	Res 2	Garden soil	630	Yes	No	No
PA-349-03	PA-**349**-03(0-6)-050713	N312001-**46**	5/7/2013	**0–6**	**Res 2**	Back yard soil	1400	Yes	No	No
PA-349-03	PA-349-03(6-14)-071613	N312001-54	7/16/2013	6–14	Res 2	Back yard soil	680	Yes	No	No
PA-351-01	PA-351-01(0-12)-050713	N312001-BI	5/7/2013	0–12	Res 2	Garden soil	390	Yes	No	No
PA-369-01	PA-**369**-01(0-2)-050713	N312001-**45**	5/7/2013	0–2	**Res 2**	Back yard soil	480	Yes	No	No
PA-369-01	PA-**369**-01(0-6)-050713	N312001-**DK**	5/7/2013	**0–6**	**Res 2**	Back yard soil	1500	Yes	No	No
PA-369-02	PA-369-02(0-12)-050713	N312001-BG	5/7/2013	0–12	Res 2	Garden soil	1700	Yes	No	No
PA-369-03,04	PA-**369**-03,04(0-6)-050713	N312001-**91**	5/7/2013	**0–6**	**Res 2**	Front yard soil	2300	Yes	No	No
PA-370-01	PA-**370**-01(0-6)-050713	N312001-**DL**	5/7/2013	**0–6**	**Res 1**	Back yard soil	700	Yes	Yes	No
PA-370-01	PA-370-01(0-6)-050713D	N312001-DM	5/7/2013	0–6	Res 1	Back yard soil	950	Yes	No	No
PA-370-02	PA-370-02(0-12)-050713	N312001-CJ	5/7/2013	0–12	Res 1	Garden soil	1700	Yes	Yes	No
PA-370-02	PA-370-02(0-12)-050713D	N312001-DN	5/7/2013	0–12	Res 2	Garden soil	1700	Yes	No	No
PA-371-01	PA-**371**-01(0-6)-050713	N312001-**DO**	5/7/2013	**0–6**	**Res 2**	Back yard soil	1800	Yes	No	Yes
PA-371-02	PA-371-02(0-6)-050713	N312001-**DP**	5/7/2013	**0–6**	**Res 2**	Front yard soil	320	Yes	Yes	No
PA-371-02	PA-371-02(0-6)-050713D	N312001-96	5/7/2013	0–6	Res 2	Front yard soil	410	Yes	Yes	No
PA-375-01	PA-**375**-01(0-6)-050713	N312001-**DQ**	5/7/2013	**0–6**	**Res 1**	Back yard soil	1800	Yes	Yes	No
PA-375-02	PA-375-02(0-12)-050713	N312001-BF	5/7/2013	0–12	Res 1	Garden soil	2500	Yes	No	No
PA-464-01	PA-464-01(0-6)-050813	N312001-**CA**	5/8/2013	**0–6**	Res 3	Yard (east 1/2 lot)	910	Yes	Yes	No
PA-464-02	PA-**464**-02(0-6)-050813	N312001-**DR**	5/8/2013	**0–6**	Res 3	Yard (west 1/2 lot)	240	Yes	Yes	No
PA-464-03	PA-464-03(0-12)-050813	N312001-BK	5/8/2013	0–12	Res 3	Garden soil	670	Yes	No	No
PA-464-04	PA-464-04(0-12)-050813	N312001-BL	5/8/2013	0–12	Res 3	Garden soil	450	Yes	No	No
PA-464-04	PA-464-04(0-12)-050813D	N312001-BM	5/8/2013	0–12	Res 3	Garden soil	390	Yes	No	No
PA-465-01	PA-**465**-01(0-6)-050913	N312001-**BZ**	5/9/2013	**0–6**	Res 3	Yard soil	370	Yes	Yes	No
PA-465-01	PA-465-01(0-6)-050913D	N312001-DS	5/9/2013	0–6	Res 3	Yard soil	340	Yes	No	No
PA-465-02,03,04	PA-465-02,03,04(0-12)-050913	N312001-BO	5/9/2013	0–12	Res 3	Garden/drip zone	350	Yes	No	No
PA-466-01	PA-**466**-01(0-6)-050913	N312001-**DT**	5/9/2013	**0–6**	**Res 2**	Yard (east 1/2 lot)	730	Yes	Yes	No
PA-466-02	PA-**466**-02(0-6)-050913	N312001-**CE**	5/9/2013	**0–6**	**Res 2**	Yard (west 1/2 lot)	650	Yes	Yes	No
PA-466-05	PA-466-05(0-6)-050913	N312001-81	5/8/2013	0–6	Res 2	Drip zone soil	2400	Yes	Yes	No
PA-467-01	PA-**467**-01(0-6)-050913	N312001-**49**	5/8/2013	**0–6**	**Res 2**	Back yard soil	1400	Yes	No	No

Table 1. LIST OF SAMPLES[a]
Additional Characterization of Lead in Soils
Pilsen Neighborhood, Chicago, Illinois

Location ID	Field Sample ID	Laboratory Information Management System (LIMS) No.	Sampling Date	Depth Interval (inches)	Sampling Area	Sample Description	Lead concentration (mg/kg)[b]	Elemental Results[b]	Lead Isotope Ratio Results	SEM/EDS Results
PA-468-01	PA-**468**-01(0-6)-050913	N312001-**50**	5/8/2013	**0–6**	**Res 2**	Back yard soil	1300	Yes	Yes	No
PA-469-01	PA-**469**-01(0-6)-051013	N312001-**CH**	5/10/2013	**0–6**	**Res 3**	Field – NW quadrant	130	Yes	Yes	No
PA-469-01	PA-469-01(0-6)-051013D	N312001-85	5/10/2013	0–6	Res 3	Field – NW quadrant	120	Yes	No	No
PA-469-01	PA-469-01(6-15)-071113	N312001-86	7/11/2013	6–15	Res 3	Field – NW quadrant	340	Yes	Yes	No
PA-469-02	PA-**469**-02(0-6)-051013	N312001-**83**	5/10/2013	**0–6**	**Res 3**	Field – NE quadrant	100	Yes	No	No
PA-469-02	PA-469-02(6-15)-071113	N312001-84	7/11/2013	6–15	Res 3	Field – NE quadrant	330	Yes	No	No
PA-469-03	PA-**469**-03(0-6)-051013	N312001-**88**	5/10/2013	**0–6**	**Res 3**	Field – SW quadrant	120	Yes	No	No
PA-469-03	PA-469-03(6-15)-071113	N312001-89	7/11/2013	6–15	Res 3	Field – SW quadrant	560	Yes	No	No
PA-469-03	PA-469-03(6-15)-071113D	N312001-90	7/11/2013	6–15	Res 3	Field – SW quadrant	250	Yes	No	No
PA-469-04	PA-**469**-04(0-6)-051013	N312001-**87**	5/10/2013	**0–6**	**Res 3**	Field – SE quadrant	110	Yes	No	No
PA-469-04	PA-469-04(0-6)-051013D	N312001-DV	5/10/2013	0–6	Res 3	Field – SE quadrant	80	Yes	No	No
PA-469-05	PA-469-05(0-6)-051013	N312001-DW	5/10/2013	0–6	Res 3	Playground	340	Yes	Yes	No
PA-470-01	PA-**470**-01(0-6)-070913	N312001-**15**	7/9/2013	**0–6**	**Res 2**	Back yard soil	3200	Yes	No	No
PA-471-01	PA-**471**-01(0-6)-070913	N312001-**16**	7/9/2013	**0–6**	**Harrison Park**	Back yard soil	1900	Yes	No	No
PA-472-01	PA-**472**-01(0-6)-070913	N312001-**17**	7/9/2013	**0–6**	**Harrison Park**	Back yard soil	940	Yes	No	No
PA-472-01	PA-472-01(0-6)-070913D	N312001-18	7/9/2013	0–6	Harrison Park	Back yard soil	1200	Yes	No	No
PA-473-01	PA-**473**-01(0-6)-070913	N312001-**19**	7/9/2013	**0–6**	**Harrison Park**	Back yard soil	1700	Yes	No	No
PA-473-01	PA-473-01(6-18)-070913	N312001-20	7/9/2013	6–18	Harrison Park	Back yard soil	1600	Yes	No	No
PA-473-01	PA-473-01(18-24)-070913	N312001-21	7/9/2013	18–24	Harrison Park	Back yard soil	140	Yes	No	No
PA-474-01	PA-**474**-01(0-6)-071013	N312001-**22**	7/10/2013	**0–6**	**Harrison Park**	Back yard soil	2600	Yes	No	Yes
PA-474-01	PA-474-01(6-18)-071013	N312001-23	7/10/2013	6–18	Harrison Park	Back yard soil	2300	Yes	No	No
PA-474-02	PA-**474**-02(0-6)-071013	N312001-**97**	7/10/2013	**0–6**	**Harrison Park**	Front yard soil	2200	Yes	No	No
PA-475-01	PA-**475**-01(0-6)-071013	N312001-**24**	7/10/2013	**0–6**	**Harrison Park**	Back yard soil	3700	Yes	No	Yes
PA-476-01	PA-**476**-01(0-6)-071013	N312001-**25**	7/10/2013	**0–6**	**Harrison Park**	Back yard soil	2000	Yes	No	No
PA-477-01	PA-**477**-01(0-6)-071013	N312001-**26**	7/10/2013	**0–6**	**Harrison Park**	Back yard soil	1700	Yes	No	No
PA-477-01	PA-477-01(6-18)-071013	N312001-27	7/10/2013	6–18	Harrison Park	Back yard soil	1100	Yes	No	No
PA-478-01	PA-**478**-01(0-6)-071013	N312001-**AN**	7/10/2013	**0–6**	**Harrison Park**	Front/back comp	1400	Yes	No	No
PA-478-01	PA-478-01(0-6)-071013D	N312001-AO	7/10/2013	0–6	Harrison Park	Front/back comp	1700	Yes	No	No
PA-479-01	PA-**479**-01(0-6)-071113	N312001-**98**	7/11/2013	**0–6**	**Harrison Park**	Front yard soil	1200	Yes	No	No
PA-480-01	PA-480-01(0-6)-071113	N312001-**99**	7/11/2013	**0–6**	**Harrison Park**	Front yard soil	3200	Yes	No	Yes
PA-481-01	PA-**481**-01(0-6)-071113	N312001-**28**	7/11/2013	**0–6**	**Harrison Park**	Back yard soil	1600	Yes	No	No
PA-482-01	PA-**482**-01(0-6)-071113	N312001-**AA**	7/11/2013	**0–6**	**Res 3**	Front yard soil	210	Yes	No	No
PA-482-01	PA-482-01(6-18)-071113	N312001-AB	7/11/2013	6–18	Res 3	Front yard soil	250	Yes	No	No
PA-483-01	PA-**483**-01(0-6)-071213	N312001-**29**	7/12/2013	**0–6**	**Res 2**	Back yard soil	200	Yes	No	No

Table 1. LIST OF SAMPLES[a]
Additional Characterization of Lead in Soils
Pilsen Neighborhood, Chicago, Illinois

Location ID	Field Sample ID	Laboratory Information Management System (LIMS) No.	Sampling Date	Depth Interval (inches)	Sampling Area	Sample Description	Lead concentration (mg/kg)[b]	Elemental Results[b]	Lead Isotope Ratio Results	SEM/EDS Results
PA-483-01	PA-483-01(6-24)-071213	N312001-30	7/12/2013	6–24	Res 2	Back yard soil	140	Yes	No	No
PA-484-01	PA-**484**-01(0-6)-071213	N312001-**31**	7/12/2013	**0–6**	**Harrison Park**	Back yard soil	1700	Yes	No	No
PA-484-01	PA-484-01(6-18)-071213	N312001-32	7/12/2013	6–18	Harrison Park	Back yard soil	4300	Yes	No	No
PA-485-01	PA-**485**-01(0-6)-071213	N312001-**33**	7/12/2013	**0–6**	**Harrison Park**	Back yard soil	510	Yes	No	No
PA-486-01	PA-**486**-01(0-6)-071213	N312001-**34**	7/12/2013	**0–6**	**Harrison Park**	Back yard soil	880	Yes	No	No
PA-486-01	PA-486-01(6-24)-071213	N312001-35	7/12/2013	6–24	Harrison Park	Back yard soil	1100	Yes	No	No
PA-486-01	PA-486-01(6-24)-071213D	N312001-36	7/12/2013	6–24	Harrison Park	Back yard soil	960	Yes	No	No
PA-487-01	PA-**487**-01(0-6)-071513	N312001-**37**	7/15/2013	**0–6**	**Harrison Park**	Back yard soil	1400	Yes	No	No
PA-488-01	PA-**488**-01(0-6)-071513	N312001-**AC**	7/15/2013	**0–6**	**Harrison Park**	Front yard soil	410	Yes	No	No
PA-489-01	PA-489-01(0-6)-081213	N312001-AF	8/12/2013	0–6	Little Italy	Front yard soil	160	Yes	No	No
PA-489-01	PA-489-01(6-18)-081213	N312001-AG	8/12/2013	6–18	Little Italy	Front yard soil	92	Yes	No	No
PA-490-01	PA-**490**-01(0-6)-081213	N312001-**AH**	8/12/2013	**0–6**	**Little Italy**	Front yard soil	220	Yes	No	No
PA-491-01	PA-**491**-01(0-6)-081213	N312001-**AI**	8/12/2013	**0–6**	**Little Italy**	Front yard soil	260	Yes	No	No
PA-491-01	PA-491-01(6-18)-081213	N312001-AJ	8/12/2013	6–18	Little Italy	Front yard soil	270	Yes	No	No
PA-491-01	PA-491-01(6-18)-081213D	N312001-AK	8/12/2013	6–18	Little Italy	Front yard soil	260	Yes	No	No
PA-492-01	PA-**492**-01(0-6)-081313	N312001-**AL**	8/13/2013	**0–6**	**Little Italy**	Front yard soil	260	Yes	No	No
PA-493-01	PA-**493**-01(0-6)-081313	N312001-**AM**	8/13/2013	**0–6**	**Little Italy**	Front yard soil	190	Yes	No	No
PA-494-01	PA-**494**-01(0-6)-081313	N312001-**79**	8/13/2013	**0–6**	**Little Italy**	Back yard common area	120	Yes	No	No
PA-495-01	PA-**495**-01(0-6)-081313	N312001-**55**	8/13/2013	**0–6**	**Res 3**	Back yard soil	930	Yes	No	No
PA-495-01	PA-495-01(6-24)-081313	N312001-56	8/13/2013	6–24	Res 3	Back yard soil	1800	Yes	No	No
PA-496-01	PA-**496**-01(0-6)-081313	N312001-**57**	8/13/2013	**0–6**	**Res 3**	Back yard soil	230	Yes	No	No
PA-497-01	PA-**497**-01(0-6)-081313	N312001-**58**	8/13/2013	**0–6**	**Res 3**	Back yard soil	460	Yes	No	No
PA-498-01	PA-**498**-01(0-6)-081313	N312001-**59**	8/13/2013	**0–6**	**Res 3**	Back yard soil	270	Yes	No	No
PA-498-01	PA-498-01(0-6)-081313D	N312001-60	8/13/2013	0–6	Res 3	Back yard soil	280	Yes	No	No
PA-498-01	PA-498-01(6-15)-081313	N312001-61	8/13/2013	6–15	Res 3	Back yard soil	550	Yes	No	No
PA-499-01	PA-**499**-01(0-6)-081413	N312001-**AP**	8/14/2013	**0–6**	**Res 3**	Front yard soil	1200	Yes	No	No
PA-500-01	PA-**500**-01(0-6)-081413	N312001-**62**	8/14/2013	**0–6**	**Little Italy**	Back yard soil	760	Yes	No	No
PA-500-01	PA-500-01(6-24)-081413	N312001-63	8/14/2013	6–24	Little Italy	Back yard soil	930	Yes	No	No
PA-501-01	PA-**501**-01(0-6)-081413	N312001-**AQ**	8/14/2013	**0–6**	**Little Italy**	Front yard soil	66	Yes	No	No
PA-502-01	PA-**502**-01(0-6)-081413	N312001-**64**	8/14/2013	**0–6**	**Harrison Park**	Back yard soil	780	Yes	No	No
PA-502-01	PA-502-01(6-24)-081413	N312001-65	8/14/2013	6–24	Harrison Park	Back yard soil	580	Yes	No	No
PA-503-01	PA-**503**-01(0-6)-081413	N312001-**AR**	8/14/2013	**0–6**	**Harrison Park**	Front yard soil	1400	Yes	No	No
PA-503-01	PA-503-01(6-24)-081413	N312001-AS	8/14/2013	6–24	Harrison Park	Front yard soil	840	Yes	No	No
PA-504-01	PA-**504**-01(0-6)-081513	N312001-**AT**	8/15/2013	**0–6**	**Res 3**	Front yard soil	390	Yes	No	No

Table 1. LIST OF SAMPLES[a]
Additional Characterization of Lead in Soils
Pilsen Neighborhood, Chicago, Illinois

Location ID	Field Sample ID	Laboratory Information Management System (LIMS) No.	Sampling Date	Depth Interval (inches)	Sampling Area	Sample Description	Lead concentration (mg/kg)[b]	Elemental Results[b]	Lead Isotope Ratio Results	SEM/EDS Results
PA-505-01	PA-**505**-01(0-6)-081513	N312001-**66**	8/15/2013	**0–6**	**Res 3**	Back yard soil	1300	Yes	No	No
PA-505-01	PA-505-01(0-6)-081513D	N312001-67	8/15/2013	0–6	Res 3	Back yard soil	1400	Yes	No	No
PA-506-01	PA-**506**-01(0-6)-081513	N312001-**68**	8/15/2013	**0–6**	**Res 3**	Back yard soil	940	Yes	No	No
PA-507-01	PA-**507**-01(0-6)-081513	N312001-**69**	8/15/2013	**0–6**	**Harrison Park**	Back yard soil	270	Yes	No	No
PA-508-01	PA-**508**-01(0-6)-081513	N312001-**70**	8/15/2013	**0–6**	**Res 3**	Back yard soil	580	Yes	No	No
PA-508-01	PA-508-01(6-24)-081513	N312001-71	8/15/2013	6–24	Res 3	Back yard soil	140	Yes	No	No
PA-509-01	PA-**509**-01(0-6)-081513	N312001-**72**	8/15/2013	**0–6**	**Res 3**	Back yard soil	1400	Yes	No	No
PA-510-01	PA-**510**-01(0-6)-081513	N312001-**AU**	8/15/2013	**0–6**	**Res 3**	Front yard soil	1700	Yes	No	Yes
PA-511-01	PA-**511**-01(0-6)-081613	N312001-**AV**	8/16/2013	**0–6**	**Little Italy**	Front yard soil	210	Yes	No	No
PA-512-01	PA-**512**-01(0-6)-081613	N312001-**AW**	8/16/2013	**0–6**	**Little Italy**	Front yard soil	320	Yes	No	No
PA-513-01	PA-**513**-01(0-6)-081613	N312001-**AX**	8/16/2013	**0–6**	**Little Italy**	Front yard soil	170	Yes	No	No
PA-513-01	PA-513-01(0-6)-081613D	N312001-AY	8/16/2013	0–6	Little Italy	Front yard soil	140	Yes	No	No
PA-514-01	PA-**514**-01(0-6)-081613	N312001-**73**	8/16/2013	**0–6**	**Res 3**	Back yard soil	410	Yes	No	No
PA-514-01	PA-514-01(6-24)-081613	N312001-74	8/16/2013	6–24	Res 3	Back yard soil	760	Yes	No	No
PA-515-01	PA-**515**-01(0-6)-081613	N312001-**75**	8/16/2013	**0–6**	**Res 3**	Back yard soil	1600	Yes	No	Yes
PA-516-01	PA-**516**-01(0-6)-081613	N312001-**76**	8/16/2013	**0–6**	**Harrison Park**	Back yard soil	520	Yes	No	No
PA-516-01	PA-516-01(0-6)-081613D	N312001-77	8/16/2013	0–6	Harrison Park	Back yard soil	560	Yes	No	No
PA-516-01	PA-516-01(6-18)-081613	N312001-78	8/16/2013	6–18	Harrison Park	Back yard soil	550	Yes	No	No
PA-84-01	PA-**84**-01(0-6)-050813	N312001-**DX**	5/8/2013	**0–6**	**Res 2**	Front yard soil	600	Yes	Yes	No
PA-84-02	PA-**84**-02(0-6)-050813	N312001-**47**	5/8/2013	**0–6**	**Res 2**	Back yard soil	1100	Yes	No	No
PA-84-02	PA-84-02(0-6)-050813D	N312001-48	5/8/2013	0–6	Res 2	Back yard soil	740	Yes	No	No
PA-92-01	PA-**92**-01(0-6)-050813	N312001-**DU**	5/8/2013	**0–6**	**Res 2**	Back yard soil	880	Yes	Yes	No
PA-92-01	PA-92-01(6-12)-070913	N312001-52	7/9/2013	6–12	Res 2	Back yard soil	920	Yes	No	No
PA-92-01	PA-92-01(12-24)-070913	N312001-53	7/9/2013	12–24	Res 2	Back yard soil	1000	Yes	No	No
PA-92-02	PA-92-02(0-12)-050813	N312001-BN	5/8/2013	0–12	Res 2	Garden soil	400	Yes	No	No
PA-RR01,02	PA-RR01,02(0-6)-050613	N312001-BV	5/6/2013	**0–6**	**Railroad**	Composite	4000	Yes	Yes	Yes
PA-RR01,02	PA-RR01,02(6-24)-050613	N312001-BW	5/6/2013	6–24	Railroad	Composite	1700	Yes	Yes	No
PA-RR01,02	PA-RR01,02(6-24)-050613D	N312001-CU	5/6/2013	6–24	Railroad	Composite	1500	Yes	No	No
PA-RR04,06	PA-RR04,06(0-6)-050613	N312001-BX	5/6/2013	**0–6**	**Railroad**	Composite	11000	Yes	Yes	Yes
PA-RR04,06	PA-RR04,06(6-24)-050613	N312001-BY	5/6/2013	6–24	Railroad	Composite	1700	Yes	Yes	No
PA-RR07,08	PA-RR07,08(6-24)-050613	N312001-BU	5/6/2013	6–24	Railroad	Composite	5500	Yes	Yes	No
PA-RR07,08	PA-RR07,08(0-6)-050613	N312001-CV	5/6/2013	**0–6**	**Railroad**	Composite	6800	Yes	Yes	No
PA-RR10,12	PA-RR10,12(0-6)-050613	N312001-BR	5/6/2013	**0–6**	**Railroad**	Composite	1800	Yes	No	No
PA-RR10,12	PA-RR10,12(6-24)-050613	N312001-BT	5/6/2013	6–24	Railroad	Composite	2400	Yes	No	No

Table 1. LIST OF SAMPLES[a]
Additional Characterization of Lead in Soils
Pilsen Neighborhood, Chicago, Illinois

Location ID	Field Sample ID	Laboratory Information Management System (LIMS) No.	Sampling Date	Depth Interval (inches)	Sampling Area	Sample Description	Lead concentration (mg/kg)[b]	Elemental Results[b]	Lead Isotope Ratio Results	SEM/EDS Results
PA-RR11,13	PA-RR11,13(0-6)-050613	N312001-BQ	5/6/2013	**0–6**	**Railroad**	Composite	940	Yes	No	No
PA-RR11,13	PA-RR11,13(6-24)-050613	N312001-BS	5/6/2013	6–24	Railroad	Composite	1000	Yes	Yes	No
PA-RR14,15,16	PA-RR14,15,16(0-6)-050613	N312001-BP	5/6/2013	**0–6**	**Railroad**	Composite	1500	Yes	Yes	No
PA-RR14,15,16	PA-RR14,15,16(6-24)-050613	N312001-CG	5/6/2013	6–24	Railroad	Composite	2200	Yes	No	No
Perez	040001	N105006-12	1/03/11	n.a.[c]	Perez Elementary	TSP filter	1.09[d]	No	Yes	(NEIC 2011)
Perez	040016	N105006-11	4/2/10	n.a.[c]	Perez Elementary	TSP filter	1.40[d]	No	Yes	(NEIC 2011)
Perez	040041	N105006-13	8/30/10	n.a.[c]	Perez Elementary	TSP filter	0.90[d]	No	Yes	(NEIC 2011)
Perez	040058	N105006-10	12/10/10	n.a.[c]	Perez Elementary	TSP filter	1.53[d]	No	Yes	(NEIC 2011)

[a] Soil sampling areas were shown in colored text for easier differentiation; soil areas designated Res 1, Res 2, and Res 3 were defined in Canar et al. (2014) and EPA (2014b).
[b] Lead data for unsieved soil samples from STAT Analysis Corp by SW 846 6020 ICP-MS (EPA, 2014a and b) (milligrams per kilogram [mg/kg]).
[c] n.a. = not applicable.
[d] Data collected by the CCDEC and available from EPA (2011) (micrograms per cubic meter [µg/m^3]).

MICROSCOPY ANALYSIS

SEM with EDS was conducted in December 2013 and January, June, and July 2014 on 17 soil samples (Table 1). Two soil samples each were from the alley and railroad, four each were from the Res 1 and Res 2 areas, two were from the Res 3 area, and three soil samples were from the Harrison Park area.

The objective of the SEM analysis was to characterize the composition, morphology, and size of Pb-bearing particles and other distinctive particles in soil samples from the areas examined and selected by Pb concentration and location. Soil from the Harrison Park area was examined for comparison to soil with possible historical Pb contamination.

Soil samples were mounted onto 12-millimeter (mm) diameter, aluminum SEM specimen stubs via carbon adhesive tabs. Specimens were carbon-coated using a Denton Vacuum bench-top carbon evaporator.

Sample specimens were analyzed in accordance with the NEIC operating procedure *Scanning Electron Microscope Operation*, NEICPROC/00-072R5. A JEOL JSM-6460LV SEM with a Thermo Scientific energy dispersive X-ray spectrometer with a silicon drift detector and Noran System Seven (NSS version 3.0) software were used for analysis. The following instrument parameters were used: acceleration voltage was 20 kiloelectronvolts (keV), working distance was 10 mm, magnification was varied as needed, and the count acquisition time for spectra was 30 seconds. Both secondary electron imaging (SEI) and backscattered electron imaging (BEI) were used to document particle morphology, texture, and size. BEI was useful for locating Pb-bearing particles among particles of soil. In BEI, features having compositions of higher mean atomic number (Z) appear brighter. Because Pb has a much higher atomic number relative to most other elements typically found in soils, Pb-bearing particles may be distinguished from other particles in BEI. SEI as well as BEI produced images depicting the morphology, texture, and size of Pb-bearing particles. Energy dispersive spectra of X-ray emissions from analyzed particles were collected at selected spots to document elemental composition at those locations and, in some cases, from wider areas for comparison to adjacent material.

Soil mounts were systematically scanned in BEI mode to search for Pb-bearing particles and, along with SEI, to identify other particles with distinctive composition or morphology. Examination of each stub was concluded after documentation of approximately 10 to 24 particles. Pb-bearing particles and other distinctive particles were manually classified by composition and particle shape. Proper EDS calibration was verified daily with Al and cobalt (Co) standards in an SPI Supplies reference standard set.

LEAD ISOTOPE RATIO ANALYSIS

Pb isotopic analyses were conducted from summer 2013 to January 2014 at the USGS High Resolution MC-ICP-MS Laboratory in Denver, Colorado. Twelve soil samples from an alley south of the H. Kramer facility, 8 soil samples collected from the railroad tracks to the west of the H. Kramer facility, 36 residential soil samples, 3 Little Italy soil samples, 3 Harrison Park soil samples; 4 H. Kramer baghouse samples; and 4 TSP filters collected at Perez Elementary School were selected by Pb concentration and location and analyzed for Pb isotope compositions. Lead isotope ratio results of soil samples were compared to each other, and to the Pb isotope results of H. Kramer baghouse dust and TSP filters.

Sample Preparation and Separation

Approximately 0.2-gram aliquots of each sample were accurately weighed and digested in aqua-regia solution (2.5% nitric acid [HNO_3] and 7.5% hydrochloric acid [HCl]) at approximately 95 degrees Celsius (°C) for 1 hour. The digestates were filtered and diluted to 50 milliliters (mL) with 18.2 mega ohm (MΩ) resistivity water.

In order to measure Pb isotope composition with high precision and accuracy, Pb must be separated from the sample matrix and analyzed as a single element. Isolation of Pb from a matrix is achieved by processing samples through a column filled with a resin that uptakes Pb. The columns for Pb separation were prepared using Samco pipets (Cat #242, 8.5 centimeters [cm] x 2.5 mm, National Packaging Services, Inc., Secaucus, NJ, USA) with the tips cut off and fitted with Bel-Art porous frits (0.70-µm pore size, Bel-Art Products, Pequannock, NJ, USA). The columns were loaded using 0.25 mL of precleaned Eichrom Sr (Eichrom, Lisle, IL, USA) specific resin (Gale, 1996). The resin-loaded columns were rinsed using five 1-mL aliquots of Milli-Q™ water and conditioned using three 1-mL aliquots of 2M HCl (Seastar Chemicals, British Columbia, Canada). All chromatographic separation work was performed in Class 100 laminar flow hoods within a Class 1000 clean room. All samples were prepared to yield an adequate volume (10–20 mL) of solution with a final Pb concentration of 10 parts per billion (ppb) after column separation. Samples were reconstituted in 0.5-mL 2M HCl and loaded on the preconditioned Eichrom Sr specific resin. The loaded samples were allowed to absorb to the top of the resin bed before they were rinsed with two 0.5-mL aliquots of 2M HCl, followed by an additional two 1-mL 2M HCl aliquots to remove the matrix elements. Pb was removed from the column using eight 1-mL aliquots of 6M HCl. The eluted Pb fraction was collected in pre-cleaned Savillex® vials and evaporated to dryness. The dried Pb samples were reconstituted in 10–20-mL 2% HNO_3 and allowed to sit overnight prior to MC-ICP-MS analyses.

Method of Analysis

All Pb isotope analyses were conducted using a Nu Instruments HR®, double-focusing MC-ICP-MS. Soil- and baghouse-separated Pb samples were spiked with National Institute of

Standards and Technology (NIST) Standard Reference Material (SRM) 997 Thalium (Tl) isotope standard at the concentration equivalent to Pb (10 ppb) and introduced into the MC-ICP-MS using a desolvating nebulizer (Aridus II). The Perez TSP filters were sampled directly three times from three distinct areas on the filters using a New Wave 213 nanometer (nm) laser ablation system coupled to the MC-ICP-MS. The NIST SRM 997 Tl standard was introduced to the laser ablation sample stream through a laser ablation gas mixing chamber. Laser ablation analysis consisted of five minutes of data collection with a spot size of 55 μm, an energy density of 1.5 to 2.5 joules per cubic centimeter (J/cm^2), a laser scan rate of 10 μm per second, and laser power ranging from 50 to 55% at a frequency of 10 hertz (Hz). Prepared soil samples were analyzed using 30 cycles with 10-second integration per cycle, for a total duration of 5 minutes per Pb isotope measurement. A typical analysis procedure involved a 4–5 sample set bracketed by NIST SRM 981 Pb isotope standard. Mass bias was corrected using the exponential law (Ridley, 2005) using a $^{205}Tl/^{203}Tl$ value of 2.3875. Greater detail on the USGS MC-ICP-MS instrument configuration and mass bias correction for Pb isotopes is described by Pribil et al. (2014).

ELEMENTAL ANALYSIS

Results of elemental analysis performed by STAT Analysis Corp according to *Test Methods for Evaluating Solid Waste, Physical/Chemical Methods* (SW-846) were evaluated by NEIC for this report. Soil samples and H. Kramer baghouse dust were prepared according to EPA Method 3050B and analyzed in accordance with EPA Method 6020 using ICP-MS (EPA, 1996; EPA, 2007). The analytical results used in this study were reported for the total sample on a dry weight basis for Sb, Cd, Cr, Cu, Pb, Sn, and Zn (EPA, 2014a and b). Elemental results of the soils were compared with each other and with the results of H. Kramer baghouse dust.

Correlation Analysis

Log-log scatterplots were created, and correlation analysis was performed to evaluate relationships between Pb with other elements within sample sets. Similar evaluations have been conducted by others (USGS, 2003; Myers and Thorbjornsen, 2004; Thorbjornsen and Myers, 2006 and 2007a). Results of correlation analysis were given as the Spearman rank correlation coefficient, r_s, because a normal distribution of data in sample populations is not assumed for its application, and because it is a better indicator in the case of a non-linear relationship. An r_s is calculated by correlating rankings of the data values in data sets rather than correlating the data values themselves. The Spearman rank correlation coefficient is more robust than the Pearson product-moment correlation coefficient for the reasons stated above, and tends to minimize the effects of extreme values (outliers). An r_s indicates the strength or weakness of a relationship between the intensities or concentrations of a pair of elements. An r_s of unity (1), either positive or negative, indicates a perfect correlation, and an r_s of zero indicates that there is no evidence of a correlation. Weak correlations may be indicated by $|r_s| < 0.3$, moderate correlations by $0.3 < |r_s| < 0.7$, and strong correlations by $0.7 < |r_s| < 1$ (Gerstman, 2013; Laerd, 2013). Thus, an r_s of 0.90

indicates a relatively strong positive relationship, while an r_s of 0.40 indicates a considerably weaker relationship. The sign (+ or -) of the r_s indicates a positive or negative correlation between the parameters of a pair of elements, increasing for both in a positive monotonic relationship, and decreasing for one element while increasing for the other in a negative relationship.

For each r_s, a p-value was calculated. P-values are probabilities based, in part, on the number of data pairs, n, used in the correlation analysis. Typically, p-values less than a significance level set at $\alpha = 0.05$ suggest a high level of confidence that a statistically significant, non-zero correlation exists between the intensities or concentrations of a pair of elements. Both the r_s and p-value are used to evaluate the strength of association between two variables. Thus, a p-value of 0.0001 or less indicates a high level of confidence that the variables are correlated, and a p-value of 0.0500 or greater indicates a lower level of confidence. Both the r_s and the p-value are used to evaluate the strength of association between two variables (Miller and Miller, 1993; Good and Hardin, 2003).

ANALYTICAL RESULTS

The following analytical results are presented: (1) microscopy results of individual particles by SEM/EDS, (2) Pb isotope ratio measurements by MC-ICP-MS, (3) elemental analysis by ICP-MS (EPA, 2014a and b), and (4) metals composition of H. Kramer slag material (H. Kramer, 2014a). Analytical results of the soil areas (alley, railroad, Res 1, Res 2, Res 3, Harrison Park, and Little Italy); TSP filters; and H. Kramer baghouse dust and slag composition are evaluated, compared, and discussed.

MICROSCOPY RESULTS

A summary of SEM results is presented in **Table 2** for Pb-bearing and other distinctive particle types and for phase types in Pb-bearing particles with multi-phase assemblages or agglomerations. A count of single-phase particle types and Pb-bearing multi-phase particles is included in **Table 2**. Particle and phase types were based on the dominant elemental compositions observed. Particle morphologies generally ranged from very angular to sub-rounded. Particles with unique morphologies were also classified by the morphology exhibited. For example, spherical morphology of metal oxide particles in baghouse dust indicated those particles condensed from a high-temperature fume (Schwartz et al., 1955; Buckle and Pointon, 1976; EPA, 1977; Machemer, 2004; NEIC, 2011a and b, 2012). Documented particles ranged from sub-micrometer to 100s μm in diameter. Some particles exhibited distinct spherical cavities, typical of vesicles, holes formed in molten material by escaping gas bubbles and typical in slag material (van Oss, 2003). A phase, as referred to here, represented material with a predominant elemental composition based on EDS response. A multi-phase particle contained zones with different dominant elemental compositions, such as Fe-oxide or Si-oxide with a dominant Fe or Si EDS response, respectively. Multi-phase, angular particles, micrometer-scale and greater, are characteristic of slag material (CLEMEX, 2008; Pistorius and Kotzé, 2009; Perederly et al., 2012; Bernal et al., 2014; Piatak et al., 2014). The composition of non-ferrous slag is dominated by Fe and Si with lesser amounts of Al and Ca (Piatak et al., 2014). Slag from a brass and bronze foundry contains high Cu and Zn relative to Pb (EPA, 1995; Shen and Forssberg, 2003). Many spectra are presented at approximately full scale (0 to 14 keV) and at an expanded scale in the higher energy region (approximately 7 to 14 keV). Expanded scales allow the evaluation of relative spectral responses for Cu, Pb, and Zn in this higher energy region. In addition, expanded scales allow Pb and sulfur (S), which generally interfere with each other in the lower energy region around 2.3 keV, to be clearly distinguished because S does not have a response in the higher energy region.

Alley and Railroad Soils

Pb-bearing particles in alley and railroad soils typically occurred as single-phase particles, micrometer to hundreds of micrometers in scale (1s–100s μm), or as multi-phase

particles, 10s–100s μm in scale. Pb-oxide, Fe-oxide, Si-oxide, and Zn-oxide were common single-phase particle types (**Figures 5–9**). Cu and Zn were commonly associated with Pb-oxide particles, and Cu and Pb were commonly associated with Zn-oxide particles. Fe-oxide and Si-oxide particles typically exhibited greater spectral response for Zn than Pb. Less frequently observed were Sn-oxide and Cu-oxide particles that typically contained Pb and Zn (**Figures 7** and **10**, respectively) and Fe-sulfate and barium (Ba)-sulfate particles. Ca-oxide/carbonate particles exhibited a slight to no clear spectral response for Pb.

Micrometer-scale Zn-oxide particles (<10 μm) were less commonly observed (**Figure 6a**), although this may have been because they were more difficult to observe because of their relatively small size compared to the abundant and much larger Pb-bearing particles (10s–100s μm). The occurrence of micrometer-scale Zn-oxide particles with hexagonal crystal symmetry was also noted in railroad soils (**Figure 6b**). Micrometer-scale, Zn-oxide particles were consistent in size range and composition with baghouse dust from a brass and bronze foundry (**Figure 6c**), that also included spherical and hexagonal Zn-oxide particles (NEIC, 2011a, 2012).

The most common phases in the typically much larger multi-phase, Pb-bearing particles in alley and railroad soils were similar to those in the single-phase particles and included Pb-oxide, Fe-oxide, Si-oxide, and Zn-oxide. **Figure 11** shows a multi-phase, Pb-bearing particle in railroad soil containing Fe-oxide and Si-oxide phases. The composition of non-ferrous slag is dominated by Fe and Si (Piatak et al., 2014). Also similar to the single-phase particles, Cu and Zn were commonly associated with Pb-oxide phases, and Cu and Pb were commonly associated with Zn-oxide phases. Fe-oxide and Si-oxide phases typically exhibited greater spectral response for Zn than Pb. Less frequently observed were Cu-oxide and Sn-oxide phases; Ba-sulfate, Ca-oxide/carbonate, and carbon (C)-rich phases (**Figure 12**) were also present. Ca-oxide/carbonate phases typically exhibited a slight to no clear spectral response for Pb. **Figures 5b** and **12** show particles in railroad and alley soils with cavities consistent with vesicles, textures typical in slag material (van Oss, 2003).

The variety of Pb-bearing particles in alley and railroad soils described above was consistent with the composition of slag from a brass and bronze foundry because of the presence of Pb-bearing Cu-oxide, Sn-oxide, and Zn-oxide particles and because greater spectral responses for Cu and Zn relative to Pb were common in Fe-oxide and Si-oxide phases in particles typical of slag (**Table 2**). Multi-phase, angular particles, micrometer-scale and greater, are characteristic of slag material (CLEMEX, 2008; Pistorius and Kotzé, 2009; Perederly et al., 2012; Bernal et al., 2014; Piatak et al., 2014). Slag from a brass and bronze foundry contains high Cu and Zn relative to Pb (EPA, 1995; Shen and Forssberg, 2003).

Res 1 Soils

Lead-bearing particles in Res 1 soils typically occurred as single-phase particles, 1s–10s μm in scale, or as multi-phase particles, 10s–100s μm in scale. Pb-oxide, Fe-oxide, and Si-oxide

particles were common single-phase particle types. Fe-oxide particles typically exhibited greater spectral response for Zn than Pb. Other particle types included Fe-sulfate and Cu-oxide. **Figure 13** shows a Cu-oxide particle in Res 1 soils with ovoid and irregularly shaped cavities consistent with dissolution, a weathering process, and vesicles, textures typical in slag material (van Oss, 2003).

The most common phases in the typically much larger multi-phase, Pb-bearing particles in Res 1 soils were similar to those in the single-phase particles and included Pb-oxide, Fe-oxide, Fe-sulfate, Ba-sulfate, Ca-oxide/carbonate, Ca-phosphate, Si-oxide, and C-rich phases. **Figure 14** shows a multi-phase, Pb-bearing particle in Res 1 soil containing Fe-oxide and Si-oxide phases. Fe-oxide and Si-oxide phases typically exhibited greater spectral response for Zn than Pb, consistent with the composition of slag from a brass and bronze foundry because slag from a brass and bronze foundry contains high Cu and Zn relative to Pb (EPA, 1995; Shen and Forssberg, 2003).

Res 2 Soils

Lead-bearing particles in Res 2 soils typically occurred as single-phase particles, 1s–10s μm in scale, or as multi-phase particles, 10s–100s μm in scale. Pb-oxide and Fe-oxide particles were the common single-phase particle types observed. Fe-oxide particles typically exhibited greater spectral response for Zn than Pb. No single-phase Pb-bearing particle types were observed in two of the four Res 2 soils examined.

The most common phases in the typically much larger multi-phase, Pb-bearing particles in Res 2 soils were similar to those in the single-phase particles and included Pb-oxide, Fe-oxide, Fe-sulfate, Ba-sulfate, Ca-oxide/carbonate, Ca-phosphate, Si-oxide, and C-rich phases. **Figure 15** shows a multi-phase, Pb-bearing particle in Res 2 soil containing Fe-oxide and Si-oxide phases. Fe-oxide and Si-oxide phases typically exhibited greater spectral response for Zn than Pb, consistent with the composition of slag from a brass and bronze foundry because slag from a brass and bronze foundry contains high Cu and Zn relative to Pb (EPA, 1995; Shen and Forssberg, 2003).

Res 3 Soils

Lead-bearing particles in Res 3 soils typically occurred as single-phase particles, 1s–10s μm in scale, or as multi-phase particles, 10s–100s μm in scale. Pb-oxide, Fe-oxide, and Si-oxide particles were the common single-phase particle types observed.

The most common phases in the typically much larger multi-phase, Pb-bearing particles in Res 3 soils were similar to those in the single-phase particles and included Pb-oxide, Fe-oxide, Ba-sulfate, Ca-oxide/carbonate, and Si-oxide phases. **Figure 16** shows a multi-phase, Pb-bearing particle in Res 3 soil containing Si-oxide and Ca-oxide/carbonate phases. Si-oxide

phases typically exhibited much greater spectral response for Pb than Zn or Cu. Much greater spectral responses for Pb relative to Cu and Zn were not characteristic of slag composition from a brass and bronze foundry because slag from a brass and bronze foundry contains high Cu and Zn relative to Pb (EPA, 1995; Shen and Forssberg, 2003).

Harrison Park Soils

Pb-bearing particles in Harrison Park soils containing possible historical Pb contamination typically occurred as single-phase particles, 1s–10s μm in scale, or as multi-phase particles, 10s–100s μm in scale. Pb-oxide and Si-oxide were common single-phase particle types (**Figures 17** and **18**). **Figure 18** shows a particle of Harrison Park soil with pitted surface consistent with dissolution, a weathering process, and vesicles, textures typical in slag material (van Oss, 2003).

However, unlike in the alley and railroad soils, Cu and Zn were less commonly associated with Pb-oxide particles and exhibited much lower spectral responses when observed. Furthermore, although Cu, Pb, and Zn were found associated with Si-oxide particles, Pb typically exhibited a much greater spectral response than Cu and Zn. Pb-bearing, multi-phase particles were also found in Harrison Park soils containing Fe-oxide and Ca-oxide/carbonate (**Figure 19**). Si-oxide was also observed in Pb-bearing, multi-phase particles in Harrison Park soils. The variety of Pb-bearing particles in Harrison Park soils described above was not characteristic of slag composition from a brass and bronze foundry because Pb-bearing Cu-oxide, Sn-oxide, and Zn-oxide particles were not observed and because much greater spectral responses for Pb relative to Cu and Zn were common in particles typical of slag. Slag from a brass and bronze foundry contains high Cu and Zn relative to Pb (EPA, 1995; Shen and Forssberg, 2003).

Synopsis of SEM Results

The micrometer-scale Zn-oxide particles found in railroad soil were consistent with bag-house dust from a brass and bronze foundry (**Figures 6a and c**). In particular, the spherical morphology of micrometer-scale Zn-oxide particles noted in railroad soil was indicative of condensation from a high-temperature fume (Schwartz et al., 1955; Buckle and Pointon, 1976; EPA, 1977; Machemer, 2004; NEIC, 2011a and b, 2012), the process in which baghouse dust is formed. Hexagonal crystal symmetry associated with Zn-oxide particles was also noted in railroad soil (**Figure 6b**), consistent with zincite (ZnO), which may exhibit a hexagonal structure (Mindat, 2011; Webmineral, 2011). In addition to micrometer-scale Zn-oxide particles with crystallite morphology, spherical and hexagonal Zn-oxide particles were also observed in H. Kramer baghouse dust (NEIC, 2011a, 2012). However, in comparison to micrometer-scale Zn-oxide particles in baghouse dust, micrometer-scale Zn-oxide particles found in railroad soil typically appeared to have undergone dissolution weathering because of dissolution textures and general lack of crystallite morphology that indicated exposure to moisture, a process baghouse

dust is not expected to encounter. Dissolution of Zn-oxide particles may be expected as a result of exposure to moisture (Cernik et al., 1995; Wilcke and Kaupenjohann, 1998; Manceau et al., 2000; Voegelin et al., 2005).

Of likely greater importance were the variety and abundance of larger Pb-bearing particles (10s–100s μm) in alley, railroad, Res 1, and Res 2 soils that contained Fe, Pb, Si, and Zn-oxides and/or Ca-oxide/carbonates (**Figures 7–15**). These particles were abundant, consistently angular, frequently multi-phase in composition, and occurred sporadically with vesicular textures. These multi-phase, micrometer-scale and greater, angular particles were characteristic of slag material (CLEMEX, 2008; Pistorius and Kotzé, 2009; Perederly et al., 2012; Bernal et al., 2014; Piatak et al., 2014). Because Cu and Zn were commonly associated with Pb-oxide particles and Zn exhibited relatively high spectral responses relative to Pb in non-Pb-oxide phases, these particles were consistent with the composition of brass and bronze foundry slag (EPA, 1995; Shen and Forssberg, 2003). High Cu and Zn relative to Pb were typical in copper and brass smelting slags. Thus, the predominant morphology, size, and composition of Pb-bearing particles in the soils of the alley, railroad, Res 1, and Res 2 areas were consistent with brass and bronze foundry slag.

Furthermore, the presence of Pb-oxide, Cu-oxide, Sn-oxide, and Zn-oxide particles in both alley and railroad soils (**Figures 5a, 7, and 10**, respectively) was also consistent with the composition of slag from a brass and bronze foundry (EPA, 1995; Shen and Forssberg, 2003). Pb-oxide particles in railroad soil were found with vesicles (**Figure 5b**), textures typical in slag material (van Oss, 2003). Pb-oxide is also a primary raw material for Pb alloying in brass and bronze products (H. Kramer, 2011; Omenazu, 2011). Sn-oxide and Cu-oxide particles were also observed in H. Kramer baghouse dust (NEIC, 2011a, 2012).

Slag material was observed in one railroad and eight alley soil borings (EPA, 2014a), including two soil locations (alley AY-18, railroad RR-02) with soil examined by SEM/EDS in this study. Slag originates from industrial processes such as smelting (primary or secondary) and is not consistent with coal fly ash, leaded paint, leaded gasoline, automobile battery lead, or tire dust (Friedlander, 1973; Hurst et al., 1996; Calvert, 2004; Lee and von Lehmden, 2012; Kaster, 2014).

Although Fe, Pb, and Si-oxides and Ca-oxide/carbonates in similar sized, angular Pb-bearing particles (10s–100s μm) were common in Res 3 soils (**Figure 16**) and in Harrison Park soils (**Figures 17–19**) that represented possible historical Pb contamination, Cu and Zn were less commonly associated with Pb-oxide particles and exhibited much lower spectral responses relative to Pb in non-Pb phases, such as Si-oxide, compared to alley and railroad soils. These relative elemental responses in Pb-bearing particles in the Harrison Park and Res 3 soils were dissimilar to those in Pb-bearing particles in the alley and railroad soils and were not characteristic of slag composition from a brass and bronze foundry (EPA, 1995; Shen and Forssberg, 2003). High Cu and Zn relative to Pb were typical in copper and brass smelting slags.

Comparison of relative spectral responses of Cu, Pb, and Zn in typical Pb-bearing, multi-phase particles in soils from the alley, railroad, Res 1, Res 2, Res 3, and Harrison Park areas appears in the "Discussion" section (**Figures 34a–f**).

Table 2. SUMMARY OF SEM DATA COLLECTED FROM SOIL SAMPLES
Additional Characterization of Lead in Soils
Pilsen Neighborhood, Chicago, Illinois

Sampling Site	Field Sample Number (LIMS Number)	Pb Concentration[a] (mg/kg)	Particle count of Pb-bearing and other distinctive particle types with single phase[b] (recurring concomitant elements)	Multi-phase Pb-bearing particle count	Phase types in Pb-bearing particles with multiple phases[b,c] (recurring concomitant elements)
Railroad	PA-**RR04,06** (0-6) (N312001-**BX**)	11000	15 **Pb-oxide** (Al, Ca, Cu, Fe, P, Si, Zn) 1 **Ca-oxide/carbonate** (Cu, **Zn>Pb**) 1 **Zn-oxide**, 10s–100s μm (Al, Ca, Cu, Fe, P, **Pb**, Si) 4 **Zn-oxide**, μm-scale (Ca, Cu, Fe. P, **Pb**, Si)[d] 1 Spherical **Zn-oxide** (Ca, Cu, Fe, **Pb**)[d] 1 Hexagonal **Zn-oxide** crystallite[d]	5	**Pb-oxide** (Cu, Zn) **Fe-oxide** (Al, Ca, Cu, P, **Pb**, Si, Zn) **Ca-oxide/carbonate** (Cu, Fe, Mg, Si, Zn) **Zn-oxide** (Al, Ca, Cu, Fe, P, **Pb**, Si) **Cu-oxide** (Al, Ca, Fe, Si; **Zn>Pb**) **C-rich** (Al, Ca, Cu, Fe, Si, Zn)
Railroad	PA-**RR01,02** (0-6) (N312001-**BV**)	4000	2 **Pb-oxide** (Ca, Cu, Fe, P, Si, Zn) 6 **Fe-oxide** (Al, Ca, Cu, Si, Sn; **Zn>Pb**) 2 **Ca-oxide/carbonate** (Al, Cu, Fe, Mg, Si, Zn) 3 **Sn-oxide** (Al, Ca, Cu, Fe, **Pb**, Si, Zn) 2 **Si-oxide** (Al, Ca, Cu, Fe, Mn; **Zn>Pb**) 1 Spherical **Fe-oxide** (Al, Ca, Cu, **Pb**, Si, Zn) 1 Pseudo-hexagonal **Fe-oxide** crystallite	11	**Pb-oxide** (Ca, Cu, Fe, Si, Zn) **Fe-oxide** (Al, Ca, Cu, Si, Sn; **Zn>Pb**) **Ca-oxide/carbonate** (Al, Cu, Fe, Mg, Si, Zn) **Sn-oxide** (Ca, Cu, Fe, **Pb**, Si, Zn) **Si-oxide** (Al, Ca, Cu, Fe, Mn, P; **Zn>Pb**) **Zn-oxide** (Al, Ca, Cu, Fe, **Pb**, Si) **C-rich** (Ca, Cu, Fe, Si, Zn)
Alley	PA-**AY18** (6-12) (N312001-**03**)	3400	10 **Fe-oxide** (Al, Ca, Cu, Si; **Zn>Pb**) 1 **Ba-sulfate** (Al, Ca, Cu, Fe, Si, Zn) 1 **Ca-oxide/carbonate** (Al, Fe, Si, **Cu, Zn>Pb**) 4 **Si-oxide** (Al, Ca, Cu, Fe, Mg, Mn; **Zn>Pb**) 5 **Cu-oxide** (Al, Ca, Fe, Si; **Zn>Pb**) 1 **Zn-oxide** (Al, Ca, Cu, Fe, **Pb**, Si) 1 Spherical **Fe-oxide** (Al, Ca, Cu, Si, Zn) 1 Spherical **Si-oxide** (Al, Ca, Cu, Fe, Zn)	5	**Fe-oxide** (Al, Ca, Cu, Si; **Zn>Pb**) **Sn-oxide** (Ca, Cu, Fe, **Pb**, Si, Zn) **Si-oxide** (Al, Ca, Cu, Fe, K, Mg; **Zn>Pb**) **Cu-oxide** (Al, Ca, Fe, Si; **Zn>Pb**) **Zn-oxide** (Al, Ca, Cu, Fe, Si) **C-rich** (Al, Si)
Alley	PA-**AC07** (0-6) (N312001-**01**)	940	2 **Pb-oxide** (Al, Ca, Cu, Fe, Mg, P, Si, Zn) 11 **Fe-oxide** (Al, Ca, Mg, P, Si; **Cu, Zn>Pb**) 2 **Fe-sulfate** (Al, Ca, Si; **Cu, Zn>Pb**) 1 **Ba-sulfate** (Al, Ca, Cu, Mg, Si, Zn) 1 **Ca-oxide/carbonate** (Al, Mg, Si) 1 **Si-oxide** (Al, Ca, Fe, K, Ti; **Cu, Zn>Pb**) 1 **Sn-oxide** (Cu, Si) 1 **Zn-oxide** (Al, Ca, Cu, Fe, **Pb**, Si)	6	**Fe-oxide** (Al, Ca, K, Mg, P, S, Si; **Cu, Zn>Pb**) **Ba-sulfate** **Ca-oxide/carbonate** (Al, Cu, Fe, Mg, S, Si, Zn) **Si-oxide** (Al, Ca, Fe, K, Mg; **Cu, Zn>Pb**) **C-rich** (Al, Ca, Cu, S, Si, Zn)
Res 1	**122**-01 (0-6) (N312001-**14**)	1900	2 **Pb-oxide** (Al, Ba, Ca, Cu, Fe, P, S, Si, Zn) 1 **Si-oxide** (Al, Ca, Cu, Fe, K, Mg; **Zn>Pb**)	9	**Pb-oxide** (Al, Ca, Cu, Fe, P, Si, Zn) **Fe-oxide** (Al, Ca, Cu, K, Si, Ti; **Zn>Pb**) **Ba-sulfate** (Al, Ca, Cu, **Pb**, Si, Zn) **Si-oxide** (Al, Ca, Cu, Fe, K, Mg; P, **Zn>Pb**)
Res 1	**127**-01 (0-6) (N312001-**CY**)	2500	2 **Pb-oxide** (Al, Ca, Cu, Fe, K, Mg, Mn, P, S, Si, Ti, Zn) 4 **Fe-oxide** (Al, Ca, Cu, P, Si; **Zn>Pb**) 1 **Fe-sulfate** (Al, Ca, Cu, Si; **Zn>Pb**) 5 **Si-oxide** (Al, Ca, Cu, Fe, K, Mg, Ti, P; **Zn>Pb**)	12	**Pb-oxide** (Al, Ca, Cu, Fe, P, Si, Zn) **Fe-oxide** (Al, Ca, Cu, K, Mg, Mn, P, S, Si; **Zn>Pb**) **Fe-sulfate** (Al, Ca, Cu, Si; **Zn>Pb**) **Ca-oxide/carbonate** (Al, Cu, Fe, Mg, P, Si; **Zn>Pb**) **Si-oxide** (Al, Ca, Cu, Fe, K, Mg, P, Ti; **Zn>Pb**)
Res 1	**272**-01 (0-6) (N312001-**DD**)	2000	2 **Pb-oxide** (Al, Ca, Cu, Fe, P, Si, Zn) 4 **Fe-oxide** (Al, Ca, Cu, P, Si; **Zn>Pb**) 3 **Si-oxide** (Al, Ca, Cu, Fe, K, Mg, Mn, P, TI; **Zn>Pb**) 1 **Cu-oxide** (Al, Ca, Fe, Si; **Zn>Pb**)	3	**Fe-oxide** (Al, Ca, Cu, K, Mg, Mn, P, Si; **Zn>Pb**) **Si-oxide** (Al, Ca, Cu, Fe, K, Mg, Mn, P, Ti; **Zn>Pb**)
Res 1	**274**-01 (0-6) (N312001-**DE**)	1900	1 **Pb-oxide** (Al, Ca, Cu, Fe, P, Si, Zn) 2 **Fe-oxide** (Al, Ca, Cu, P, Si; **Zn>Pb**)	7	**Fe-oxide** (Al, Ca, Cu, P, Si; **Zn>Pb**) **Ca-phosphate** (Al, Cu, Fe, Si; **Zn>Pb**) **Si-oxide** (Al, Ca, Cu, Fe, K, Mn, P; **Zn>Pb**) **C-rich** (Al, Cu, Fe, Si, Zn)

Table 2. SUMMARY OF SEM DATA COLLECTED FROM SOIL SAMPLES
Additional Characterization of Lead in Soils
Pilsen Neighborhood, Chicago, Illinois

Sampling Site	Field Sample Number (LIMS Number)	Pb Concentration[a] (mg/kg)	Particle count of Pb-bearing and other distinctive particle types with single phase[b] (recurring concomitant elements)	Multi-phase Pb-bearing particle count	Phase types in Pb-bearing particles with multiple phases[b,c] (recurring concomitant elements)
Res 2	**104**-02 (0-6) (N312001-**CW**)	1400	Not observed	10	**Pb-oxide** (Al, Ca, Fe, P, Si, Zn) **Fe-oxide** (Al, Ca, Cu, K, P, **Pb**, Si, Zn) **Fe-sulfate** (Al, Ca, Cu, K, **Pb**, Si, Zn) **Ca-oxide/carbonate** (Al, Fe, K, Mg, Si, Zn) **Ca-phosphate** (Al, Cu, Fe, K, S, Si, Ti; **Zn>Pb**) **Si-oxide** (Al, Ca, Cu, Fe, K, Mg, Ti; **Zn>Pb**)
Res 2	**125**-01 (0-6) (N312001-**CC**)	1500	Not observed	12	**Fe-oxide** (Al, Ca, Cu, K, Mn, P, Si; **Zn>Pb**) **Ba-sulfate** **Ca-phosphate** (Al, Cu, Fe, K, Si; **Zn>Pb**) **Si-oxide** (Al, Ca, Cu, Fe, K, Mg, Mn; **Zn>Pb**) **C-rich** (Al, Ca, Cu, Fe, P, Si, Zn)
Res 2	**141**-02 (0-6) (N312001-**CI**)	1600	2 **Pb-oxide** (Al, Ca, Cu, Fe, K, P, Si, Zn) 2 **Fe-oxide** (Al, Ca, Cu, P, **Pb**, Si, Zn)	7	**Pb-oxide** (Al, Ca, Cu, Fe, P, Si, Zn) **Fe-oxide** (Al, Ca, Cr, Cu K, Mg, P, **Pb**, S, Si, Zn) **Ca-oxide/carbonate** (Mg) **Si-oxide** (Al, Ca, Cu, Fe, K, Mn; **Zn>Pb**)
Res 2	**371**-01 (0-6) (N312001-**DO**)	1800	2 **Pb-oxide** (Al, Ca, Cu, Fe, P, Si, Zn) 4 **Fe-oxide** (Al, Ca, Cu, P, Si; **Zn>Pb**)	8	**Fe-oxide** (Al, Ca, Cu, K, P, **Pb**, Si, Zn) **Fe-sulfate** (Al, Ca, Cu, K, P, Si; **Zn>Pb**) **Ca-phosphate** (Al, Cu, Fe, Si; **Zn>Pb**) **Si-oxide** (Al, Ca, Cu, Fe, K, Mg, **Pb**, Zn)
Res 3	**510**-01 (0-6) (N312001-**AU**)	1700	3 **Pb-oxide** (Al, Ca, Cu, Fe, Si) 1 **Fe-oxide** (Al, Ca, Cu, P, **Pb**, Si, Zn) 5 **Si-oxide** (Al, Ca, Fe, K, P; **Pb>>Cu, Zn**)	3	**Pb-oxide** (Al, Ca, Cu, Fe, P, Si, Zn) **Fe-oxide** (Al, Ca, Cu, P, **Pb**, Si, Zn) **Ba-sulfate** **Ca-oxide/carbonate** (Al, Fe, K, Si) **Si-oxide** (Al, Ca, Cl, Fe, K, Mg, P; **Pb>>Cu, Zn**)
Res 3	**515**-01 (0-6) (N312001-**75**)	1600	9 **Pb-oxide** (Al, Ca, Cl, Cu, Fe, P, Si, Zn) 2 **Fe-oxide** (Al, Ca, Cu, P, **Pb**, Si, Zn)	3	**Pb-oxide** (Al, Ca, Cu, Fe, P, Si, Zn) **Si-oxide** (Al, Ca, Fe, K, P; **Pb>>Cu, Zn**)
Harrison Park[e]	**480**-01 (0-6) (N312001-**99**)	3200	10 **Pb-oxide** (Al, Ca, Cu, Fe, K, P, Si, Zn) 1 **Ca-oxide/carbonate** (Al, Fe, Mg, P, **Pb**, Si, Zn) 9 **Si-oxide** (Al, Ca, Fe, K, Mg, Na, P, Ti; **Pb>>Cu, Zn**) 2 **C-rich** (Al, Ca, P, **Pb**, Si) 1 Spherical **Fe-oxide** (Al, Ca, K, Si) 1 Spherical **Si-oxide** (Al, Fe, K)	3	**Fe-oxide** (Al, Ca, K, **Pb**, Si, Zn) **Ca-oxide/carbonate** (Al, Fe, Mg, Si) **Si-oxide** (Al, Ca, Fe, K, Mg, Mn, P; **Pb>>Zn**)
Harrison Park[e]	**474**-01 (0-6) (N312001-**22**)	2600	2 **Pb-oxide** (Al, Ca, Cu, Fe, Si, V) 3 **Fe-oxide** (Al, Ca, Cu, P, **Pb**, S, Si, Zn) 2 **Si-oxide** (Al, Ca, Fe, K, Mg, P, Ti; **Pb>>Cu, Zn**)	5	**Fe-oxide** (Al, Ca, P, **Pb**, Si, Zn) **Ca-oxide/carbonate** (Al, Cu, Fe, Mg, P, Si, Ti; **Pb>Cu, Zn**) **Si-oxide** (Al, Fe) **C-rich** (Al, Ca, S, Si)
Harrison Park[e]	**475**-01 (0-6) (N312001-**24**)	3700	8 **Pb-oxide** (Al, Ca, Cl, Cu, Fe, K, P, Si, Zn) 4 **Si-oxide** (Al, Ca, Cl, Fe, K, Mg, P, Ti; **Pb>>Cu, Zn**)	1	**Pb-oxide** (Al, Ca, Cu, Fe, P, Si, Zn) **Si-oxide** (Al, Ca, Fe, K, Mg)

[a] Lead data for unsieved soil samples from STAT Analysis Corp (EPA, 2014a and b).
[b] For distinction and contrast, Cu>Pb, Zn>Pb, etc. is in red text, and Pb>Cu, Pb>Zn, etc. is in blue text. Cu-, Sn-, and Zn- oxide particles (in red text) and Pb-oxide particles were consistent with composition of brass and bronze foundry slag. Pb-oxide was also a primary raw material for Pb alloying in brass and bronze products. See text for details.
[c] Pb-bearing particles (angular, 10s–100s µm) with multiple phases were typical of slag.
[d] Consistent with baghouse dust from brass and bronze foundry (black text).
[e] Soil with possible historical Pb contamination.

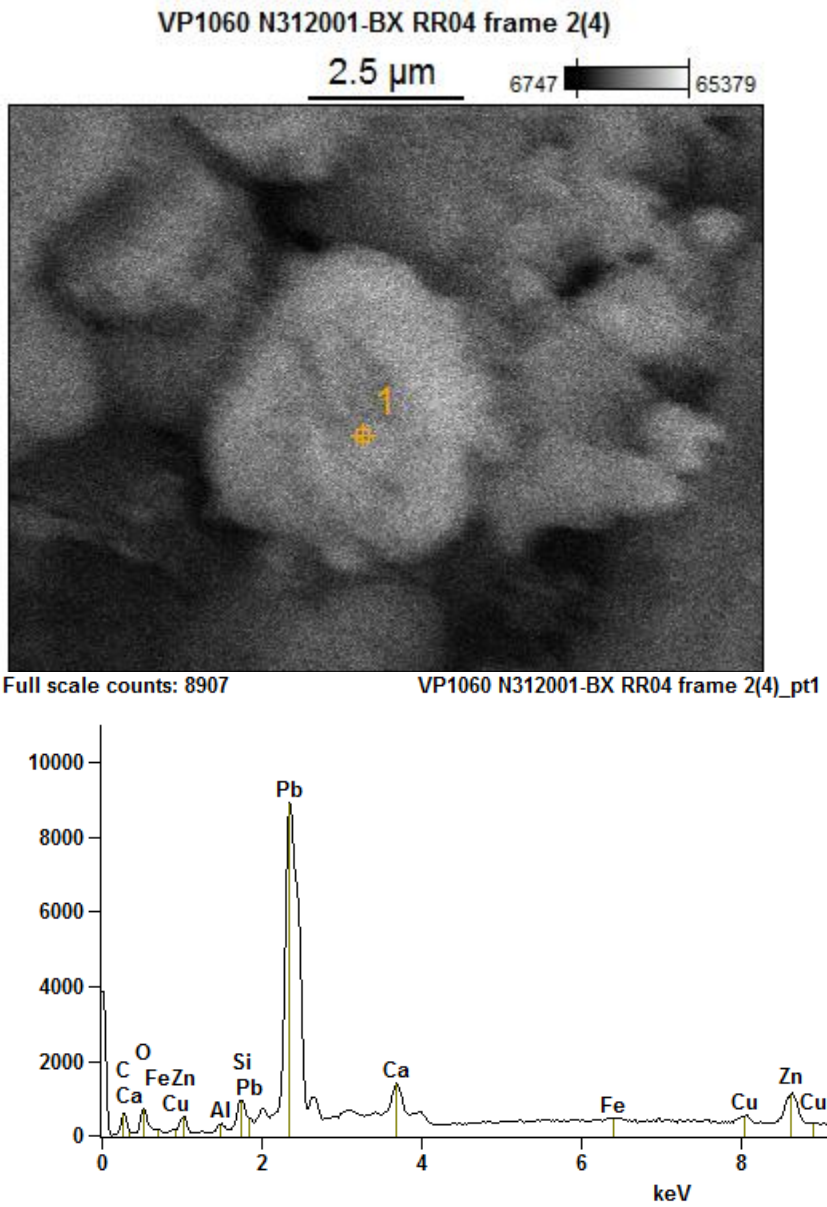

Figure 5a. Micrometer-scale Pb-oxide particle in soil from the railroad (N312001-BX). Note spectral responses for Cu and Zn.

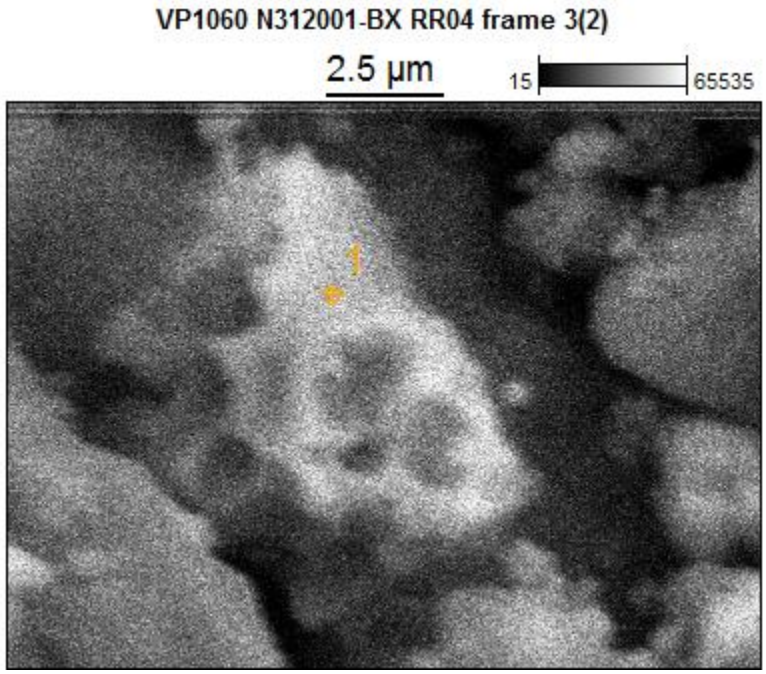

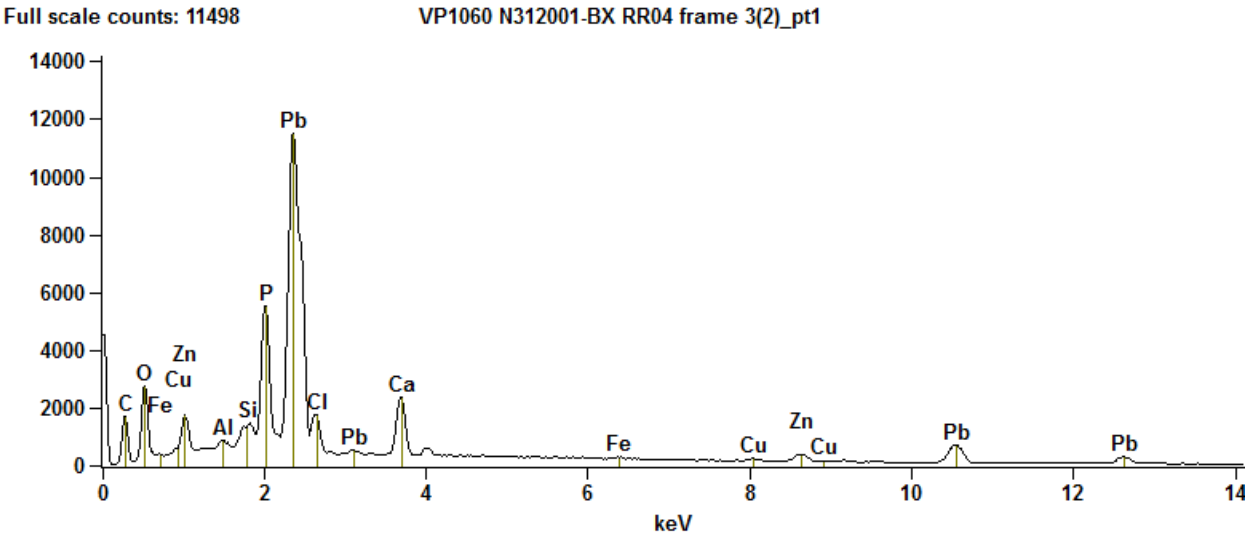

Figure 5b. Micrometer-scale Pb-oxide particle in soil from the railroad (N312001-BX). Pitted surface consistent with dissolution, and distinct spherical cavities consistent with vesicles, typical in slag material.

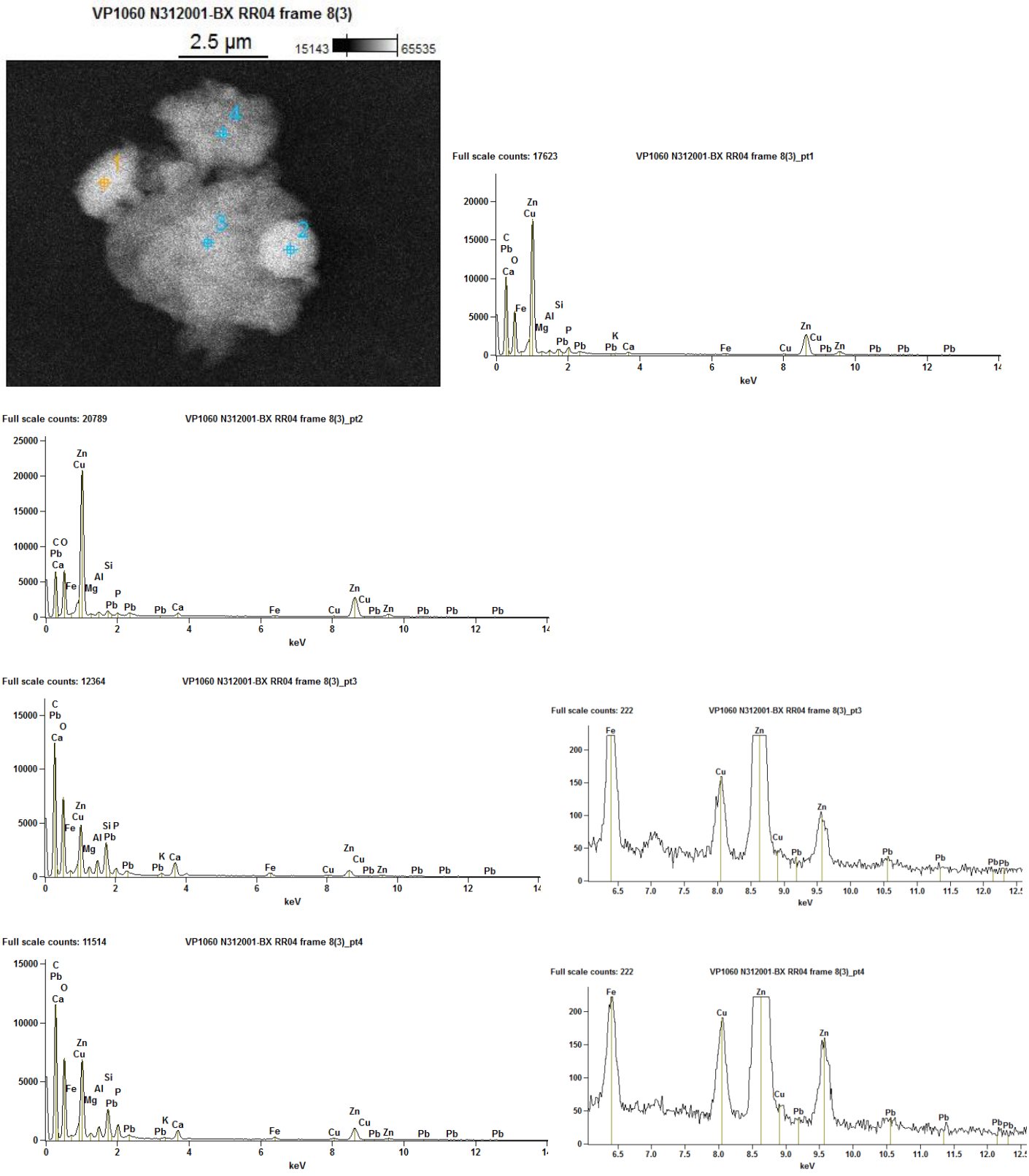

Figure 6a. Micrometer-scale Zn-oxide particles in soil from the railroad were consistent with baghouse dust from a brass and bronze foundry (NEIC, 2011a, 2012). Note spherical Zn-oxide particle (pt2) (N312001-BX).

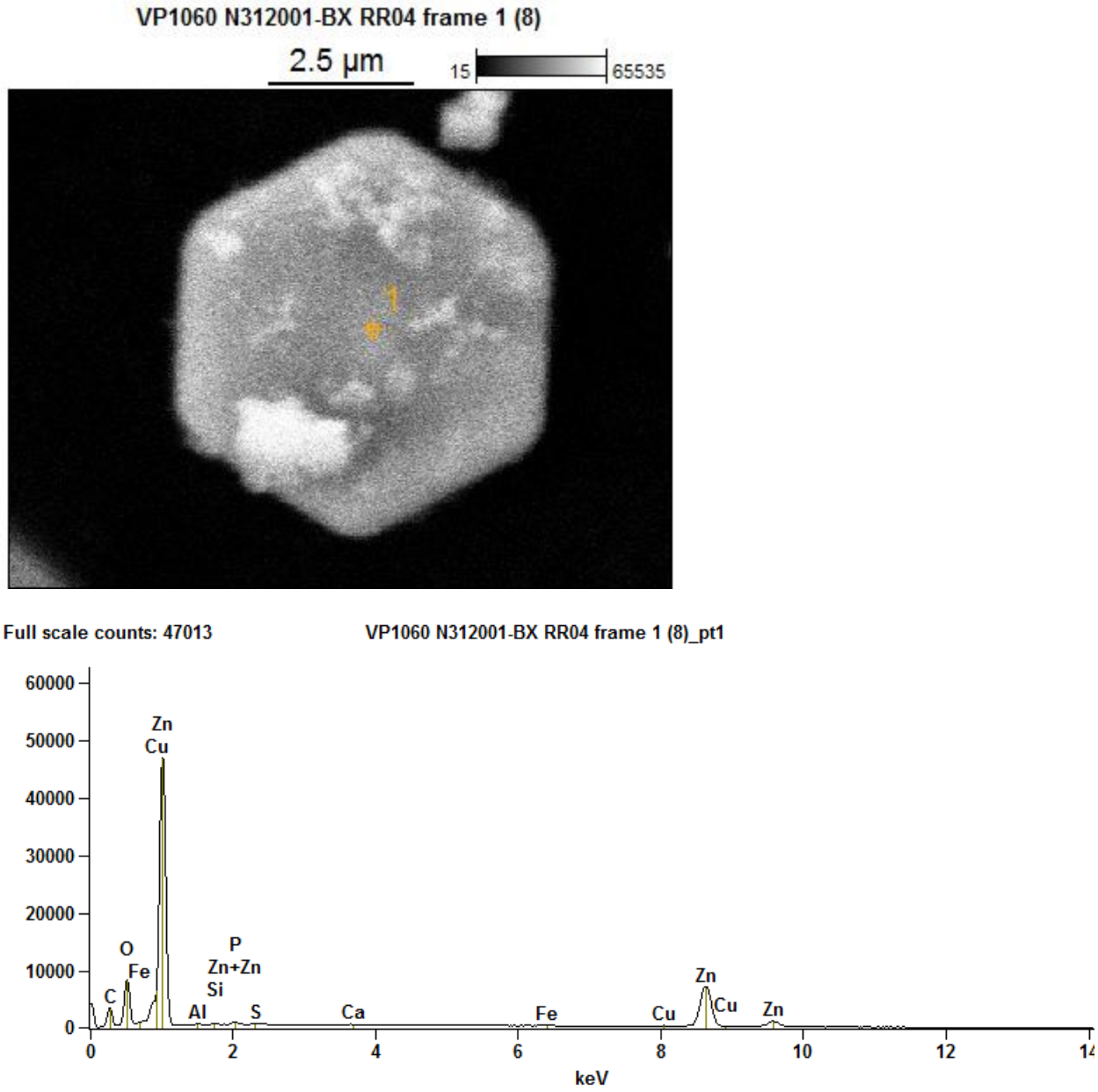

Figure 6b. Micrometer-scale Zn-oxide particle with hexagonal crystal symmetry in soil from the railroad (N312001-BX), consistent with baghouse dust from a brass and bronze foundry (NEIC, 2011a, 2012).

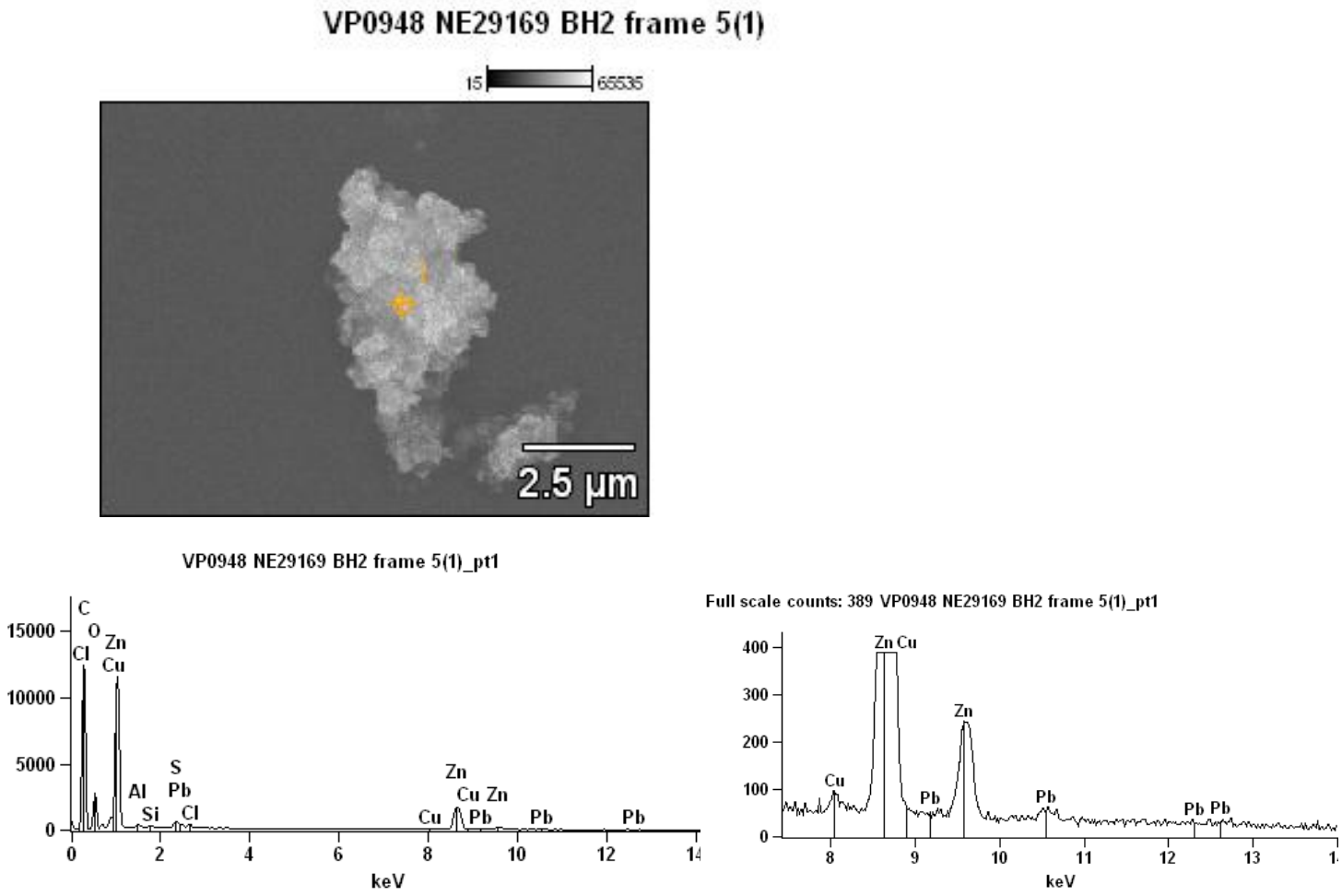

Figure 6c. SEI image of micrometer-scale aggregate of angular Zn-oxide crystallites with trace amounts of lead in dust from H. Kramer's baghouse 2 (N105006-06) (from NEIC, 2011b).

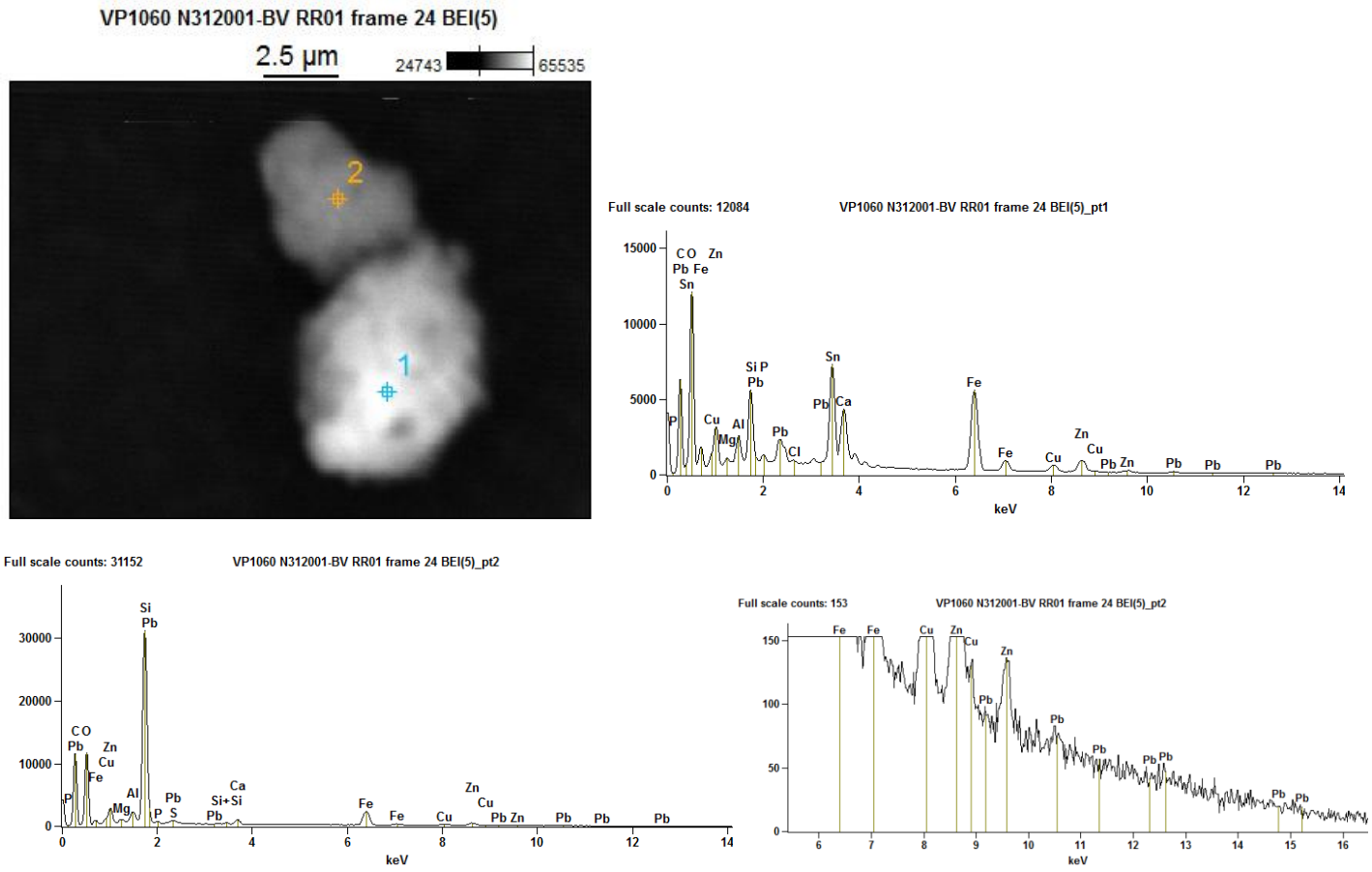

Figure 7. Micrometer-scale Sn-oxide particle (pt1) and Si-oxide particle (pt2; Zn>Pb) in soil from the railroad (N312001-BV). Relative spectral responses for Pb and Zn were consistent with composition of slag from brass and bronze foundry (EPA, 1995; Shen and Forssberg, 2003).

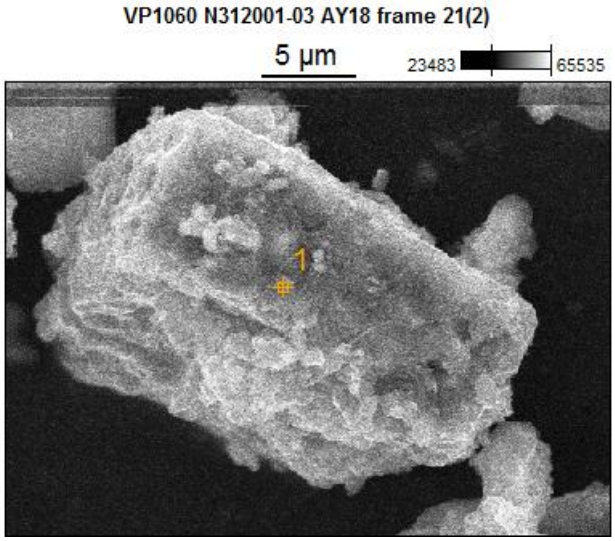

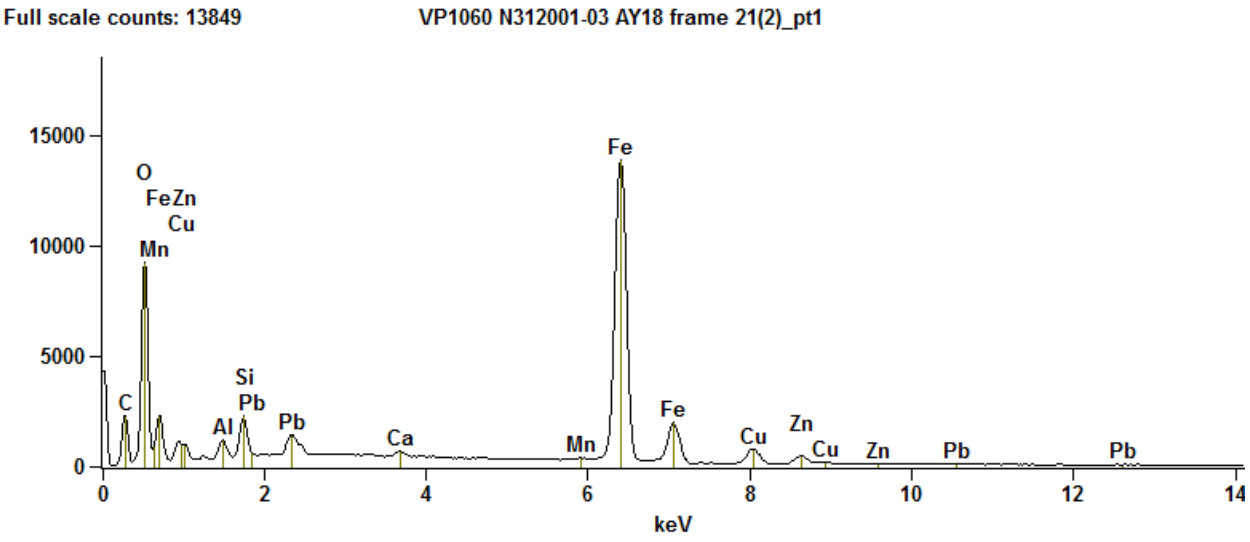

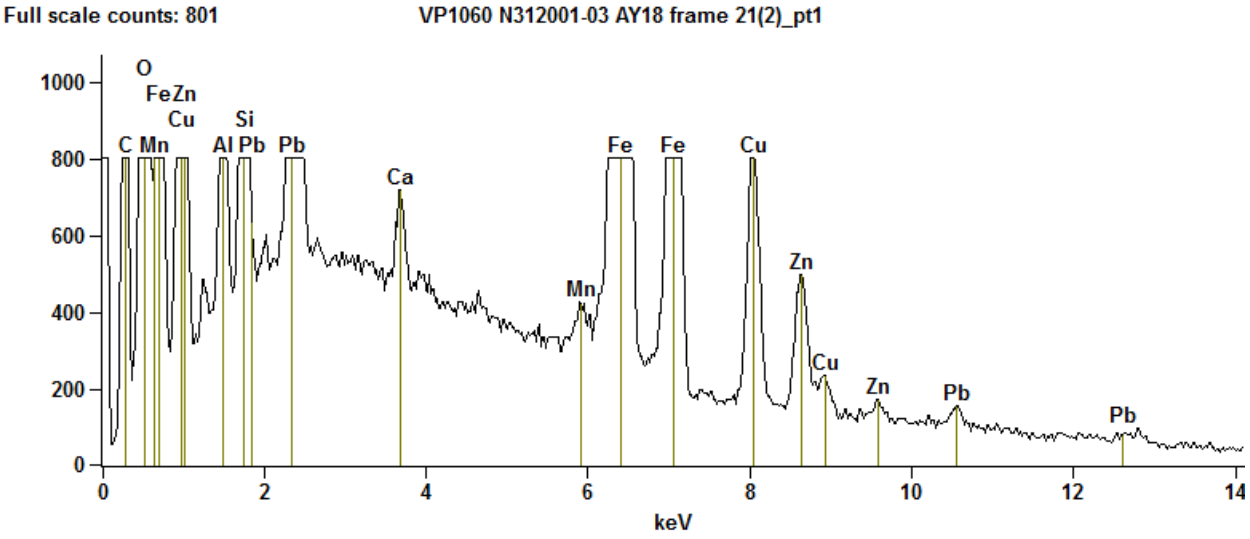

Figure 8. Angular Fe-oxide particle (10s µm; Cu>>Pb, Zn>Pb) in soil from the alley (N312001-03). Relative spectral responses for Cu, Pb, and Zn were consistent with composition of slag from brass and bronze foundry (EPA, 1995; Shen and Forssberg, 2003).

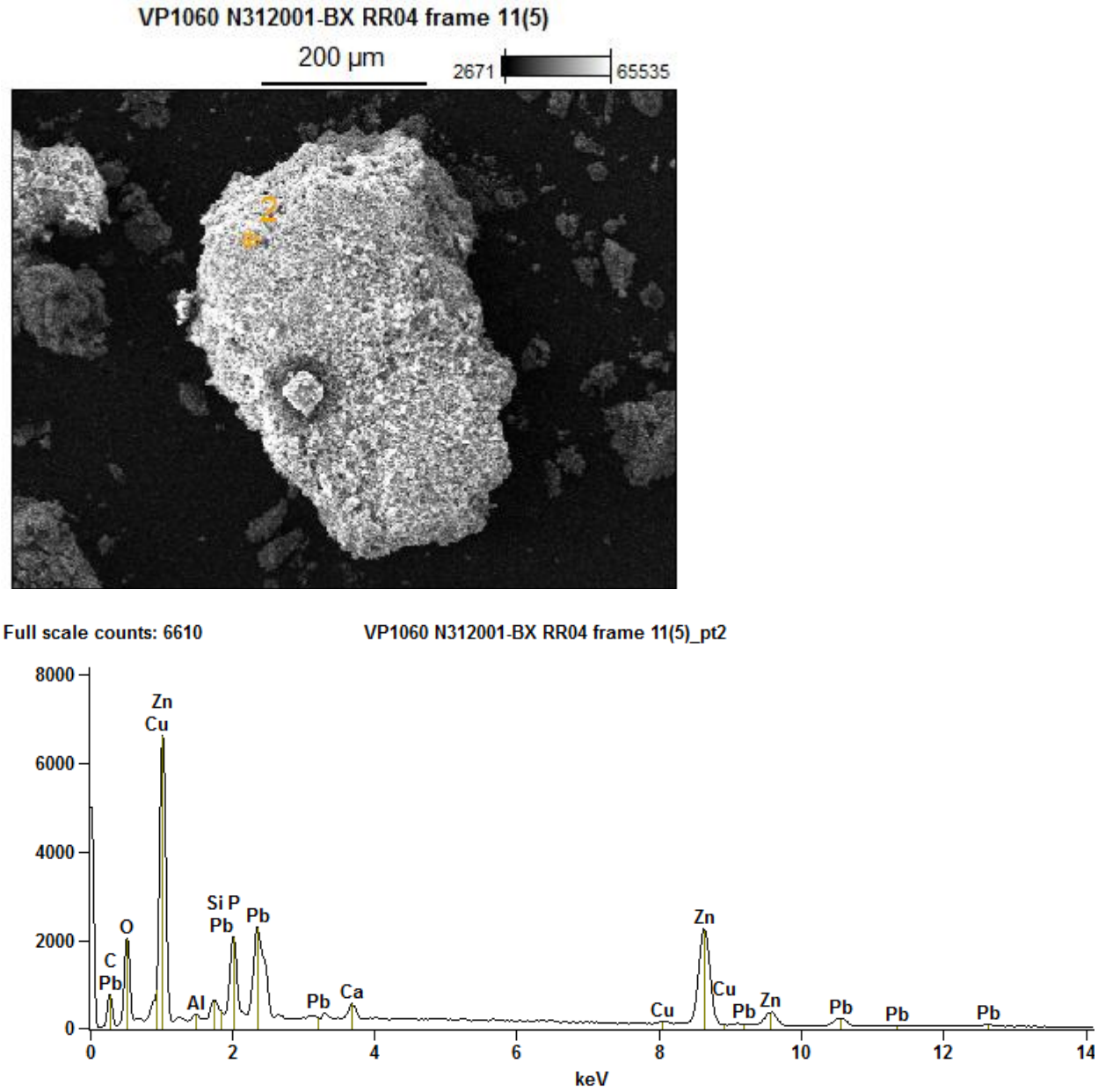

Figure 9. Sub-angular Zn-oxide particle (100s µm, Zn>>Pb) in soil from the railroad (N312001-BX). Relative spectral responses for Pb and Zn were consistent with composition of slag from brass and bronze foundry (EPA, 1995; Shen and Forssberg, 2003).

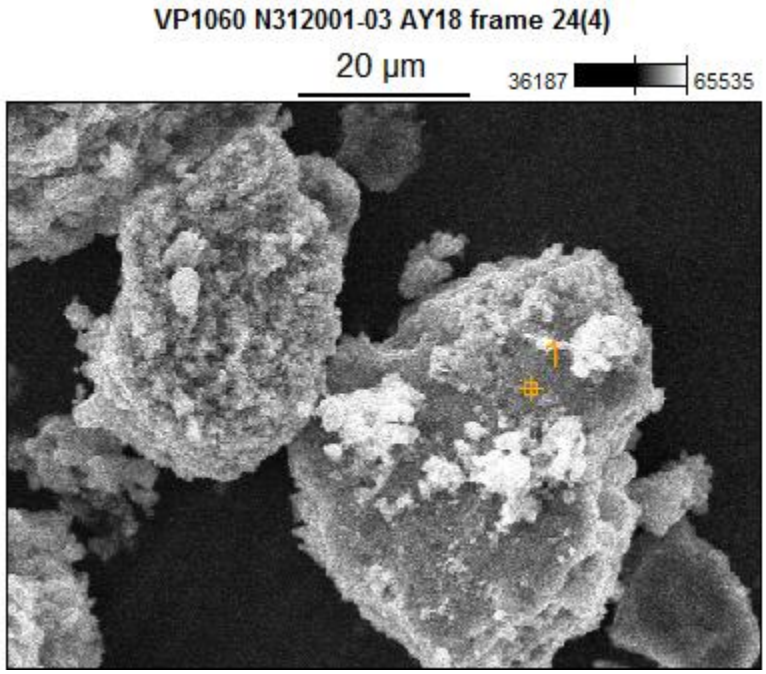

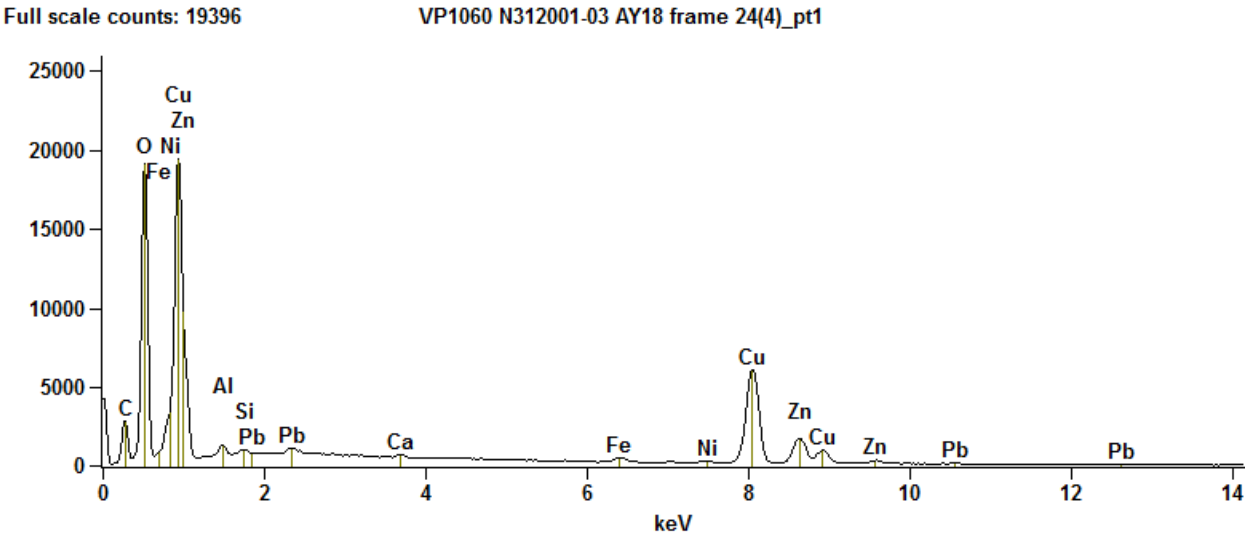

Figure 10. Sub-angular Cu-oxide particle (10s µm; Cu>>Pb, Zn>Pb) in soil from the alley (N312001-03). Relative spectral responses for Cu, Pb, and Zn were consistent with composition of slag from brass and bronze foundry (EPA, 1995; Shen and Forssberg, 2003).

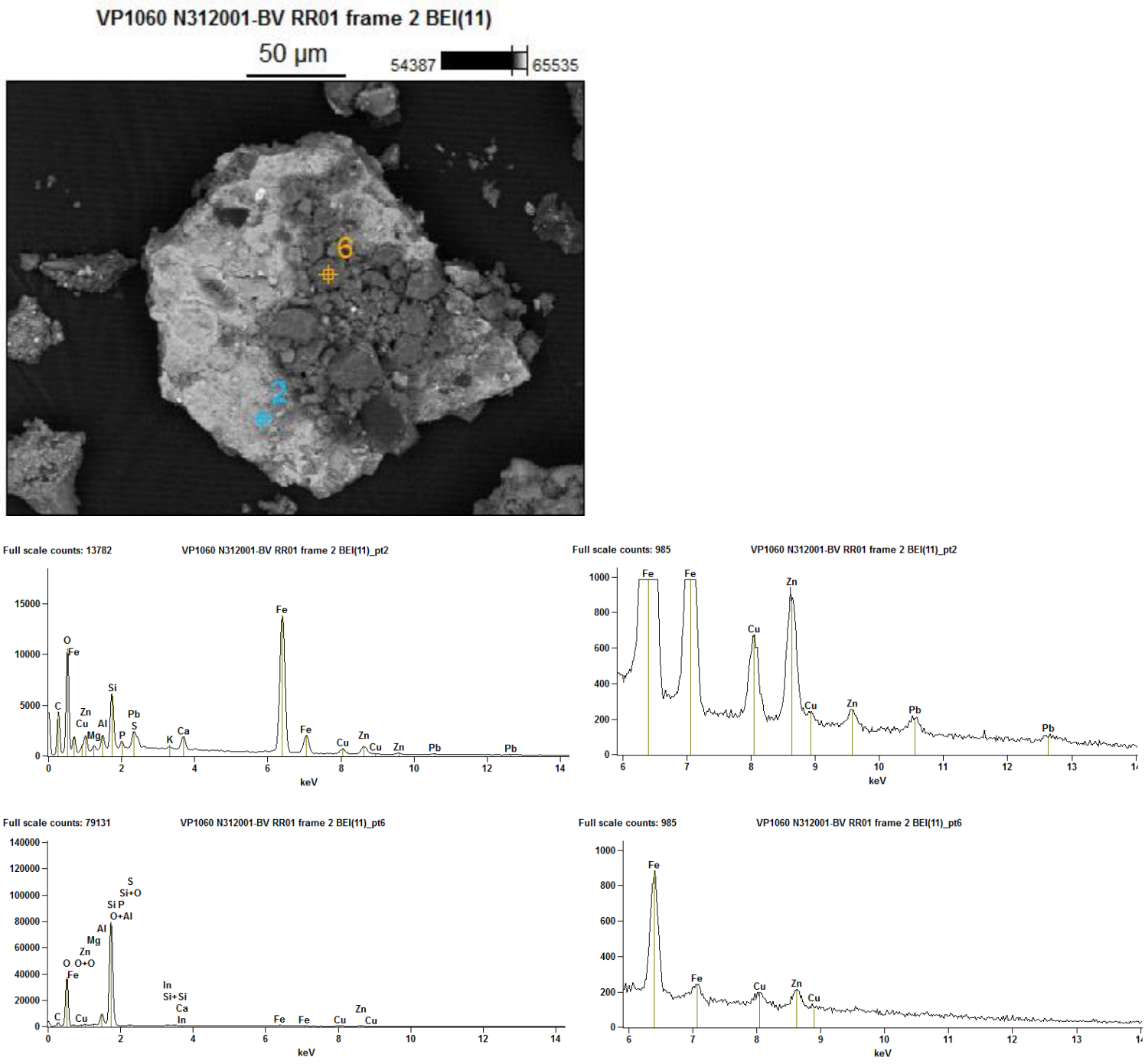

Figure 11. Angular multi-phase particle with Fe-oxide (pt2; Cu>Pb, Zn>>Pb) and Si-oxide (pt6; Cu>Pb, Zn>Pb) in soil from the railroad (N312001-BV). Relative spectral responses for Cu, Pb, and Zn were consistent with composition of slag from brass and bronze foundry (EPA, 1995; Shen and Forssberg, 2003).

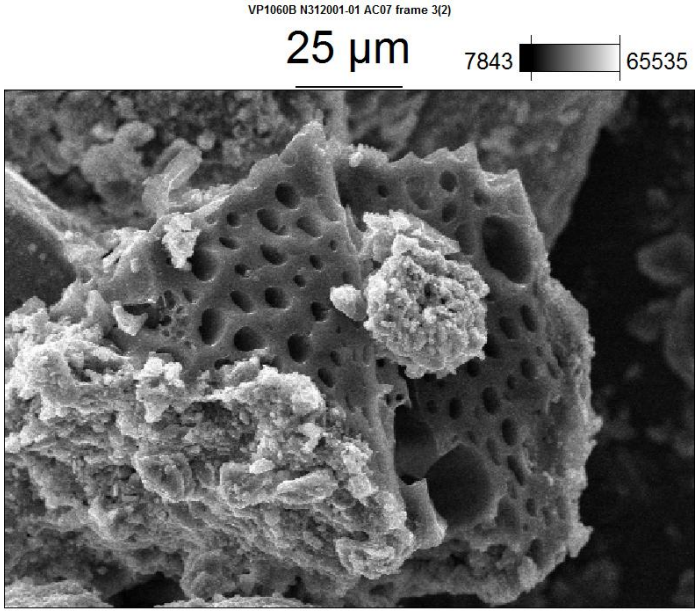
VP1060B N312001-01 AC07 frame 3(2)
25 µm
7843
65535

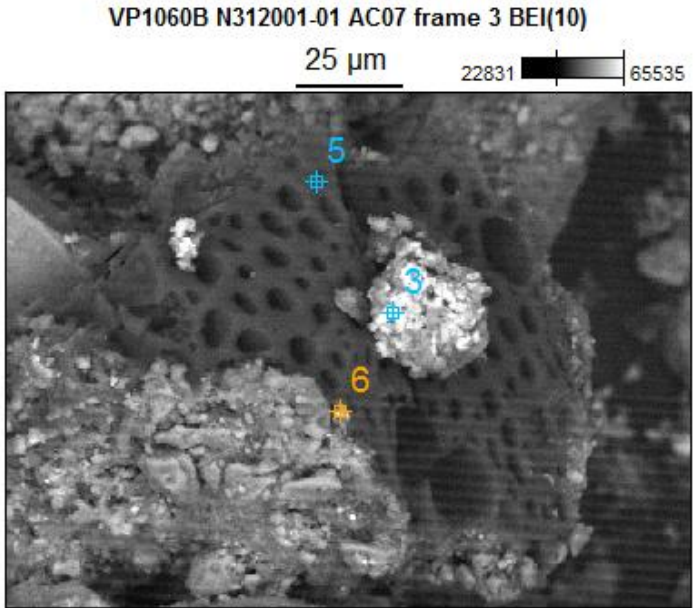
VP1060B N312001-01 AC07 frame 3 BEI(10)
25 µm
22831
65535
5
3
6

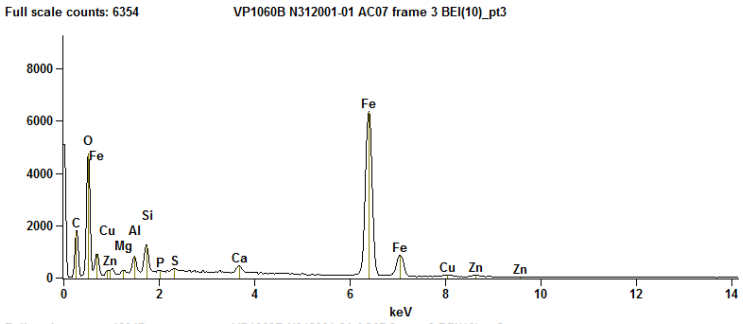
Full scale counts: 6354
VP1060B N312001-01 AC07 frame 3 BEI(10)_pt3
O
Fe
C
Cu
Al
Si
Mg
Zn
P
S
Ca
Fe
Fe
Cu
Zn
Zn
keV

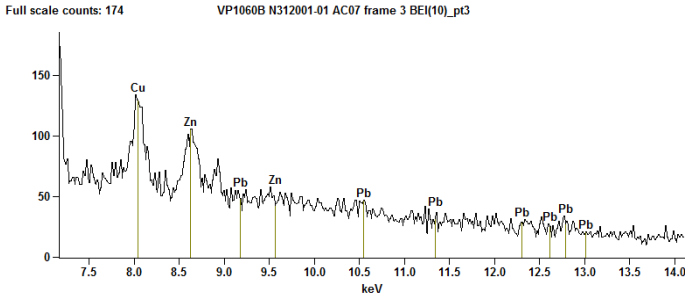
Full scale counts: 174
VP1060B N312001-01 AC07 frame 3 BEI(10)_pt3
Cu
Zn
Pb
Zn
Pb
Pb
Pb
Pb
Pb
Pb
keV

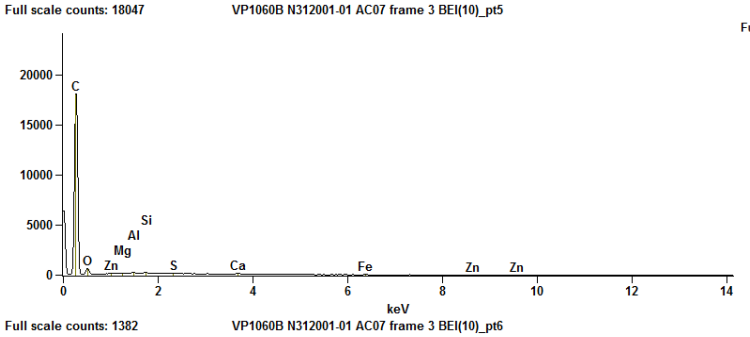
Full scale counts: 18047
VP1060B N312001-01 AC07 frame 3 BEI(10)_pt5
C
O
Si
Al
Mg
Zn
S
Ca
Fe
Zn
Zn
keV

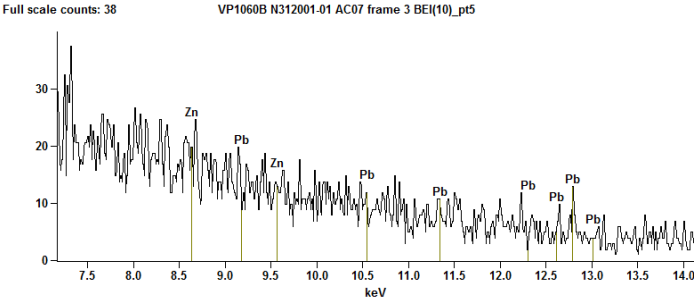
Full scale counts: 38
VP1060B N312001-01 AC07 frame 3 BEI(10)_pt5
Zn
Pb
Zn
Pb
Pb
Pb
Pb
Pb
Pb
keV

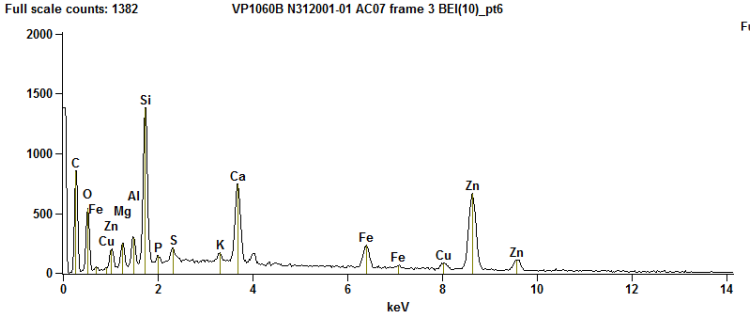
Full scale counts: 1382
VP1060B N312001-01 AC07 frame 3 BEI(10)_pt6
C
O
Fe
Mg
Zn
Cu
Al
Si
P
S
K
Ca
Fe
Fe
Cu
Zn
Zn
keV

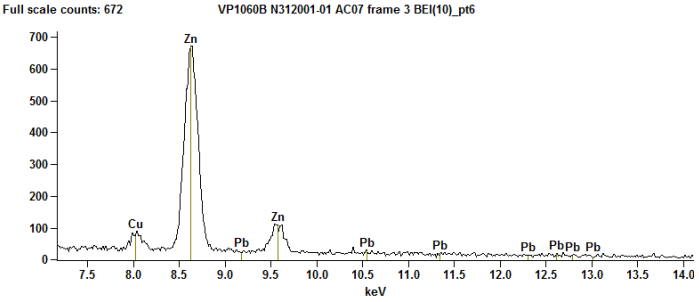
Full scale counts: 672
VP1060B N312001-01 AC07 frame 3 BEI(10)_pt6
Zn
Cu
Zn
Pb
Pb
Pb
Pb
Pb
Pb
Pb
keV

Figure 12. (Previous page) Angular multi-phase C-rich (pt5) particle (100s μm) with Si-oxide (pt6; Cu>Pb, Zn>>Pb) in soil from the alley (N312001-01). Regularly distributed spheriod and ovoid cavities consistent with vesicles, typical in slag material. Sub-angular Fe-oxide (pt3; Cu>Pb, Zn>Pb) particle (10s μm) resting on top of the C-rich particle. SEI image and full keV energy scale (left), BEI image and expanded keV energy scale (right). Relative spectral responses for Cu, Pb, and Zn were consistent with composition of slag from brass and bronze foundry (EPA, 1995; Shen and Forssberg, 2003).

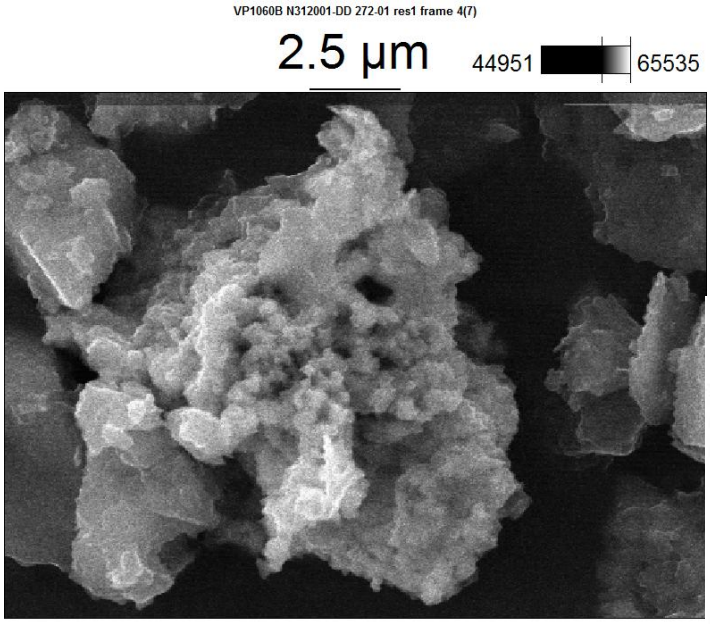

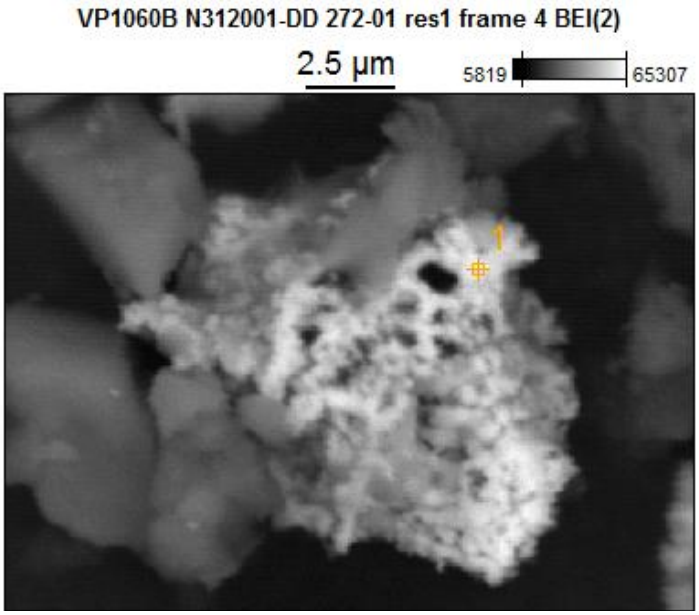

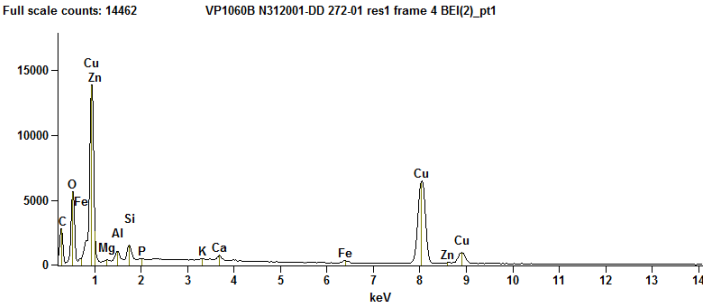

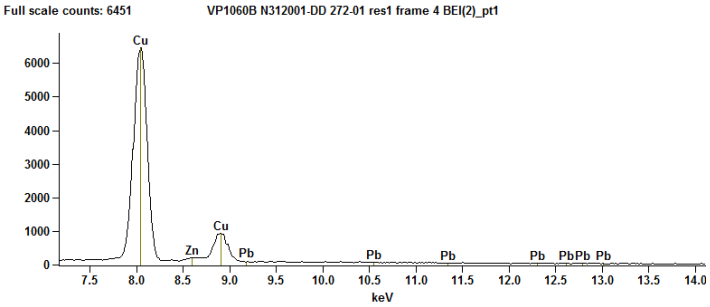

Figure 13. Angular Cu-oxide particle (ca. 10 μm; Cu>>Pb, Zn>Pb) in Res 1 soil (N312001-DD). Ovoid and irregularly shaped cavities consistent with dissolution and vesicles. SEI image and full keV energy scale (left), BEI image and expanded keV energy scale (right). Relative spectral responses for Cu, Pb, and Zn were consistent with composition of slag from brass and bronze foundry (EPA, 1995; Shen and Forssberg, 2003).

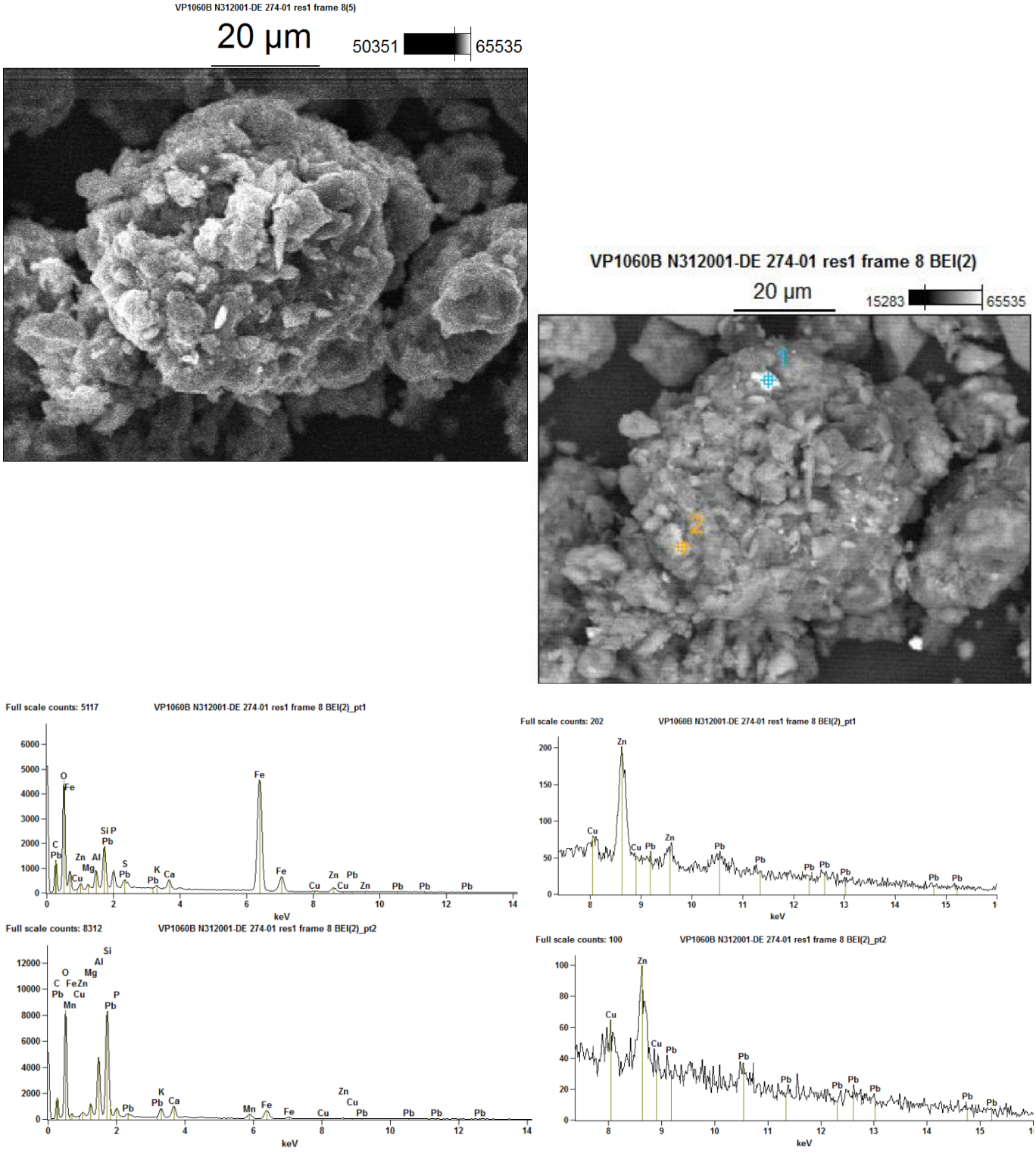

Figure 14. Angular multi-phase, Pb-bearing particle in Res 1 soil (N312001-DE) containing Fe-oxide (pt1, Zn>>Pb) and Si-oxide (pt2, Zn>Pb) phases. SEI image and full keV energy scale (left), BEI image and expanded keV energy scale (right). Relative spectral responses for Pb and Zn were consistent with composition of slag from brass and bronze foundry (EPA, 1995; Shen and Forssberg, 2003).

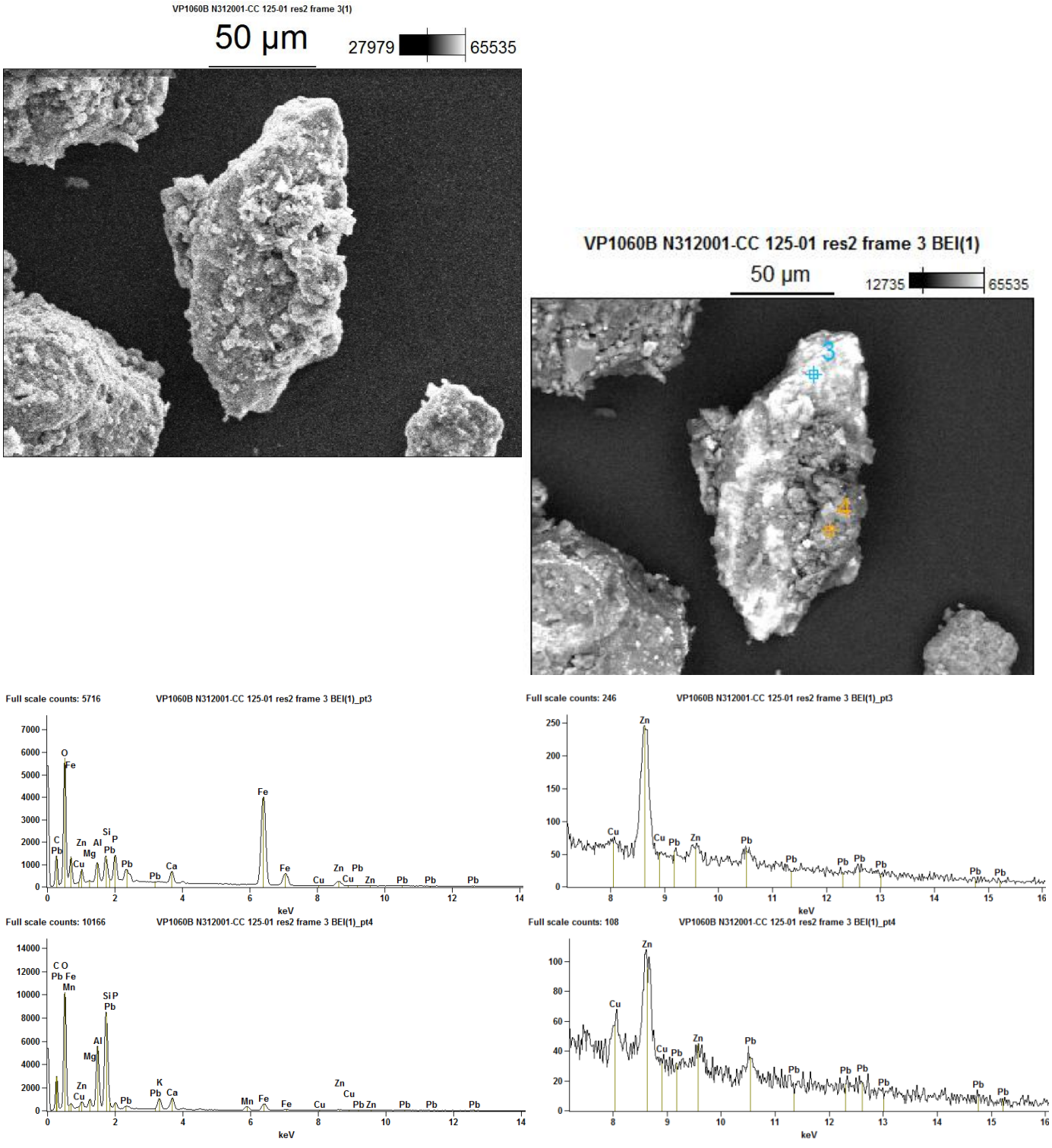

Figure 15. Angular, multi-phase, Pb-bearing particle in Res 2 soil (N312001-CC) containing Fe-oxide (pt3, Zn>>Pb) and Si-oxide (pt4, Zn>Pb) phases. SEI image and full keV energy scale (left), BEI image and expanded keV energy scales (right). Relative spectral responses for Pb and Zn were consistent with composition of slag from brass and bronze foundry (EPA, 1995; Shen and Forssberg, 2003).

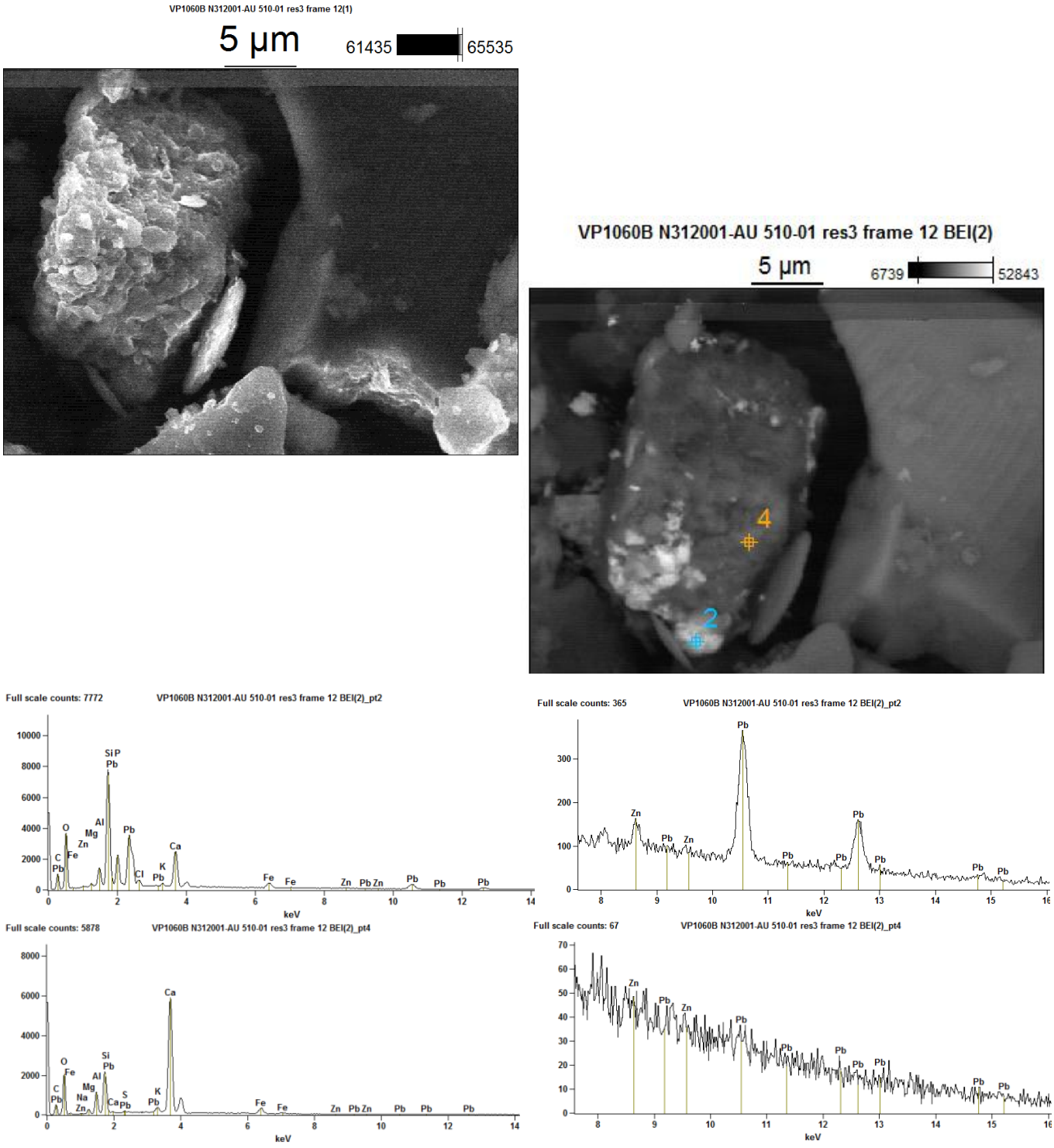

Figure 16. Sub-angular multi-phase, Pb-bearing particle in Res 3 soil (N312001-AU) containing Si-oxide (pt2; Pb>>Cu, Zn) and Ca-oxide/carbonate phases (pt4). SEI image and full keV energy scale (left), BEI image and expanded keV energy scales (right). Relative spectral responses for Cu, Pb, and Zn were not characteristic of slag composition from brass and bronze foundry (EPA, 1995; Shen and Forssberg, 2003).

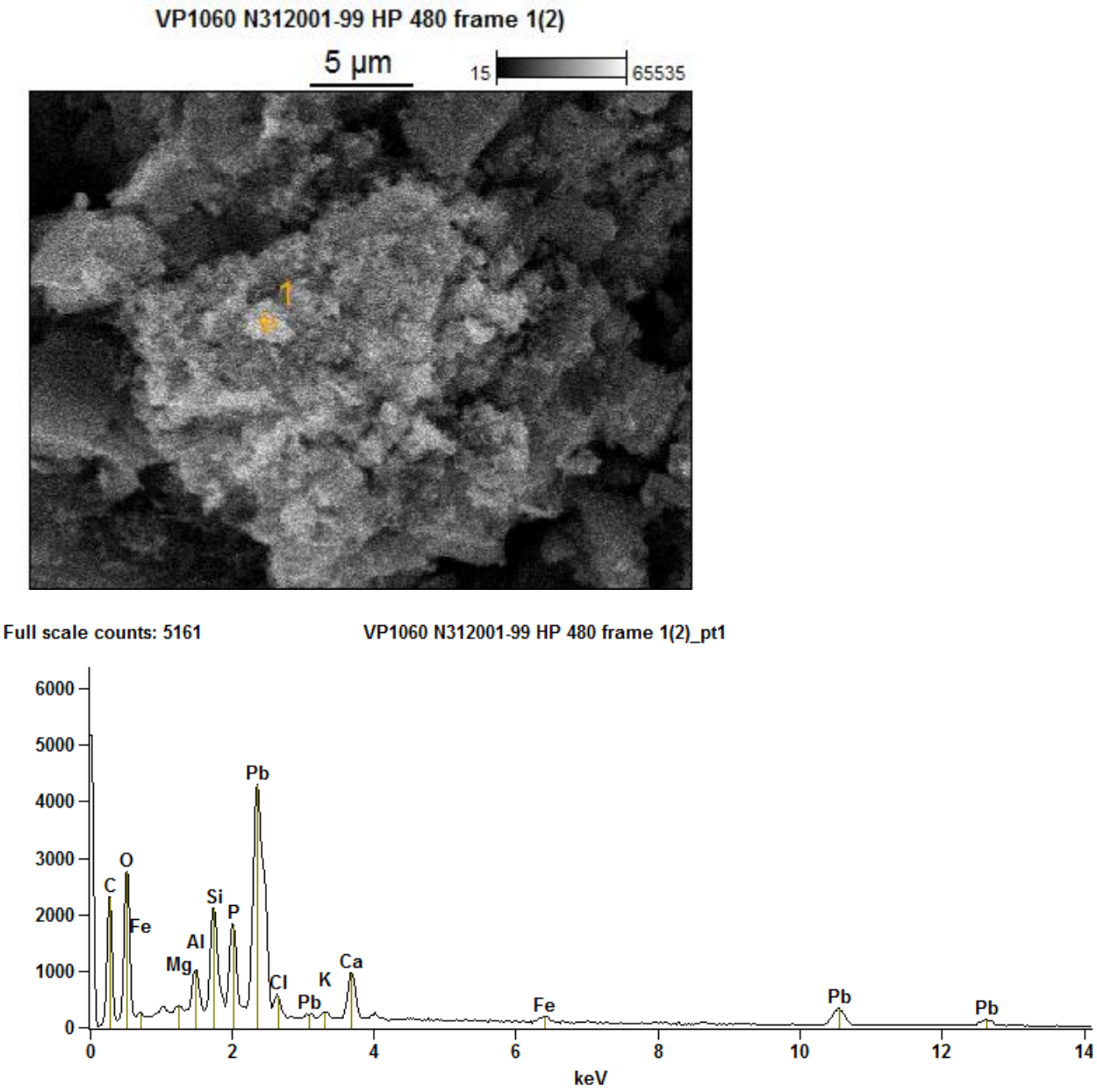

Figure 17. Angular Pb-oxide particle (10s µm) in soil from the Harrison Park area (N312001-99). Negligible spectral responses for Cu and Zn.

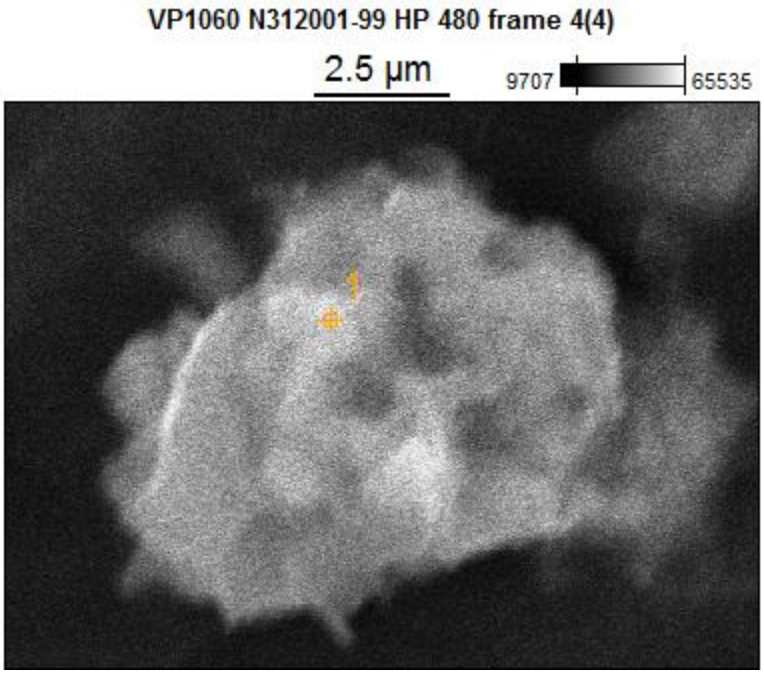

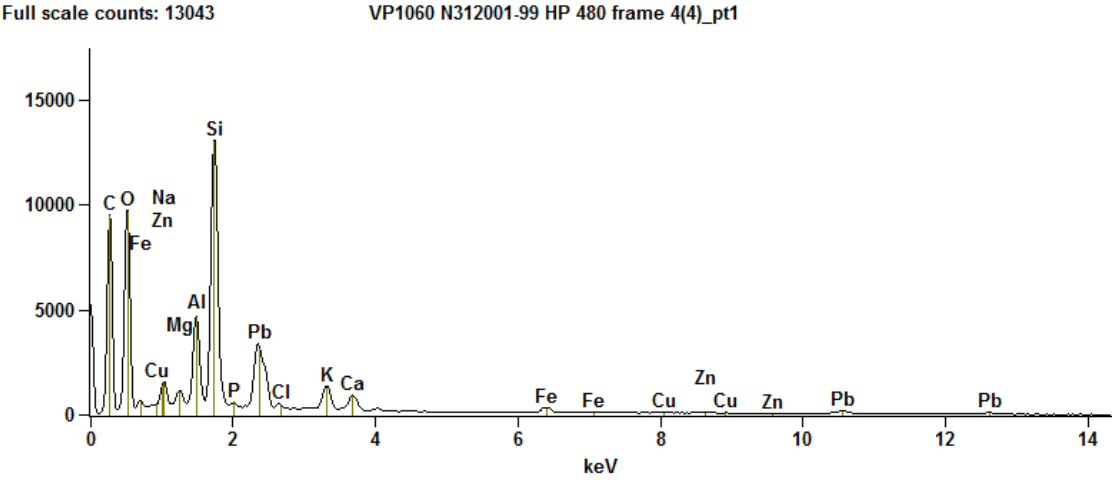

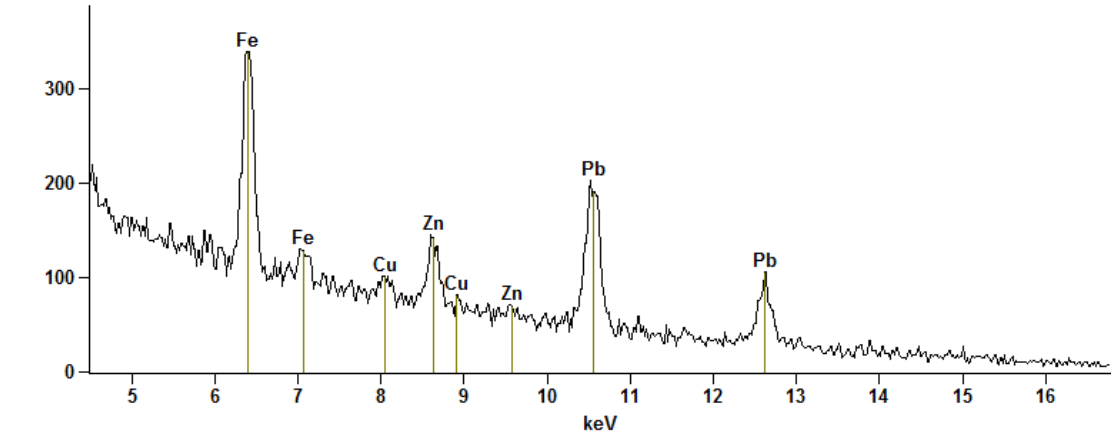

Figure 18. Angular Si-oxide particle (with Pb>>Cu and Pb>Zn) in soil from the Harrison Park area (N312001-99). Pitted surface consistent with dissolution, distinct spherical/ovoid cavities consistent with vesicles, typical in slag material. Relative spectral responses for Cu, Pb, and Zn were not characteristic of the composition of slag from brass and bronze foundry (EPA, 1995; Shen and Forssberg, 2003).

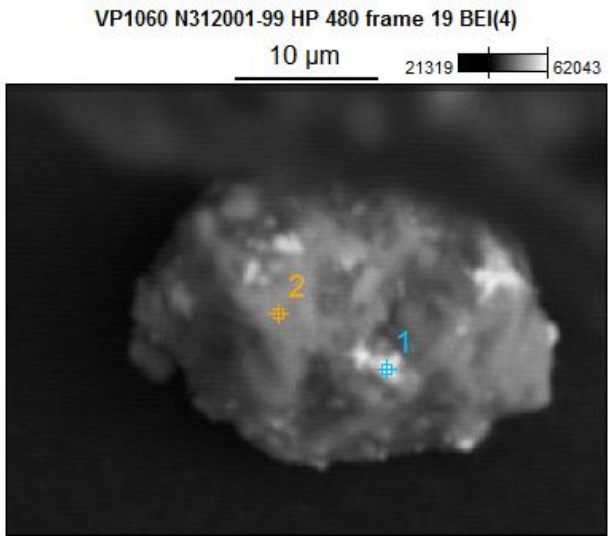

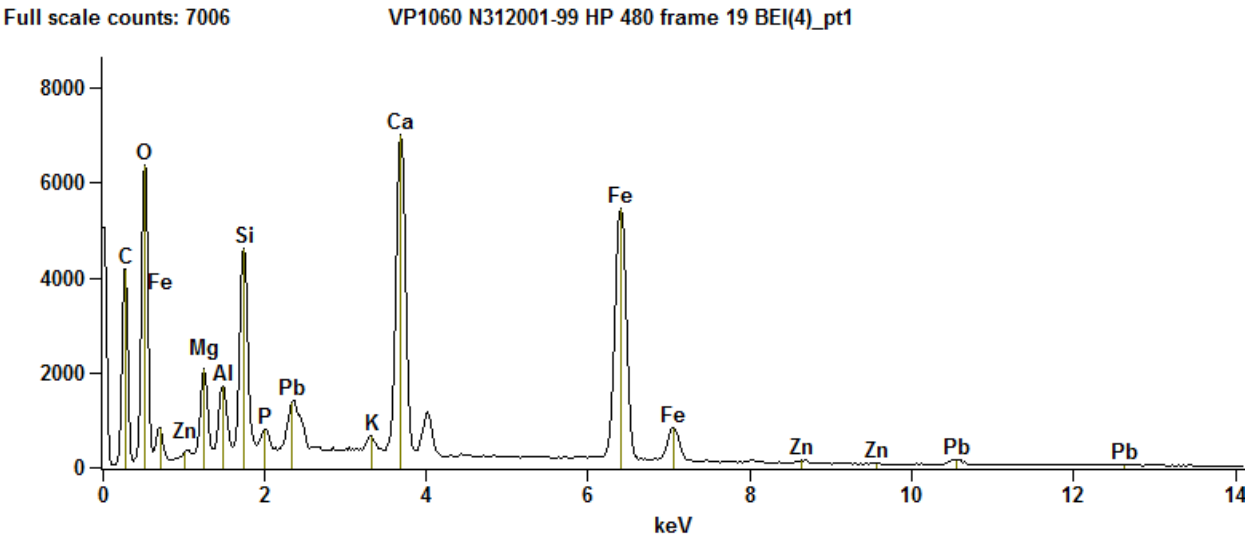

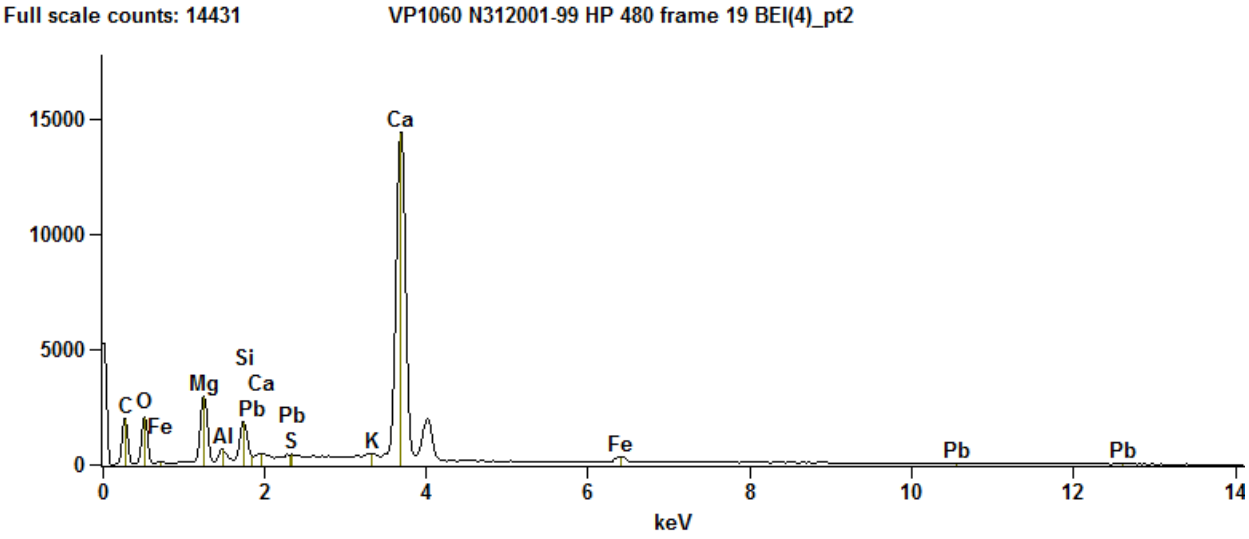

Figure 19. Sub-angular multi-phase particle with Fe-oxide (pt1, Pb>Zn) and Ca-oxide/carbonate (pt2, 10s µm) in soil from the Harrison Park area (N312001-99). Relative spectral responses for Pb and Zn were not characteristic of slag composition from brass and bronze foundry (EPA, 1995; Shen and Forssberg, 2003).

LEAD ISOTOPE RATIO RESULTS

Understanding analytical precision and accuracy for Pb isotope ratio measurements is important for evaluating and comparing Pb isotope ratio results. Instrument performance and analytical procedure reproducibility were measured by analyzing NIST SRM 2709, 2711 soil standards and NIST SRM 981 through the sample preparation process multiple times (**Table 3**). NIST SRM 981 (n=41) was analyzed throughout the analysis period, both processed through the sample preparation method and unprocessed, and resulted in an average $^{208}Pb/^{207}Pb$ of 2.3682±0.0005 (2 standard deviations[SD]) and $^{206}Pb/^{207}Pb$ of 1.0938±0.0006 (2SD). NIST SRM 981 certificate value for $^{208}Pb/^{207}Pb$ is 2.3704 and for $^{206}Pb/^{207}Pb$ is 1.0933. The NIST SRM 2709 soil standard resulted in $^{208}Pb/^{207}Pb$ of 2.4825±0.0006 (2SD) and $^{206}Pb/^{207}Pb$ of 1.2181±0.0012 (2SD), similar to the values reported by Takaoka et al. (2006) for $^{208}Pb/^{207}Pb$ of 2.482±0.002 (2SD) and $^{206}Pb/^{207}Pb$ of 1.217±0.002 (2SD). The NIST SRM 2711 soil standard resulted in $^{208}Pb/^{207}Pb$ of 2.3939±0.0007 (2SD) and $^{206}Pb/^{207}Pb$ of 1.1107±0.0008 (2SD), similar to the values reported in the Georem database of $^{208}Pb/^{207}Pb$ of 2.395 and $^{206}Pb/^{207}Pb$ of 1.111 (Jochum et al., 2005). Multiple samples were processed through the sample preparation method in duplicate and triplicate and resulted in an uncertainty for both $^{208}Pb/^{207}Pb$ of ±0.0014 and $^{206}Pb/^{207}Pb$ of ±0.0016 (2SD). Laser ablation and mass spectrometer system performance was determined by analyzing NIST 612 and a USGS synthetic basalt glass reference material (GSE 1G), as well as TSP filter samples in duplicate and triplicate. Based on direct sampling replicates by laser ablation, the isotope ratios varied within a single TSP filter for $^{208}Pb/^{207}Pb$ and $^{206}Pb/^{207}Pb$ by 2.72×10^{-4} (1SD) and 3.88×10^{-5} (1SD), respectively. The average variation among multiple TSP filters by laser ablation over a 9-month period was 5.28×10^{-4} (1SD) for $^{208}Pb/^{207}Pb$ and 1.10×10^{-3} (1SD) for $^{206}Pb/^{207}Pb$.

Table 3. Pb ISOTOPE RATIO PERFORMANCE CRITERIA: ESTIMATED UNCERTAINTY
Additional Characterization of Lead in Soils
Pilsen Neighborhood, Chicago, Illinois

	USGS this study		Woodhead, 2002		Jochum et al., 2005 (Georem database)		Takaoka et al., 2006	
Standard	$^{206}Pb/^{207}Pb$	$^{208}Pb/^{207}Pb$	$^{206}Pb/^{207}Pb$	$^{208}Pb/^{207}Pb$	$^{206}Pb/^{207}Pb$	$^{208}Pb/^{207}Pb$	$^{206}Pb/^{207}Pb$	$^{208}Pb/^{207}Pb$
NIST SRM 2709	1.2181	2.4825	n.a.[b]	n.a.[b]	1.218	2.488	1.217	2.482
NIST SRM 2711	1.1107	2.3939	n.a.[b]	n.a.[b]	1.111	2.395	n.a.[b]	n.a.[b]
NIST SRM 981[a]	1.0937	2.3684	1.093	2.369	1.093-1.100	2.360-2.374	n.a.[b]	n.a.[b]
NIST SRM 612 G	1.1034	2.3847	n.a.[b]	n.a.[b]	1.099-1.104	2.381-2.391	n.a.[b]	n.a.[b]
USGS GSE 1G	1.2626	2.4787	n.a.[b]	n.a.[b]	1.263	2.480	n.a.[b]	n.a.[b]

[a] Error for the reported USGS NIST SRM 981value is ±0.0006 (2SD) for $^{206}Pb/^{207}Pb$ and ±0.0005 (2SD) for $^{208}Pb/^{207}Pb$.
[b] n.a. = not available.

Pb isotope ratio results are presented in **Figure 20** and **Table 4**. **Figure 20** shows the three Pb isotope plot of $^{208}Pb/^{207}Pb$ versus $^{206}Pb/^{207}Pb$ isotope ratios for samples collected in the Pilsen neighborhood. Samples included soil from the alley, railroad, and Res 1, 2, and 3 areas;

H. Kramer baghouse dust; and Pb-bearing airborne particulate collected on TSP filters from the previous Pilsen air study (NEIC, 2011a, 2012).

Three-isotope plots for Pb ($^{208}Pb/^{207}Pb$ vs. $^{206}Pb/^{207}Pb$) are generally used to determine the mixing line of a two-component member system (Veron and Church, 1997; Bollhöfer and Rosman, 2001; Kylander et al., 2010; Pribil et al., 2014). The $^{208}Pb/^{207}Pb$ and $^{206}Pb/^{207}Pb$ isotope ratios of samples of interest are shown in **Figure 20**. Typically, in a two-component mixing scenario with a Pb source material and a defined Pb baseline (non-receptor or background Pb with respect to Pb from PRPs), the more concentrated Pb samples exhibit greater influence from the Pb source material and plot toward the lower left, and the less concentrated Pb samples with less influence from the Pb source material plot toward the upper right, closer to that of the defined Pb baseline. **Figure 20** illustrates the distinct Pb isotopic composition of the two end members (labeled: first component end member and second component end member), as well as a mixing zone (labeled: mixing zone) representing mixed Pb isotopic compositions of the first component end member with the second component end member in varying proportions. Samples with Pb isotope ratios plotting in the lower left portion of the mixing zone reflected greater contributions from the first component end member (source signature), and samples with Pb isotope ratios plotting in the upper right of the mixing zone exhibited greater influence from the second component end member, and minimal influence from the first component end member (source signature). Component mixing of material with different Pb isotope compositions was described by Bollhöfer and Rosman (2001) using three-isotope plots for Pb.

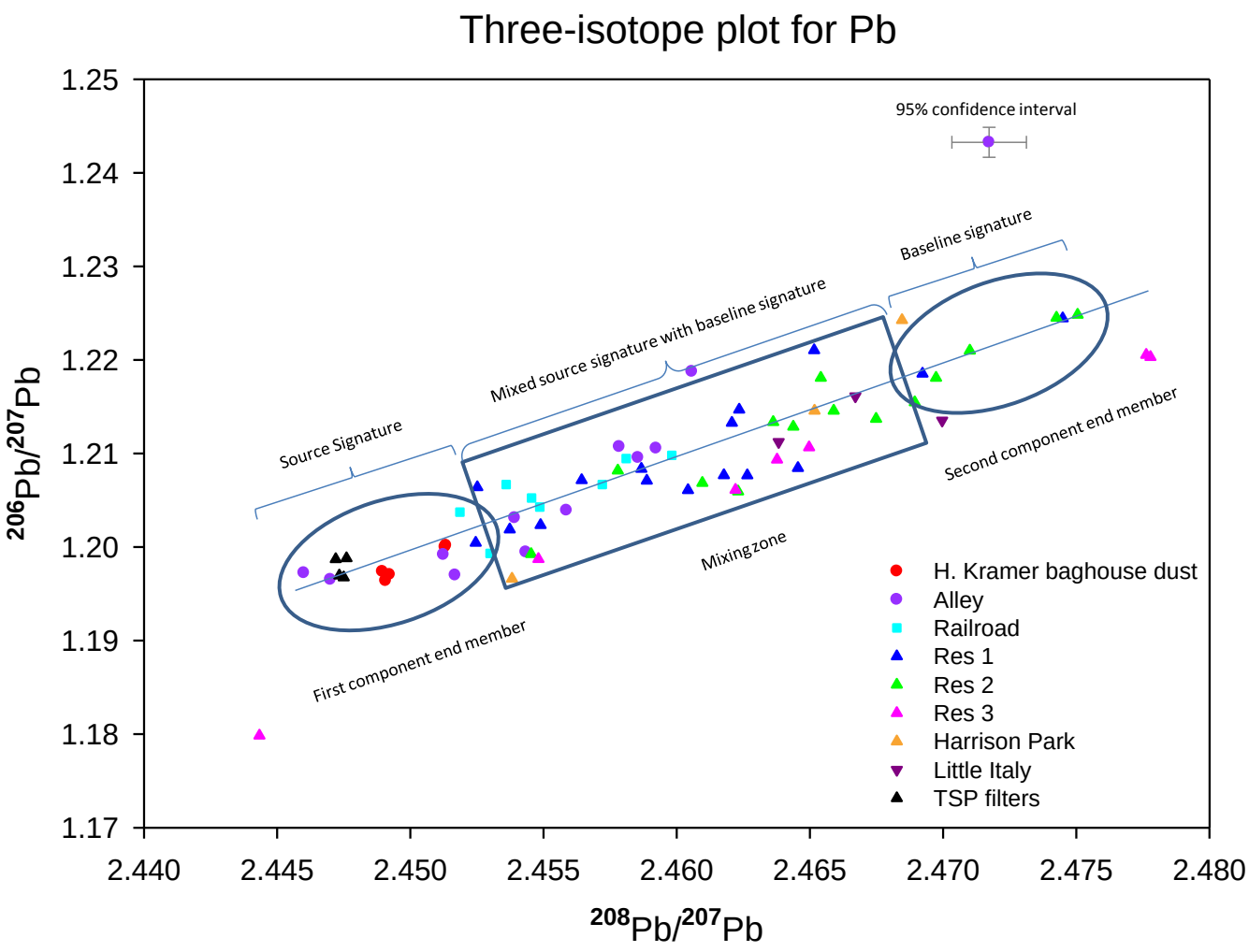

Figure 20. Three-isotope plot for Pb for the Pilsen area, Chicago, Illinois.

H. Kramer Baghouse Dust

H. Kramer baghouse dust (red circles) consisted of $^{208}Pb/^{207}Pb$ and $^{206}Pb/^{207}Pb$ from 2.4490 to 2.4513 and 1.1964 to 1.2000, respectively. The blending of various materials by H. Kramer, such as scrap metal to produce alloys rather than processing raw ore, resulted in Pb isotope ratios distinct from those of natural background Pb and of Pb from any historical primary smelting that may have impacted the area. A small Pb isotopic variation in one of the four baghouse dust samples was determined (**Figure 20**) and was most likely the result of differences in the furnace processes for which the baghouses collected emissions. Baghouse 2 controlled emissions directly from the rotary furnaces 1 and 2, while baghouses 1 and 5 controlled fugitive emissions from those furnaces (Omenazu, 2011). Baghouse 4 controlled emissions from the coreless electric induction furnaces.

TSP Filters

TSP filters (black upward triangles) resulted in the narrowest range of Pb isotope compositions, with $^{208}Pb/^{207}Pb$ and $^{206}Pb/^{207}Pb$ ranging from 2.4472 to 2.4476 and 1.1968 to 1.1988, respectively. The similar Pb isotope composition of the TSP air filters suggested a common source of airborne Pb-bearing particulate material during the time period represented by the air sampling events. TSP filters contained Pb minimally influenced by concurrent or historical Pb sources (NEIC, 2012), allowing direct comparison to current potential Pb source materials. TSP filters exhibited, within measurement uncertainty (indicated by error bars for upper right alley soil), Pb isotopic composition similar to H. Kramer baghouse dust. Results of the Pilsen air study (NEIC, 2011a, 2012) indicated Pb-bearing particulate matter collected on the TSP filters originated from process emissions at H. Kramer. The baghouse dust and the TSP filters defined the first component end member of a two-component mixing scenario.

Alley Soils

In alley soils (lavender circles), the $^{208}Pb/^{207}Pb$ and $^{206}Pb/^{207}Pb$ ratios ranged from 2.4460 to 2.4717 and 1.1967 to 1.2433, respectively. Alley soils resulted in the greatest range of Pb isotope compositions, with a 0.0257 range for $^{208}Pb/^{207}Pb$ and a 0.0466 range for $^{206}Pb/^{207}Pb$. These ranges coincided with and extended beyond the range of Pb isotopic compositions for all other soil areas. The greatest $^{208}Pb/^{207}Pb$ and $^{206}Pb/^{207}Pb$ ratios were measured in alley soil [PA-AC08(0-6)-121912], collected on the east side of the alley close to South Throop Street, and were isotopically distinct from the other samples. Alley soil PA-AC08(0-6)-121912 also exhibited one of the lowest Pb concentrations in soils for which Pb isotope ratios were determined.

Alley soils collected from the middle [PA-AC05(0-6)-121912, PA-AC06(0-6)-121912] and east side [PA-AC09(0-6)-121912, PA-AY09(12-24)-121912] of the alley exhibited Pb isotopic compositions that coincided with the TSP filters and H. Kramer baghouse dust, suggesting these four soil samples were heavily impacted by a common source of Pb consistent with H. Kramer baghouse dust as the first component end member (source Pb isotope signature). Pb isotope compositions for the other alley soils exhibited overlapping trends for both $^{208}Pb/^{207}Pb$ and $^{206}Pb/^{207}Pb$ along the Pb isotope mixing line toward the second component end member (baseline Pb isotope signature), suggesting soils with the baseline Pb isotope signature were mixed with varying amounts of material consistent with H. Kramer baghouse dust. Soils collected from the middle of the alley, exhibiting similar Pb isotopic compositions as TSP filters and H. Kramer baghouse dust, were located directly adjacent to the H. Kramer facility. The majority of alley soils (10 of 12 samples) exhibited Pb isotope compositions either similar to the first component end member or near the mixing line closest to the first component end member. Pb isotope ratios of two alley soils deviated from the mixing line (upper right) and were not isotopically similar to either the first component end member or the second component end member.

Railroad Soils

In railroad soils (teal squares), the $^{208}Pb/^{207}Pb$ and $^{206}Pb/^{207}Pb$ ratios ranged from 2.4519 to 2.4598 and 1.1993 to 1.2098, respectively. The Pb isotope ratios of railroad soils coincided with the Pb isotope ratios of alley soils, falling generally along the same component mixing line observed for the alley soils. This pattern was consistent with a common source of lead in the alley and railroad soils that was isotopically similar to TSP filters and H. Kramer baghouse dust (source Pb isotope signature).

Res 1 Soils

Res 1 soils (blue upward triangles) consisted of 16 soil samples, including garden soils (0–12 inches), a drip line soil, and a subsurface soil (6–21 inches). The $^{208}Pb/^{207}Pb$ and $^{206}Pb/^{207}Pb$ isotope ratios ranged from 2.4525 to 2.4745 and 1.2005 to 1.2244, respectively. There was no discernible difference isotopically between garden, drip line, subsurface or surface soils within each residential area. Two Res 1 soils [PA-123-01(0-12)-050313, PA-291-03(0-12)-050113] resulted in Pb isotopic composition consistent with the baseline Pb isotope signature (second component end member). Five Res 1 soils [PA-127-01(6-21)-071613, PA-180-01(0-6)-050213, PA-274-01(0-6)-050113, PA-274-02(0-6)-050113, PA-370-02(0-12)-050713] collected north and northeast of the H. Kramer facility resulted in Pb isotopic composition more consistent with alley and railroad soils, the TSP filters, and H. Kramer baghouse dust (sample BH4) (**Figure 20**, left portion of the mixing zone). The remaining nine Res 1 soils exhibited Pb isotopic compositions varying between the source Pb isotope signature (consistent with the Pb isotope signature of the TSP filters and H. Kramer baghouse dust) and the baseline Pb isotope signature.

Res 2 Soils

Res 2 soils (green upward triangles) consisted of 14 soil samples and included garden (0–12 inches) and subsurface soils. The $^{208}Pb/^{207}Pb$ and $^{206}Pb/^{207}Pb$ isotope ratios ranged from 2.4545 to 2.4750 and 1.1993 to 1.2248, respectively. Five Res 2 soils [PA-84-01(0-6)-050813, PA-92-01(0-6)-050813, PA-104-01(12-24)-071613, PA-371-02(0-6)-050713, PA-466-02(0-6)-050913] exhibited Pb isotopic compositions similar to the baseline Pb isotope signature (second component end member). The remaining nine soils exhibited Pb isotopic compositions falling along the mixing zone between the first component end member and the second component end member. A soil's position in the mixing zone is dependent on the amount of influence that each of the two end members contribute to the Pb concentration and, hence, the Pb isotopic composition of the sample. For example, soil PA-125-01(0-6)-050313 had the highest Pb concentration of the Res 2 soils analyzed for Pb isotopes and exhibited a similar Pb isotopic composition to alley and Res 1 soils. The Res 2 soils most similar to the Pb isotopic compositions of the alley and Res 1 soils were collected nearest to the boundary between the Res 1 and 2 areas, northeast and east of H. Kramer.

Res 3 Soils

Res 3 soils (pink upward triangles) consisted of seven soil samples and included duplicate, subsurface, and playground soils from two locations within the Res 3 area. The $^{208}Pb/^{207}Pb$ and $^{206}Pb/^{207}Pb$ isotope ratios ranged from 2.4443 to 2.4778 and 1.1798 to 1.2205, respectively. A subsurface soil [PA-469-01(6-15)-071113] resulted in a distinct Pb isotopic composition, suggesting a potential Pb source not consistent with the Pb isotope ratios of the TSP filters or H. Kramer baghouse dust. Soils PA-465-01(0-6)-050913 and PA-465-01(0-6)-050913D exhibited Pb isotope ratios that may define a different baseline for Pb isotopic composition at this location. Four Res 3 soils [PA-464-01(0-6)-050813, PA-464-02(0-6)-050813, PA-469-01(0-6)-051013 and PA-469-05(0-6)-051013] resulted in similar Pb isotopic compositions as some of the Res 1 and 2 soils.

Harrison Park and Little Italy Soils

Harrison Park soils (gold upward triangles) consisted of three surface soil samples with $^{208}Pb/^{207}Pb$ and $^{206}Pb/^{207}Pb$ isotope ratios that ranged from 2.4538 to 2.4685 and 1.1966 to 1.2243, respectively. Although Harrison Park soils were chosen to represent baseline soil in the Pilsen neighborhood relative to soil adjacent to H. Kramer, two Harrison Park soils resulted in Pb concentrations of 1400 and 1700 mg/kg. These elevated concentrations suggested the presence of additional sources of Pb above baseline levels. Little Italy soils (purple downward triangles) consisted of three surface soil samples and one duplicate sample with $^{208}Pb/^{207}Pb$ and $^{206}Pb/^{207}Pb$ isotope ratios that ranged from 2.4638 to 2.4700 and 1.2112 to 1.2161, respectively. Pb concentrations in the Little Italy soils were the lowest of all the soil areas.

Comparisons of the seven soil areas, the alley, railroad, Res 1, Res 2, Res 3, Harrison Park, and Little Italy areas are considered in the "Comparison of Soil Areas" section.

Table 4. Pb ISOTOPE RATIO RESULTS
Additional Characterization of Lead in Soils
Pilsen Neighborhood, Chicago, Illinois

Sample	LIMS No.	Description	$^{206}Pb/^{207}Pb$	$^{208}Pb/^{207}Pb$
BH1	N105006-05	H. Kramer baghouse dust	1.1974	2.4490
BH2	N105006-06	H. Kramer baghouse dust	1.1971	2.4492
BH4	N105006-08	H. Kramer baghouse dust	1.2000	2.4513
BH4 Duplicate	N105006-09	H. Kramer baghouse dust	1.2000	2.4513
BH5	N105006-07	H. Kramer baghouse dust	1.1964	2.4491
PA-**AC01**(0-6)-121912[a]	N312001-**CK**	Alley – composite soil	1.2106	2.4592
PA-**AC02**(0-6)-121912	N312001-**CM**	Alley – composite soil	1.2039	2.4556
PA-**AC03**(0-6)-121912	N312001-**CO**	Alley – composite soil	1.2188	2.4606
PA-**AC03**HS(0-6)-121912	N312001-**DY**	Alley – composite soil	1.2107	2.4578
PA-**AC04**(0-6)-121912	N312001-**CP**	Alley – composite soil	1.1995	2.4543
PA-**AC05**(0-6)-121912	N312001-**EA**	Alley – composite soil	1.1965	2.4470
PA-**AC06**(0-6)-121912	N312001-**CQ**	Alley – composite soil	1.1992	2.4512
PA-**AC07**(0-6)-121912	N312001-**01**	Alley – composite soil	1.2031	2.4539
PA-**AC08**(0-6)-121912	N312001-**CR**	Alley – composite soil	1.2433	2.4717
PA-**AC09**(0-6)-121912	N312001-**02**	Alley – composite soil	1.1967	2.4517
PA-**AC10**(0-6)-121912	N312001-**CS**	Alley – composite soil	1.2096	2.4585
PA-**AY09**(12-24)-121912	N312001-**CT**	Alley – grab soil	1.1972	2.4460
PA-**RR-01,02**(0-6)-050613[b]	N312001-**BV**	Railroad – composite soil	1.2095	2.4581
PA-**RR-01,02**(6-24)-050613	N312001-**BW**	Railroad – composite soil	1.2043	2.4549
PA-**RR-04,06**(0-6)-050613	N312001-**BX**	Railroad – composite soil	1.2037	2.4519
PA-**RR-04,06**(6-24)-050613	N312001-**BY**	Railroad – composite soil	1.2067	2.4572
PA-**RR-07,08**(0-6)-050613	N312001-**CV**	Railroad – composite soil	1.2067	2.4536
PA-**RR-07,08**(6-24)-050613	N312001-**BU**	Railroad – composite soil	1.2052	2.4545
PA-**RR14,15,16**(0-6)-050613	N312001-**BP**	Railroad – composite soil	1.1993	2.4530
PA-**RR14,15,16**(6-24)-050613	N312001-**CG**	Railroad – composite soil	1.2098	2.4598
PA-**122**-01(0-6)-050313	N312001-**14**	Res 1 soil	1.2210	2.4652
PA-**122**-02(0-12)-050313	N312001-**BE**	Res 1 soil	1.2133	2.4621
PA-**123**-01(0-12)-050313	N312001-**BD**	Res 1 soil	1.2185	2.4692
PA-**127**-01(6-21)-071613	N312001-**41**	Res 1 soil	1.2064	2.4525
PA-**180**-01(0-6)-050213	N312001-**CB**	Res 1 soil	1.2019	2.4537
PA-**183**-01(0-12)-050213	N312001-**BB**	Res 1 soil	1.2084	2.4587
PA-**186**-02(0-6)-050213	N312001-**DA**	Res 1 soil	1.2077	2.4618
PA-**191**-01(0-6)-050213	N312001-**DB**	Res 1 soil	1.2147	2.4623
PA-**193**-01(0-6)-050313	N312001-**13**	Res 1 soil	1.2071	2.4589
PA-**272**-01(0-6)-050113	N312001-**DD**	Res 1 soil	1.2085	2.4645
PA-**274**-01(0-6)-050113	N312001-**DE**	Res 1 soil	1.2072	2.4564
PA-**274**-02(0-6)-050113	N312001-**DF**	Res 1 soil	1.2005	2.4525
PA-**291**-03(0-12)-050113	N312001-**DH**	Res 1 soil	1.2244	2.4745
PA-**370**-01(0-6)-050713	N312001-**DL**	Res 1 soil	1.2023	2.4549
PA-**370**-02(0-12)-050713	N312001-**CJ**	Res 1 soil	1.2061	2.4604
PA-**375**-01(0-6)-050713	N312001-**DQ**	Res 1 soil	1.2077	2.4626
PA-**84**-01(0-6)-050813	N312001-**DX**	Res 2 soil	1.2245	2.4743
PA-**92**-01(0-6)-050813	N312001-**DU**	Res 2 soil	1.2181	2.4697
PA-**104**-01(0-6)-050213	N312001-**94**	Res 2 soil	1.2146	2.4659
PA-**104**-01(12-24)-071613	N312001-**AE**	Res 2 soil	1.2248	2.4750
PA-**105**-01(0-6)-050213	N312001-**93**	Res 2 soil	1.2069	2.4610
PA-**125**-01(0-6)-050313	N312001-**CC**	Res 2 soil	1.1993	2.4545
PA-**125**-02(0-6)-050313	N312001-**CX**	Res 2 soil	1.2137	2.4675
PA-**163**-01(0-12)-050113	N312001-**AZ**	Res 2 soil	1.2134	2.4636
PA-**304**-01(0-6)-050913	N312001-**DI**	Res 2 soil	1.2181	2.4654
PA-**349**-01(0-6)-050713	N312001-**DJ**	Res 2 soil	1.2129	2.4644
PA-**371**-02(0-6)-050713	N312001-**DP**	Res 2 soil	1.2210	2.4710
PA-**466**-01(0-6)-050913	N312001-**DT**	Res 2 soil	1.2059	2.4623
PA-**466**-02(0-6)-050913	N312001-**CE**	Res 2 soil	1.2155	2.4689

Table 4. Pb ISOTOPE RATIO RESULTS
Additional Characterization of Lead in Soils
Pilsen Neighborhood, Chicago, Illinois

PA-**468**-01(0-6)-050913	N312001-**50**	Res 2 soil	1.2082	2.4578
PA-**464**-01(0-6)-050813	N312001-**CA**	Res 3 soil	1.2093	2.4638
PA-**464**-02(0-6)-050813	N312001-**DR**	Res 3 soil	1.1987	2.4548
PA-**465**-01(0-6)-050913	N312001-**BZ**	Res 3 soil	1.2205	2.4776
PA-**465**-01(0-6)-050913D	N312001-**DS**	Res 3 soil	1.2203	2.4778
PA-**469**-01(0-6)-051013	N312001-**CH**	Res 3 soil	1.2107	2.4650
PA-**469**-01(6-15)-071113	N312001-**86**	Res 3 soil	1.1798	2.4443
PA-**469**-05(0-6)-051013	N312001-**DW**	Res 3 soil	1.2061	2.4622
PA-**477**-01(0-6)-071013	N312001-**26**	Harrison Park area soil	1.2146	2.4652
PA-**480**-01(0-6)-071113	N312001-**99**	Harrison Park area soil	1.1966	2.4538
PA-**488**-01(0-6)-071513	N312001-**AC**	Harrison Park area soil	1.2243	2.4685
PA-**490**-01(0-6)-081213	N312001-**AH**	Little Italy area soil	1.2112	2.4638
PA-**493**-01(0-6)-081313	N312001-**AM**	Little Italy area soil	1.2135	2.4700
PA-**494**-01(0-6)-081313	N312001-**79**	Little Italy area soil	1.2161	2.4667
040001 (**1/03/11**)	N105006-12	TSP filter – Perez	1.1970	2.4473
040016 (**4/2/10**)	N105006-11	TSP filter – Perez	1.1968	2.4475
040041 (**8/30/10**)	N105006-13	TSP filter – Perez	1.1988	2.4476
040058 (**12/10/10**)	N105006-10	TSP filter – Perez	1.1987	2.4472

[a] Alley soil samples numbered from west to east (AC01 to AC10).
[b] Railroad soil samples numbered from north to south (RR01,02 to RR14,15,16).

ELEMENTAL ANALYSIS RESULTS

Results of elemental analysis by STAT Analysis Corp (EPA, 2014a and b) using ICP-MS are presented in **Table 5**. Elemental data reports from STAT Analysis Corp indicated that all quality control (QC) results were within acceptable limits established by EPA Method 6020, indicating the precision and accuracy of the analyses were within the ranges listed in Table 5 of EPA Method 6020 for solid matrices. Extraction and measurement bias was assumed to be consistent throughout the analysis of soil samples from all locations. In particular, residential soils were analyzed independent of the Res 1, Res 2, and Res 3 groupings because these subdivisions were only defined after the completion of the elemental analysis (Canar et al., 2014; EPA, 2014b). Conclusions made regarding the elemental data were based on elemental relationships in which individual sample measurement uncertainty was negligible. The strength of the elemental relationships observed and the associated statistical significance were indicated by the Spearman rank correlation coefficients (r_s) and p-values, respectively.

Table 5. ELEMENTAL ANALYSIS RESULTS[a]
Characterization of Lead in Soils
Pilsen Neighborhood, Chicago, Illinois

Field Sample ID	LIMS No.	Sampling Date	Sampling Area	Sample Description	Pb (mg/kg)	Sb (mg/kg)	Cd (mg/kg)	Cr (mg/kg)	Cu (mg/kg)	Sn (mg/kg)	Zn (mg/kg)
BH 1	N105006-05	3/17/2011	H. Kramer baghouse 1	Rotary furnace	51000	75.0	1500	44	12000	5800	600000
BH 2	N105006-06	3/17/2011	H. Kramer baghouse 2	Rotary furnace	42000	68.0	1100	90	12000	11000	550000
BH 4	N105006-08	3/17/2011	H. Kramer baghouse 4	Electric induction furnace	12000	180	510	92	62000	5800	400000
BH 4 duplicate	N105006-09	3/17/2011	H. Kramer baghouse 4	Electric induction furnace	13000	140	500	71	61000	5100	480000
BH 5	N105006-07	3/17/2011	H. Kramer baghouse 5	Rotary furnace	34000	49	700	<18	<4400	6300	650000
PA-AC01(0-6)-121912	N312001-CK	12/19/2012	Alley	Composite	2700	<25	10	1600	870	120	4800
PA-AC02(0-6)-121912	N312001-CM	12/19/2012	Alley	Composite	1900	<22.0	18	1700	1100	150	4400
PA-AC03(0-6)-121912	N312001-CO	12/19/2012	Alley	Composite	5600	290	42.0	260	8400	1100	8100
PA-AC03HS(0-6)-121912	N312001-DY	12/19/2012	Alley	Composite	2600	13	17	380	1500	190	4800
PA-AC04(0-6)-121912	N312001-CP	12/19/2012	Alley	Composite	5000	78	40	150	5400	600	14000
PA-AC05(0-6)-121912	N312001-EA	12/19/2012	Alley	Composite	3900	29	25	110	5700	480	13000
PA-AC06(0-6)-121912	N312001-CQ	12/19/2012	Alley	Composite	3000	130	18	53	1900	1600	5300
PA-AC07(0-6)-121912	N312001-01	12/19/2012	Alley	Composite	940	<24	9.3	24	2100	130	2600
PA-AC08(0-6)-121912	N312001-CR	12/19/2012	Alley	Composite	570	<21	4.5	17	660	65	1700
PA-AC09(0-6)-121912	N312001-02	12/19/2012	Alley	Composite	340	<19	2.1	11	580	37	750
PA-AC10(0-6)-121912	N312001-CS	12/19/2012	Alley	Composite	63	<19	<0.96	7	230	14	180
PA-RR01,02(0-6)-050613	N312001-BV	5/6/2013	Railroad	Composite	4000	19	16	64	9400	1300	26000
PA-RR04,06(0-6)-050613	N312001-BX	5/6/2013	Railroad	Composite	11000	18	140	56	11000	980	78000
PA-RR07,08(0-6)-050613	N312001-CV	5/6/2013	Railroad	Composite	6800	12	71	45	6500	540	46000
PA-RR10,12(0-6)-050613	N312001-BR	5/6/2013	Railroad	Composite	1800	14	17	53	1000	150	3800
PA-RR11,13(0-6)-050613	N312001-BQ	5/6/2013	Railroad	Composite	940	6.4	9.3	220	650	70	2200
PA-RR14,15,16(0-6)-050613	N312001-BP	5/6/2013	Railroad	Composite	1500	4.7	9.5	900	770	130	5800
PA-RR01,02(6-24)-050613	N312001-BW	5/6/2013	Railroad	Composite	1700	7.4	6.1	34	3700	560	17000
PA-RR04,06(6-24)-050613	N312001-BY	5/6/2013	Railroad	Composite	1700	<4.1	16	27	1800	240	9900
PA-RR07,08(6-24)-050613	N312001-BU	5/6/2013	Railroad	Composite	5500	9.0	49	43	3700	450	24000
PA-RR10,12(6-24)-050613	N312001-BT	5/6/2013	Railroad	Composite	2400	34	12	35	980	170	2200
PA-RR11,13(6-24)-050613	N312001-BS	5/6/2013	Railroad	Composite	1000	8.8	8.6	43	360	110	1100
PA-RR14,15,16(6-24)-050613	N312001-CG	5/6/2013	Railroad	Composite	2200	5.2	11	2000	900	120	4700
PA-122-01(0-6)-050313	N312001-14	5/3/2013	Res 1	Back yard	1900	<2.3	6.7	36	540	57	3000
PA-127-01(0-6)-050313	N312001-CY	5/3/2013	Res 1	Back yard	2500	2.6	7.6	26	520	61	3200
PA-180-01(0-6)-050213	N312001-CB	5/2/2013	Res 1	Yard (east 1/2 vacant lot)	810	42	6.0	28	300	36	2300
PA-180-02(0-6)-050213	N312001-CF	5/2/2013	Res 1	Yard (west 1/2 vacant lot)	3000	<2.2	6.5	18	330	140	2800

Table 5. ELEMENTAL ANALYSIS RESULTS[a]
Characterization of Lead in Soils
Pilsen Neighborhood, Chicago, Illinois

Field Sample ID	LIMS No.	Sampling Date	Sampling Area	Sample Description	Pb (mg/kg)	Sb (mg/kg)	Cd (mg/kg)	Cr (mg/kg)	Cu (mg/kg)	Sn (mg/kg)	Zn (mg/kg)
PA-186-01(0-6)-050213	N312001-95	5/2/2013	Res 1	Front yard	360	<2.2	1.9	23	180	19	970
PA-186-02(0-6)-050213	N312001-DA	5/2/2013	Res 1	Back yard	320	<2.3	2.0	19	160	20	900
PA-191-01(0-6)-050213	N312001-DC	5/2/2013	Res 1	Back yard	2000	39	14	28	1100	120	7200
PA-193-01(0-6)-050313	N312001-13	5/3/2013	Res 1	Back yard	580	<2.3	2.3	30	210	19	1000
PA-272-01(0-6)-050113	N312001-DD	5/1/2013	Res 1	Back yard	2000	33	6.7	21	520	190	2500
PA-274-01(0-6)-050113	N312001-DE	5/1/2013	Res 1	Back yard	1900	3.6	12	55	1100	110	4900
PA-276-01(0-6)-050113	N312001-DG	5/1/2013	Res 1	Back yard	2400	13	17	49	1600	200	6300
PA-291-01(0-6)-050113	N312001-DH	5/1/2013	Res 1	Front yard	500	<2.4	3.1	24	100	39	620
PA-370-01(0-6)-050713	N312001-DL	5/7/2013	Res 1	Back yard	700	<4.6	6.9	44	150	28	1600
PA-375-01(0-6)-050713	N312001-DQ	5/7/2013	Res 1	Back yard	1800	<4.9	11	40	680	84	2900
PA-104-01(0-6)-050213	N312001-94	5/2/2013	Res 2	Front yard	930	2.3	6.0	24	190	34	1500
PA-104-02(0-6)-050213	N312001-CW	5/2/2013	Res 2	Back yard	1400	2.8	7.6	33	340	53	2400
PA-105-01(0-6)-050213	N312001-93	5/2/2013	Res 2	Front yard	640	<2.2	2.1	23	99	30	930
PA-105-02(0-6)-050213	N312001-12	5/2/2013	Res 2	Back yard	990	<2.3	2.6	28	240	21	1100
PA-125-01(0-6)-050313	N312001-CC	5/3/2013	Res 2	Yard (west 1/2 lot)	1500	4.7	10	61	410	63	2900
PA-125-02(0-6)-050313	N312001-CX	5/3/2013	Res 2	Yard (east 1/2 lot)	1100	3.1	7.4	51	280	50	2200
PA-14-01(0-6)-050913	N312001-51	5/9/2013	Res 2	Back yard	140	<4.7	<1.2	18	55	13	220
PA-14-02(0-6)-050913	N312001-CZ	5/9/2013	Res 2	Front yard	480	<5.9	<1.5	24	96	<15	520
PA-141-01(0-6)-050713	N312001-CD	5/7/2013	Res 2	Yard (west 1/2 lot)	860	<4.7	3.3	33	200	39	700
PA-141-02(0-6)-050713	N312001-CI	5/7/2013	Res 2	Yard (east 1/2 lot)	1600	<4.6	3.5	40	190	26	970
PA-304-01(0-6)-050913	N312001-DI	5/9/2013	Res 2	Back yard	58	<4.2	<1.0	13	27	<10	130
PA-349-01(0-6)-050713	N312001-DJ	5/7/2013	Res 2	Front yard	890	<5	5.4	29	250	28	1800
PA-349-03(0-6)-050713	N312001-46	5/7/2013	Res 2	Back yard	1400	<4.2	2.5	27	99	19	930
PA-369-01(0-2)-050713	N312001-45	5/7/2013	Res 2	Back yard	480	<4.8	<1.2	<24	100	<12	560
PA-369-01(0-6)-050713	N312001-DK	5/7/2013	Res 2	Back yard	1500	<5.3	7.5	43	440	52	1700
PA-369-03,04(0-6)-050713	N312001-91	5/7/2013	Res 2	Front yard	2300	<4.6	5.8	24	410	49	2700
PA-371-01(0-6)-050713	N312001-DO	5/7/2013	Res 2	Back yard	1800	<5.1	7.7	40	450	49	2800
PA-371-02(0-6)-050713	N312001-DP	5/7/2013	Res 2	Front yard	320	<5.3	<1.3	14	54	<13	360
PA-466-01(0-6)-050913	N312001-DT	5/9/2013	Res 2	Yard (east 1/2 lot)	730	<4.5	3.4	23	210	25	900
PA-466-02(0-6)-050913	N312001-CE	5/9/2013	Res 2	Yard (west 1/2 lot)	650	<4.3	2.8	47	120	23	780
PA-467-01(0-6)-050913	N312001-49	5/8/2013	Res 2	Back yard	1400	5.2	7.0	55	250	34	1600
PA-468-01(0-6)-050913	N312001-50	5/8/2013	Res 2	Back yard	1300	5.2	5.9	36	290	30	1600
PA-470-01(0-6)-070913	N312001-15	7/9/2013	Res 2	Back yard	3200	<5.2	12	39	430	120	3500
PA-483-01(0-6)-071213	N312001-29	7/12/2013	Res 2	Back yard	200	<4.1	1.2	17	35	<10	180
PA-84-01(0-6)-050813	N312001-DX	5/8/2013	Res 2	Front yard	600	<4.5	2.0	19	56	30	470

Table 5. ELEMENTAL ANALYSIS RESULTS[a]
Characterization of Lead in Soils
Pilsen Neighborhood, Chicago, Illinois

Field Sample ID	LIMS No.	Sampling Date	Sampling Area	Sample Description	Pb (mg/kg)	Sb (mg/kg)	Cd (mg/kg)	Cr (mg/kg)	Cu (mg/kg)	Sn (mg/kg)	Zn (mg/kg)
PA-84-02(0-6)-050813	N312001-47	5/8/2013	Res 2	Back yard	1100	<4.5	4.5	31	110	26	880
PA-92-01(0-6)-050813	N312001-BN	5/8/2013	Res 2	Back yard	880	<4.5	4.9	25	170	140	1300
PA-464-01(0-6)-050813	N312001-CA	5/8/2013	Res 3	Yard (east 1/2 lot)	910	8.6	3.2	21	170	36	750
PA-464-02(0-6)-050813	N312001-DR	5/8/2013	Res 3	Yard (west 1/2 lot)	240	<4.3	1.9	22	74	15	260
PA-465-01(0-6)-050913	N312001-BZ	5/9/2013	Res 3	Yard	370	<4.7	1.7	46	84	17	300
PA-469-01(0-6)-051013	N312001-CH	5/10/2013	Res 3	Field - NW quadrant	130	<4.5	<1.1	35	56	14	180
PA-469-02(0-6)-051013	N312001-84	5/10/2013	Res 3	Field - NE quadrant	100	<4.6	<1.1	17	44	13	170
PA-469-03(0-6)-051013	N312001-88	5/10/2013	Res 3	Field - SW Quadrant	120	<4.9	<1.2	19	50	17	160
PA-469-04(0-6)-051013	N312001-87	5/10/2013	Res 3	Field - SE quadrant	110	<4.8	<1.2	34	59	12	190
PA-482-01(0-6)-071113	N312001-AA	7/11/2013	Res 3	Front yard	210	<4.5	3.7	24	66	13	380
PA-495-01(0-6)-081313	N312001-55	8/13/2013	Res 3	Back yard	930	<3.8	2.6	25	56	16	430
PA-496-01(0-6)-081313	N312001-57	8/13/2013	Res 3	Back yard	230	<4.4	2.8	19	64	11	380
PA-497-01(0-6)-081313	N312001-58	8/13/2013	Res 3	Back yard	460	<4.4	2.2	18	53	15	350
PA-498-01(0-6)-081313	N312001-59	8/13/2013	Res 3	Back yard	270	<3.9	1.5	16	38	<9.7	200
PA-499-01(0-6)-081413	N312001-AP	8/14/2013	Res 3	Front yard	1200	<4.5	2.5	14	86	26	500
PA-504-01(0-6)-081513	N312001-AT	8/15/2013	Res 3	Front yard	390	<4.8	1.8	21	41	26	240
PA-505-01(0-6)-081513	N312001-66	8/15/2013	Res 3	Back yard	1300	<5.3	5.5	53	170	33	1300
PA-506-01(0-6)-081513	N312001-68	8/15/2013	Res 3	Back yard	940	<4.6	4.1	28	94	17	780
PA-508-01(0-6)-081513	N312001-70	8/15/2013	Res 3	Back yard	580	<4.4	2.7	26	52	<11	400
PA-509-01(0-6)-081513	N312001-72	8/15/2013	Res 3	Back yard	1400	<5.0	4.7	40	120	53	830
PA-510-01(0-6)-081513	N312001-AU	8/15/2013	Res 3	Front yard	1700	<4.3	4.1	28	100	25	790
PA-514-01(0-6)-081613	N312001-73	8/16/2013	Res 3	Back yard	410	<4.3	2.1	23	59	<11	370
PA-515-01(0-6)-081613	N312001-75	8/16/2013	Res 3	Back yard	1600	9.2	7.4	22	140	29	1100
PA-471-01(0-6)-070913	N312001-16	7/9/2013	Harrison Park	Back yard	1900	<5.4	7.2	46	230	40	2000
PA-472-01(0-6)-070913	N312001-17	7/9/2013	Harrison Park	Back yard	940	<4.6	5.6	45	130	52	1100
PA-473-01(0-6)-070913	N312001-19	7/9/2013	Harrison Park	Back yard	1700	<5.2	9.1	87	160	43	970
PA-474-01(0-6)-071013	N312001-22	7/10/2013	Harrison Park	Back yard	2600	<5.1	3.5	34	130	180	870
PA-474-02(0-6)-071013	N312001-23	7/10/2013	Harrison Park	Front yard	2200	<4.9	3.1	26	95	24	740
PA-475-01(0-6)-071013	N312001-24	7/10/2013	Harrison Park	Back yard	3700	<5.0	6.6	53	160	55	1700
PA-476-01(0-6)-071013	N312001-25	7/10/2013	Harrison Park	Back yard	2000	<5.0	8.5	34	170	32	1800
PA-477-01(0-6)-071013	N312001-26	7/10/2013	Harrison Park	Back yard	1700	<5.1	4.1	42	98	26	720
PA-478-01(0-6)-071013	N312001-AN	7/10/2013	Harrison Park	Front & back composite	1400	<4.3	17	220	230	42	1400
PA-479-01(0-6)-071113	N312001-98	7/11/2013	Harrison Park	Front yard	1200	<4.3	5.3	53	140	33	970

Table 5. ELEMENTAL ANALYSIS RESULTS[a]
Characterization of Lead in Soils
Pilsen Neighborhood, Chicago, Illinois

Field Sample ID	LIMS No.	Sampling Date	Sampling Area	Sample Description	Pb (mg/kg)	Sb (mg/kg)	Cd (mg/kg)	Cr (mg/kg)	Cu (mg/kg)	Sn (mg/kg)	Zn (mg/kg)
PA-480-01(0-6)-071113	N312001-AA	7/11/2013	Harrison Park	Front yard	3200	<4.8	4.9	58	180	37	1300
PA-481-01(0-6)-071113	N312001-29	7/11/2013	Harrison Park	Back yard	1600	<4.5	5.4	30	120	36	1300
PA-484-01(0-6)-071213	N312001-31	7/12/2013	Harrison Park	Back yard	1700	5.4	75	770	740	110	2300
PA-485-01(0-6)-071213	N312001-33	7/12/2013	Harrison Park	Back yard	510	<4.8	1.8	21	100	<12	390
PA-486-01(0-6)-071213	N312001-34	7/12/2013	Harrison Park	Back yard	880	<4.7	4.4	32	130	26	840
PA-487-01(0-6)-071513	N312001-37	7/15/2013	Harrison Park	Back yard	1400	<5.0	3.1	<25	140	65	600
PA-488-01(0-6)-071513	N312001-AC	7/15/2013	Harrison Park	Front yard	410	<4.7	1.7	<24	56	17	390
PA-502-01(0-6)-081413	N312001-64	8/14/2013	Harrison Park	Back yard	780	<4.8	7.3	60	300	20	610
PA-503-01(0-6)-081413	N312001-AR	8/14/2013	Harrison Park	Front yard	1400	<4.7	6.1	25	130	21	830
PA-507-01(0-6)-081513	N312001-69	8/15/2013	Harrison Park	Back yard	270	<4.0	3.2	15	48	<9.9	280
PA-516-01(0-6)-081613	N312001-76	8/16/2013	Harrison Park	Back yard	520	<4.8	5.3	32	70	<12	500
PA-490-01(0-6)-081213	N312001-AH	8/12/2013	Little Italy	Front yard	220	<4.4	1.6	19	33	<11	150
PA-491-01(0-6)-081213	N312001-AI	8/12/2013	Little Italy	Front yard	260	<4.8	1.8	21	68	16	270
PA-492-01(0-6)-081313	N312001-AL	8/13/2013	Little Italy	Front yard	260	<4.4	2.7	24	66	13	210
PA-493-01(0-6)-081313	N312001-AM	8/13/2013	Little Italy	Front yard	190	<4.3	1.8	16	45	<11	170
PA-494-01(0-6)-081313	N312001-79	8/13/2013	Little Italy	Back yard common area	120	<4.6	2.0	33	46	<12	170
PA-500-01(0-6)-081413	N312001-62	8/14/2013	Little Italy	Back yard	760	<4.4	3.4	26	72	27	620
PA-501-01(0-6)-081413	N312001-AQ	8/14/2013	Little Italy	Front yard	66.0	<5.2	1.4	22	28	<13	150
PA-511-01(0-6)-081613	N312001-AU	8/16/2013	Little Italy	Front yard	210	<4.4	1.7	21	40	<11	170
PA-512-01(0-6)-081613	N312001-AW	8/16/2013	Little Italy	Front yard	320	<4.7	1.7	19	37	<12	230
PA-513-01(0-6)-081613	N312001-AX	8/16/2013	Little Italy	Front yard	170	4.2	1.4	31	45	<10	200
H. Kramer slag data – lower range[b]	n.a.[c]	n.a.[c]	H. Kramer	Slag	10000[b]	n.a.[c]	n.a.[c]	n.a.[c]	150000[b]	2500[b]	17500[b]
H. Kramer slag data – upper range[b]	n.a.[c]	n.a.[c]	H. Kramer	Slag	20000[b]	n.a.[c]	n.a.[c]	n.a.[c]	180000[b]	10000[b]	25000[b]
H. Kramer slag data – typical[b]	n.a.[c]	n.a.[c]	H. Kramer	Slag	12000[b]	n.a.[c]	n.a.[c]	n.a.[c]	160000[b]	4000[b]	20000[b]

[a] Metals data for unsieved soil samples from STAT Analysis Corp by SW 846 6020 ICP-MS (EPA, 2014a and b).
[b] Data of slag material composition provided by H. Kramer (2014a), representing a typical average and range of values.
[c] n.a. = not applicable/available.

Correlation Analysis Results

Spearman's rank correlation coefficients determined for the soil samples in the Pilsen neighborhood are presented in **Tables 6a** and **b**. **Table 6a** shows strong correlation of Pb with Cd, Cu, Sn, and Zn for alley, railroad, and Res 1 soils and strong to moderate correlation for Res 2 and Res 3 soils. Strong correlation indicated these four metals were co-contaminants and were likely added to soils from a single material or process (USGS, 2003; Thorbjornsen and Myers, 2007a). In contrast, Pb versus Cd, Cu, and Sn showed much weaker correlations, with less statistical significance in Harrison Park and Little Italy soils. Moderate to strong correlation for only Pb with Zn was observed in Harrison Park and Little Italy soils, supporting Harrison Park and Little Italy as non-receptor sites with respect to Pb contamination in alley, railroad, Res 1, Res 2, and Res 3 receptor areas.

Spearman's rank correlation coefficients for Pb concentration versus Cd/Pb, Cu/Pb, Sn/Pb, or Zn/Pb (Table 6b) indicated strong negative correlations for Res 3 and Little Italy and moderate to strong negative correlations for Harrison Park. Ratios of Cd/Pb, Cu/Pb, Sn/Pb, and Zn/Pb decreased with increasing Pb concentrations and suggested the presence of Pb with a different relationship (or no relationship) to Cd, Cu, Sn, and Zn compared to alley, railroad, Res 1, and Res 2 soil areas. The general lack of correlation of Pb vs Cr and the strong negative correlation of Pb vs Cr/Pb in most sampling areas indicated Cr was not associated with the Pb contamination.

These correlation coefficients were useful in evaluating elemental relationships illustrated in scatterplots in **Figures 21–27**.

Table 6a. SPEARMAN'S RANK CORRELATION COEFFICIENTS (r_s)[a]
Additional Characterization of Lead in Soils
Pilsen Neighborhood, Chicago, Illinois

	Pb Alley Soils	Pb Railroad Soils (0–6 inches)	Pb Res 1 Soils	Pb Res 2 Soils	Pb Res 3 Soils	Pb Harrison Park Soils	Pb Little Italy Soils
Sb	0.74 (0.1530) n=5	0.66 (0.1562) n=6	-0.65 (0.1646) n=6	0.51 (0.3056) n=6	n.a.[b] n=2	n.a.[b] n=1	n.a.[b] n=1
Cd	0.94 (<0.0001) n=10	0.94 (0.0048) n=6	0.69 (0.0068) n=14	0.75 (<0.0001) n=22	0.65 (0.0048) n=17	0.30 (0.1809) n=21	0.52 (0.1196) n=10
Cu	0.87 (0.0005) n=11	0.94 (0.0048) n=6	0.70 (0.0057) n=14	0.85 (<0.0001) n=27	0.64 (0.0017) n=21	0.44 (0.0445) n=21	0.46 (0.1839) n=10
Cr	0.59 (0.0556) n=11	-0.66 (0.1562) n=6	0.08 (0.7902) n=14	0.72 (<0.0001) n=26	0.24 (0.2922) n=21	0.35 (0.1476) n=19	-0.24 (0.5125) n=10
Sn	0.89 (0.0002) n=11	0.83 (0.0416) n=6	0.85 (0.0001) n=14	0.49 (0.0201) n=22	0.78 (0.0002) n=18	0.45 (0.0583) n=18	0.87 (0.3333) n=3
Zn	0.97 (<0.0001) n=11	0.94 (0.0048) n=6	0.80 (0.0006) n=14	0.88 (<0.0001) n=27	0.90 (<0.0001) n=21	0.68 (0.0007) n=21	0.77 (0.0099) n=10

[a] p-values given in parentheses;
n = number of sample results over detection limit used in evaluation;
strong correlations (-0.70 > r_s > 0.70) at 95% confidence (p-value < 0.05) in colored text.
[b] n.a. = not applicable due to small n, number of samples.

Table 6b. SPEARMAN'S RANK CORRELATION COEFFICIENTS (r_s)[a]
Additional Characterization of Lead in Soils
Pilsen Neighborhood, Chicago, Illinois

	Pb Alley Soils	Pb Railroad Soils (0–6 inches)	Pb Res 1 Soils	Pb Res 2 Soils	Pb Res 3 Soils	Pb Harrison Park Soils	Pb Little Italy Soils
Sb/Pb	0.74 (0.1530) n=5	-0.70 (0.1248) n=6	-0.65 (0.1646) n=6	0.26 (0.6141) n=6	n.a.[b] n=2	n.a.[b] n=1	n.a.[b] n=1
Cd/Pb	-0.13 (0.7261) n=10	0.49 (0.3287) n=6	-0.35 (0.2206) n=14	-0.17 (0.4518) n=22	-0.84 (<0.0001) n=17	-0.58 (0.0055) n=21	-0.84 (0.0024) n=10
Cu/Pb	-0.38 (0.2466) n=11	0.66 (0.1562) n=6	-0.13 (0.6521) n=14	-0.12 (0.5365) n=27	-0.91 (<0.0001) n=21	-0.75 (<0.0001) n=21	-0.81 (0.0041) n=10
Cr/Pb	-0.17 (0.6203) n=11	-0.94 (0.0048) n=6	-0.92 (<0.0001) n=14	-0.77 (<0.0001) n=26	-0.93 (<0.0001) n=21	-0.67 (0.0019) n=19	-0.90 (0.0004) n=10
Sn/Pb	0.12 (0.7293) n=11	0.49 (0.3287) n=6	-0.05 (0.8633) n=14	-0.55 (0.0087) n=22	-0.91 (<0.0001) n=18	-0.47 (0.0473) n=18	-0.87 (0.3333) n=3
Zn/Pb	-0.35 (0.2981) n=11	0.83 0.0416 n=6	-0.33 (0.2420) n=14	-0.08 (0.7094) n=27	-0.78 (<0.0001) n=21	-0.49 (0.0234) n=21	-0.70 (0.0245) n=10

[a] p-values given in parentheses;
n = number of sample results over detection limit used in evaluation;
strong correlations (-0.70 > r_s > 0.70) at 95% confidence (p-value < 0.05) in colored text.
[b] n.a. = not applicable due to small n, number of samples.

Scatterplots

The application of log-log scatterplots of relevant concentration pairs and suspected contaminant concentration versus elemental ratio plots was well documented by Seeley et al. (1972) and others (Schiff and Weisberg, 1999; Myers and Thorbjornsen, 2004; Thorbjornsen and Myers, 2006, 2007a and b; Machemer et al., 2007). The following log-log scatterplots using elemental data from **Table 5** (EPA, 2014a and b) were prepared and evaluated. Scatterplots of Pb concentrations versus Sb, Cd, Cu, Cr, Sn, and Zn concentrations were paired with associated scatterplots of Pb concentrations versus the concentration ratios of Sb/Pb, Cd/Pb, Cu/Pb, Cr/Pb, Sn/Pb, and Zn/Pb. Pb, Cd, Cu, Sn, and Zn were evaluated because of their association with brass and bronze foundries (Morris, 2004; H. Kramer, 2012 and 2014b). Pb versus Cu, Sn, and Zn scatterplots included the composition of slag material that was provided by H. Kramer (2014a) representing typical high, low, and average values (**Table 5**) and depicted by three points (red downward triangles). Concentrations of Sb, Cd, and Cr for H. Kramer slag were not available. However, because Cd is often associated with Zn-bearing scrap metal, Cd data patterns would be expected to be similar to the Zn data patterns. Zn was also evaluated because of its association with tire dust (Friedlander, 1973). Sb was evaluated because of its association with babbit and solder products and the smelting of antimonial Pb and battery Pb. Babbit and solder products were manufactured by Century, Loewenthal, and NL. Antimonial Pb and battery Pb smelting were also conducted by Loewenthal. Cr was evaluated because of its association with the historical use of leaded paint on homes and buildings.

The scatterplots of soil Pb concentration versus concentrations of Sb, Cd, Cu, Cr, Sn, and Zn illustrated relationships between the metals suggested by the correlation coefficients. The scatterplots of soil Pb concentration versus the ratio of (Element X)/Pb illustrated consistency or change in the ratio of (Element X)/Pb with increased soil Pb concentration, where (Element X) or (X) is Sb, Cd, Cu, Cr, Sn, or Zn. As a general guide, if a major source of Pb (contaminant or naturally occurring) did not contain a concomitant element, such as Sb, Cd, Cu, Cr, Sn, or Zn, the (X)/Pb ratios would decrease as soil Pb concentrations increased, revealing a negatively sloped trend with a moderate to strong correlation coefficient (r_s). However, if a major source of Pb contained a concomitant element, such as Sb, Cd, Cu, Cr, Sn, or Zn, the expected scatterplot would show a relatively narrow range of (X)/Pb ratios and poor correlation (r_s) with soil Pb concentration. A relatively narrow range of X/Pb ratios (little variation in the y-axis) appeared as random scatter or as a flat (horizontal) trend indicating X/Pb ratios were relatively constant with increasing soil Pb concentrations (x-axis). Such patterns indicated little, if any, relationship between (X)/Pb ratios and soil Pb concentrations, indicative of a major source of Pb containing the element (X).

Scatterplots of Pb concentrations (mg/kg) versus Cd, Cu, Sn, and Zn concentrations (mg/kg) of surface soils (0–6 inches) were paired with corresponding plots of Pb concentrations (mg/kg) versus ratios of Cd/Pb, Cu/Pb, Sn/Pb, and Zn/Pb and are presented in **Figures 21–27**.

H. Kramer baghouse dust results and H. Kramer slag data are shown in red for comparison. A list of each set of plots for each soil area in generally increasing distance from H. Kramer follows:

Figures 21a-f. Alley surface soils.

Figures 22a–f. Railroad surface soils.

Figures 23a-f. Res 1 surface soils.

Figures 24a-f. Res 2 surface soils.

Figures 25a-f. Res 3 surface soils.

Figures 26a-f. Harrison Park surface soils.

Figures 27a-f. Little Italy surface soils.

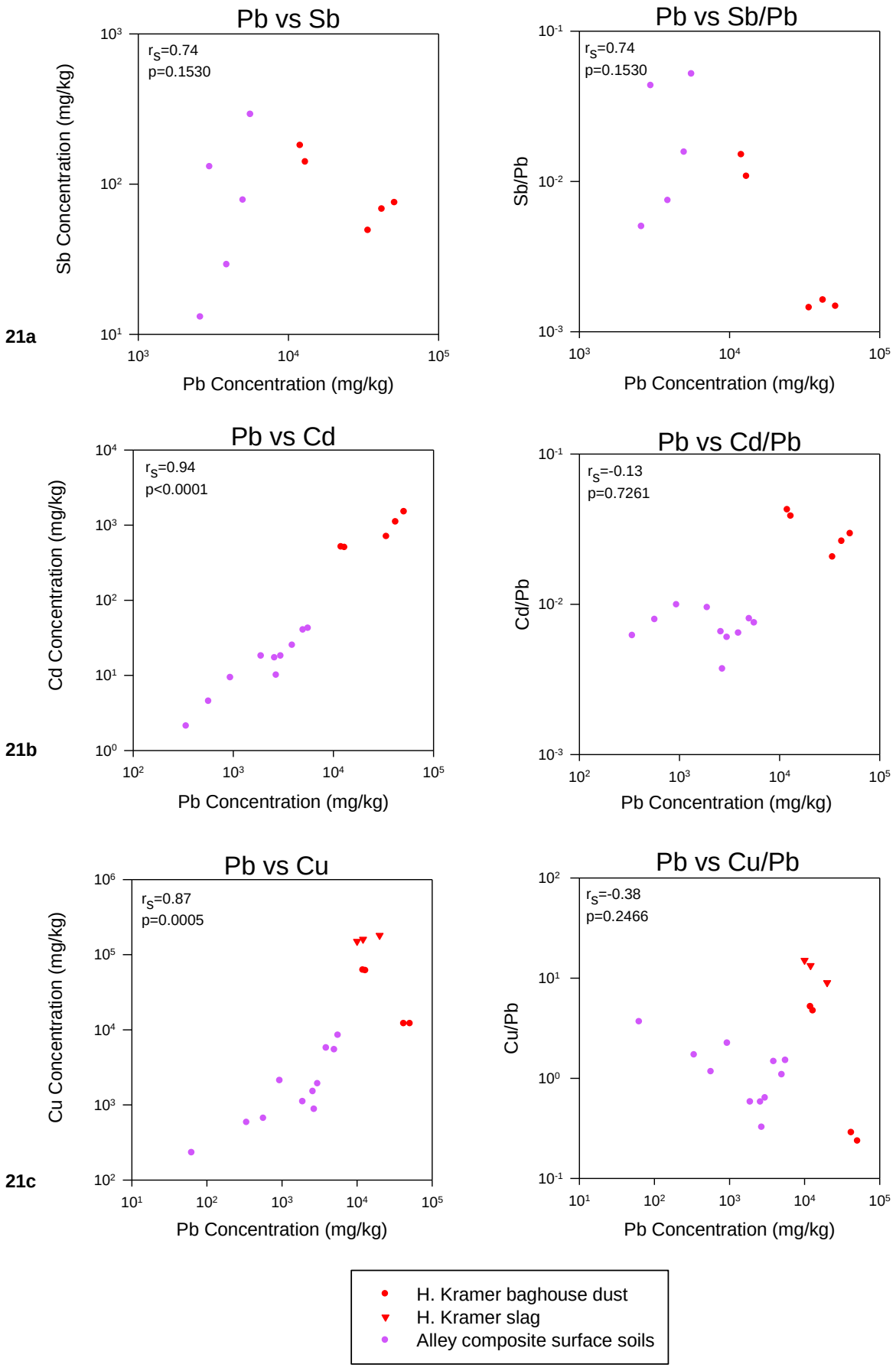

Figures 21a-c. Alley composite surface soils (0–6 inches). Slag composition from H. Kramer (2014a).

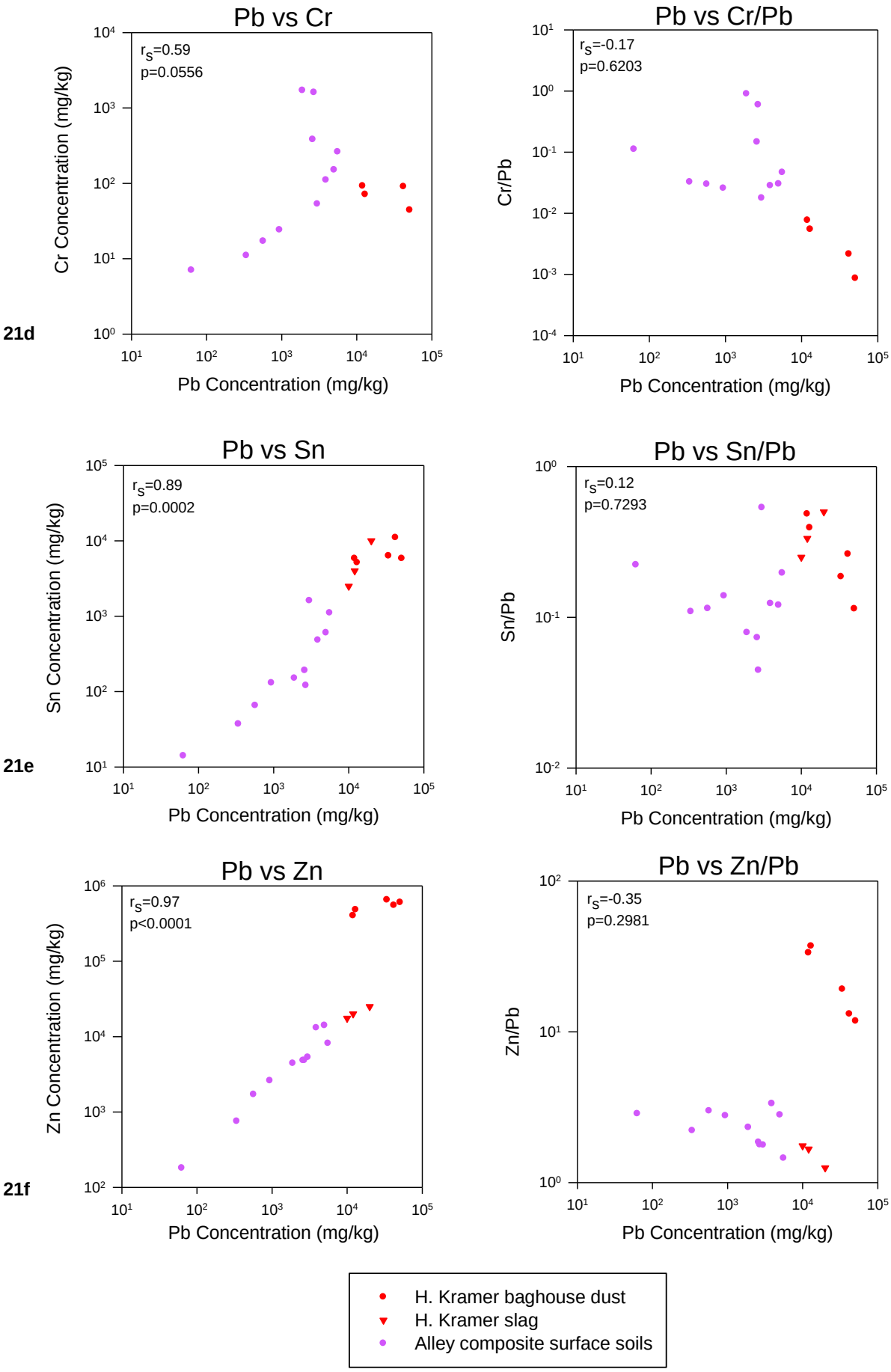

Figures 21d-f. Alley composite surface soils (0–6 inches). Slag composition from H. Kramer (2014a).

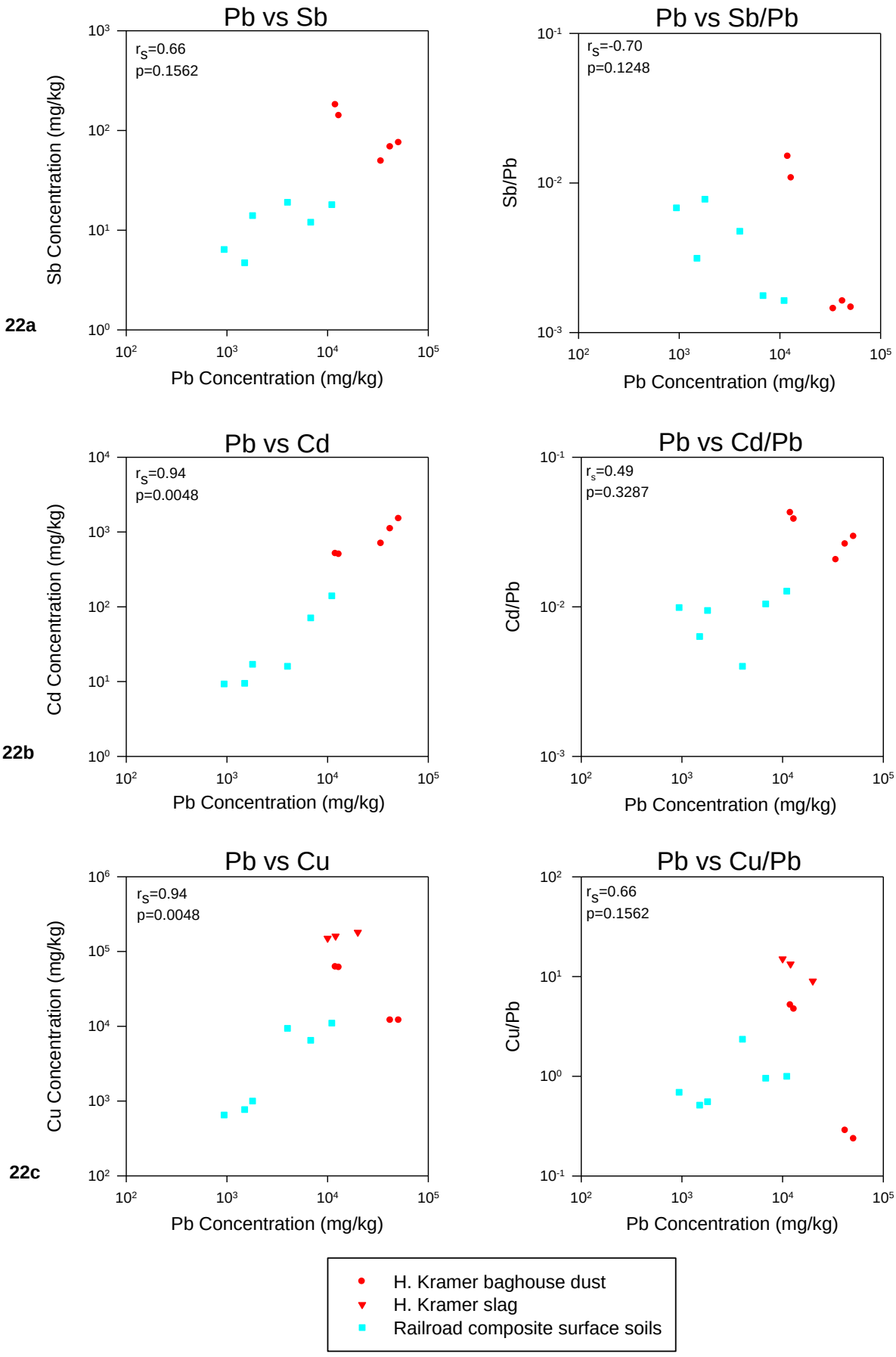

Figures 22a-c. Railroad composite surface soils (0–6 inches). Slag composition (H. Kramer, 2014a).

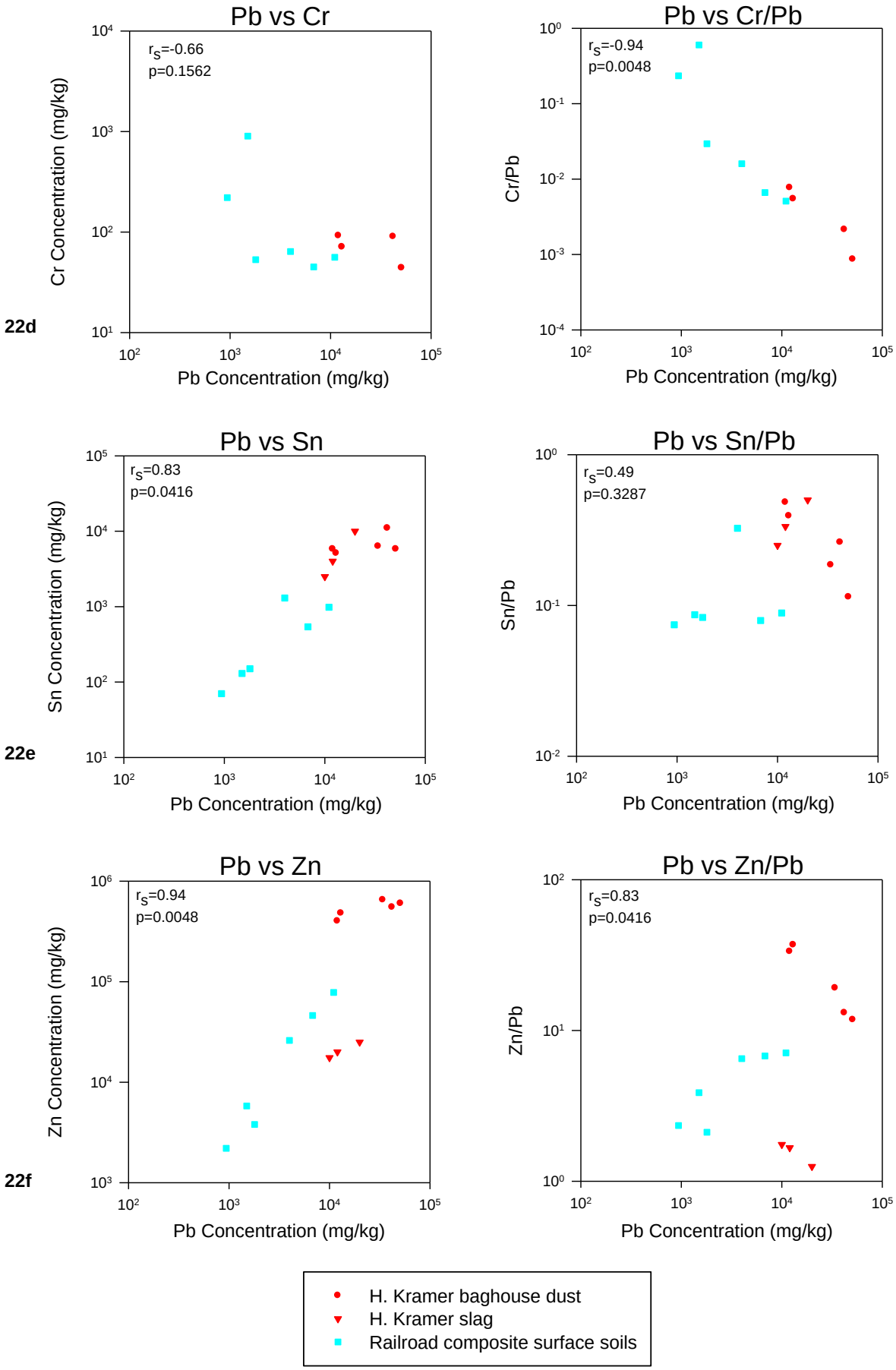

Figures 22d-f. Railroad composite surface soils (0–6 inches). Slag composition (H. Kramer, 2014a).

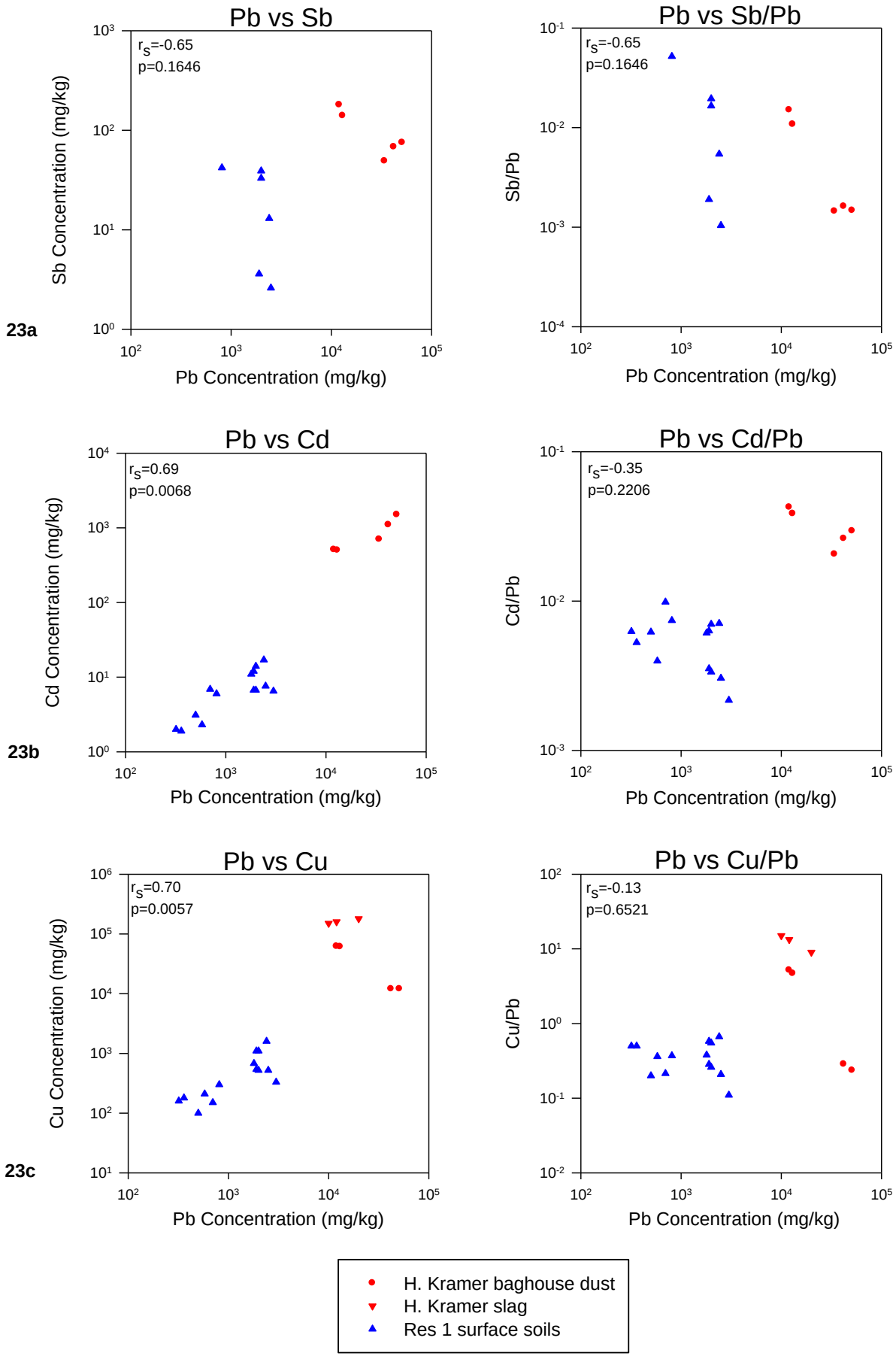

Figures 23a-c. Res 1 surface soils (0–6 inches). Slag composition from H. Kramer (2014a).

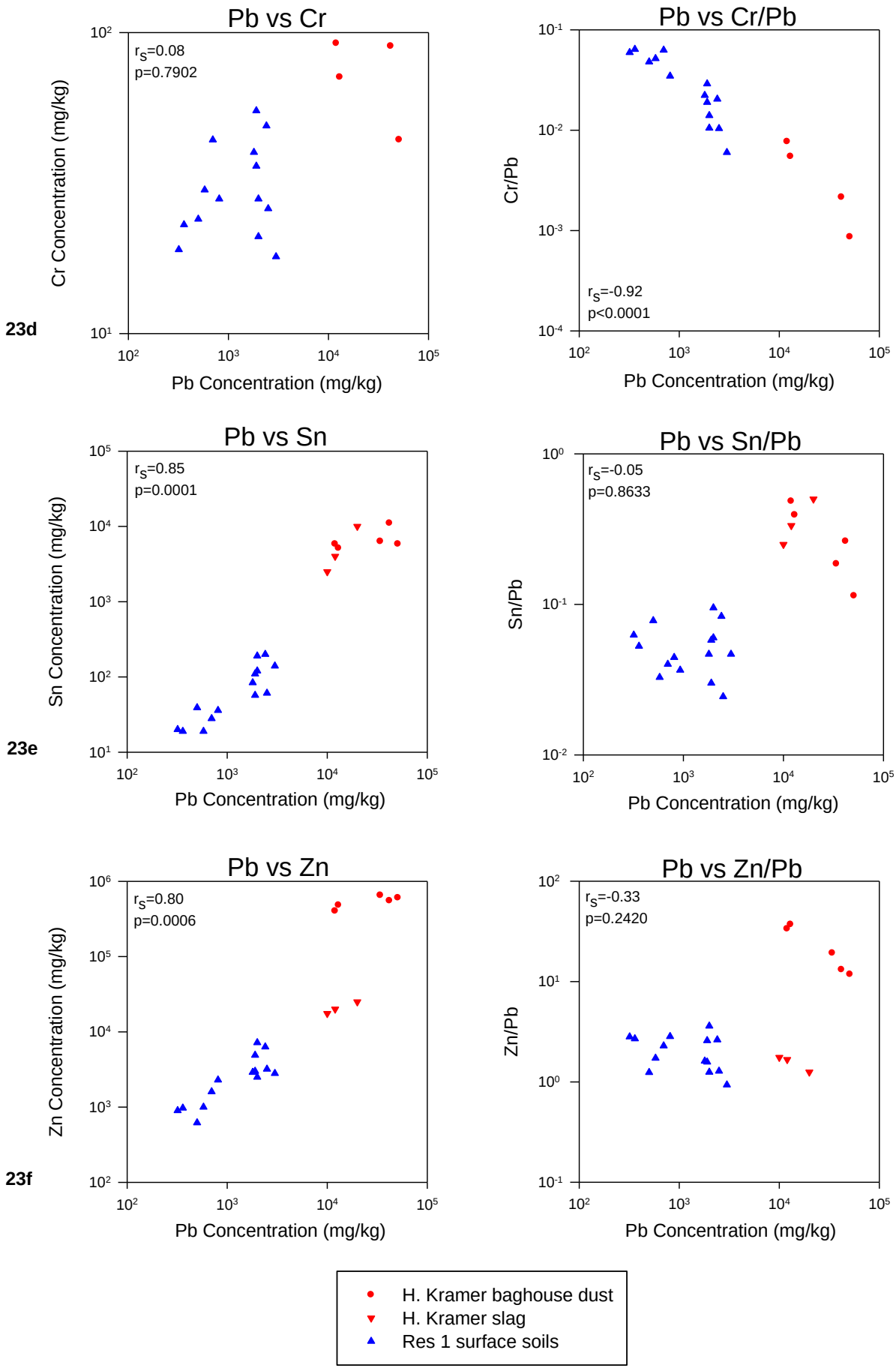

Figures 23d-f. Res 1 surface soils (0–6 inches). Slag composition from H. Kramer (2014a).

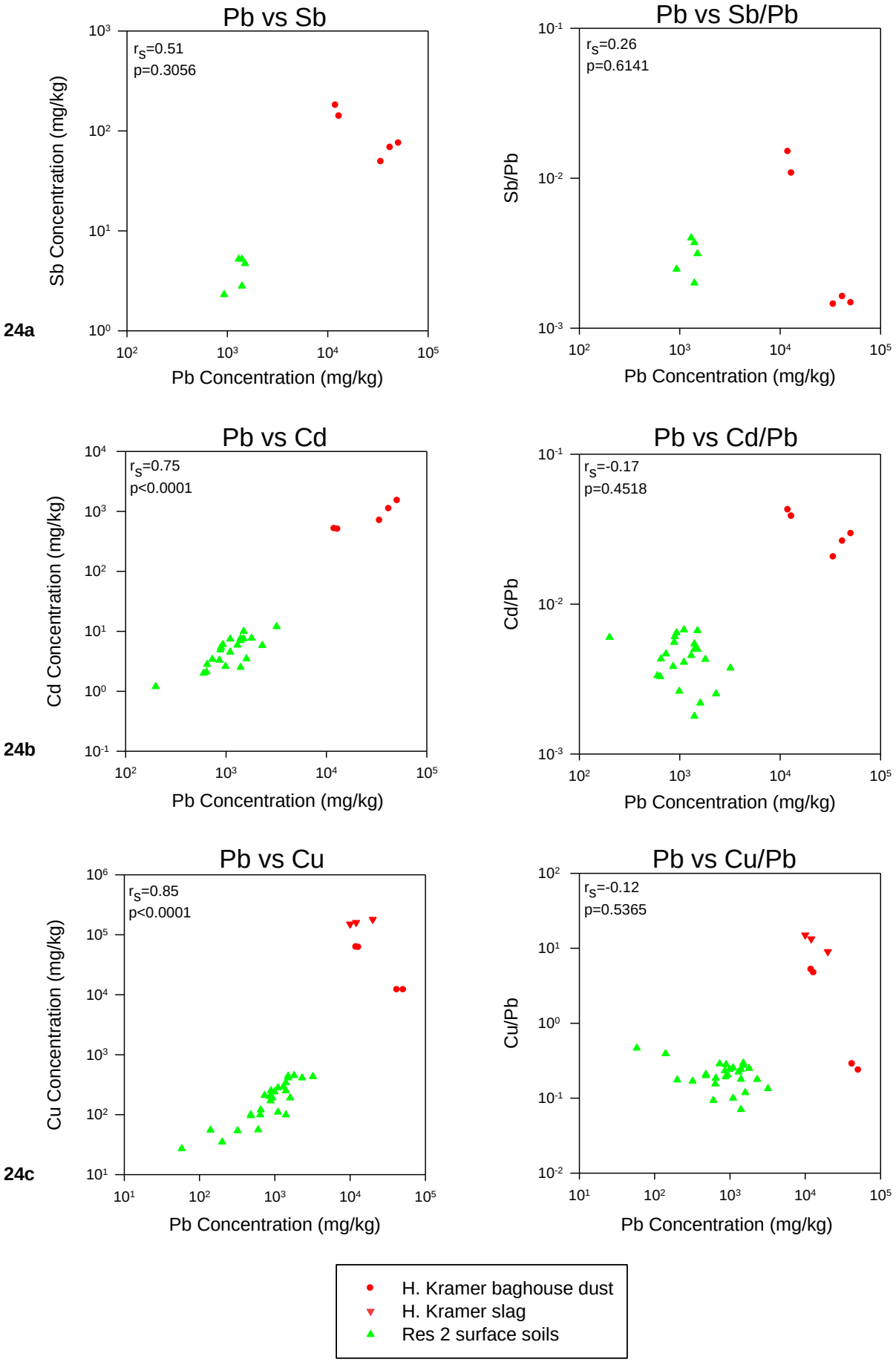

Figures 24a-c. Res 2 surface soils (0–6 inches). Slag composition from H. Kramer (2014a).

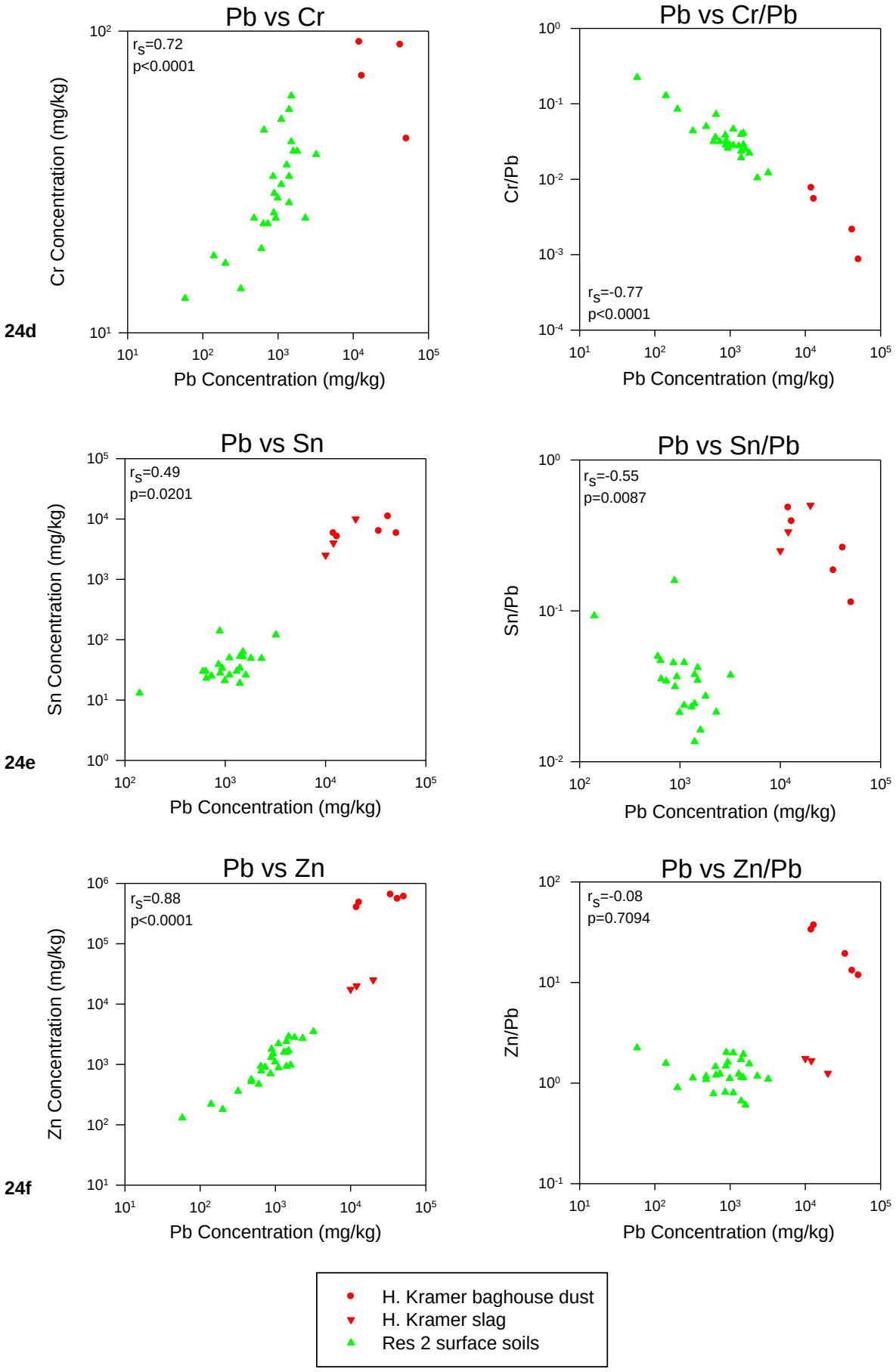

Figures 24d-f. Res 2 surface soils (0–6 inches). Slag composition from H. Kramer (2014a).

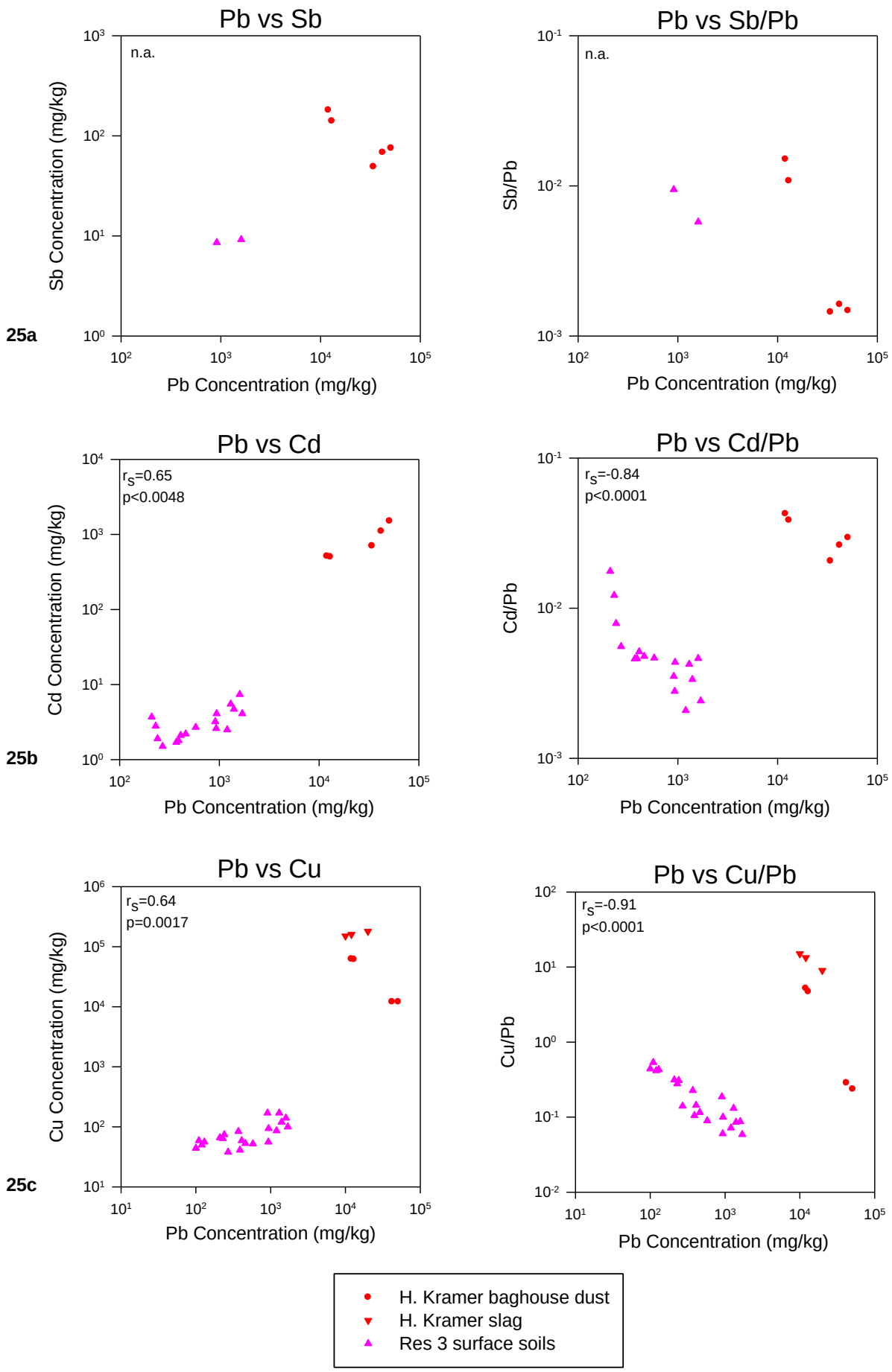

Figures 25a-c. Res 3 surface soils (0–6 inches). Slag composition from H. Kramer (2014a).

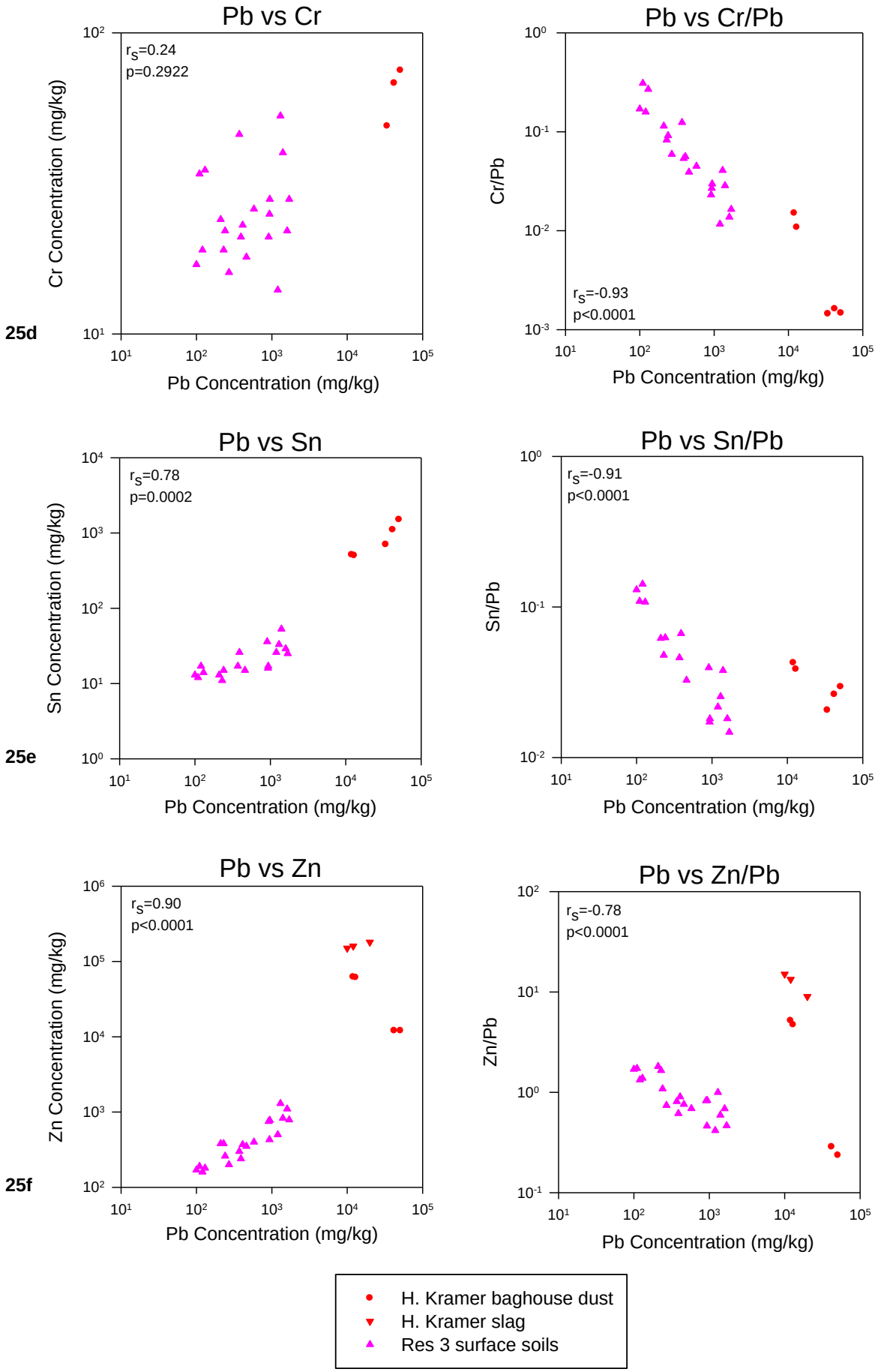

Figures 25d-f. Res 3 surface soils (0–6 inches). Slag composition from H. Kramer (2014a).

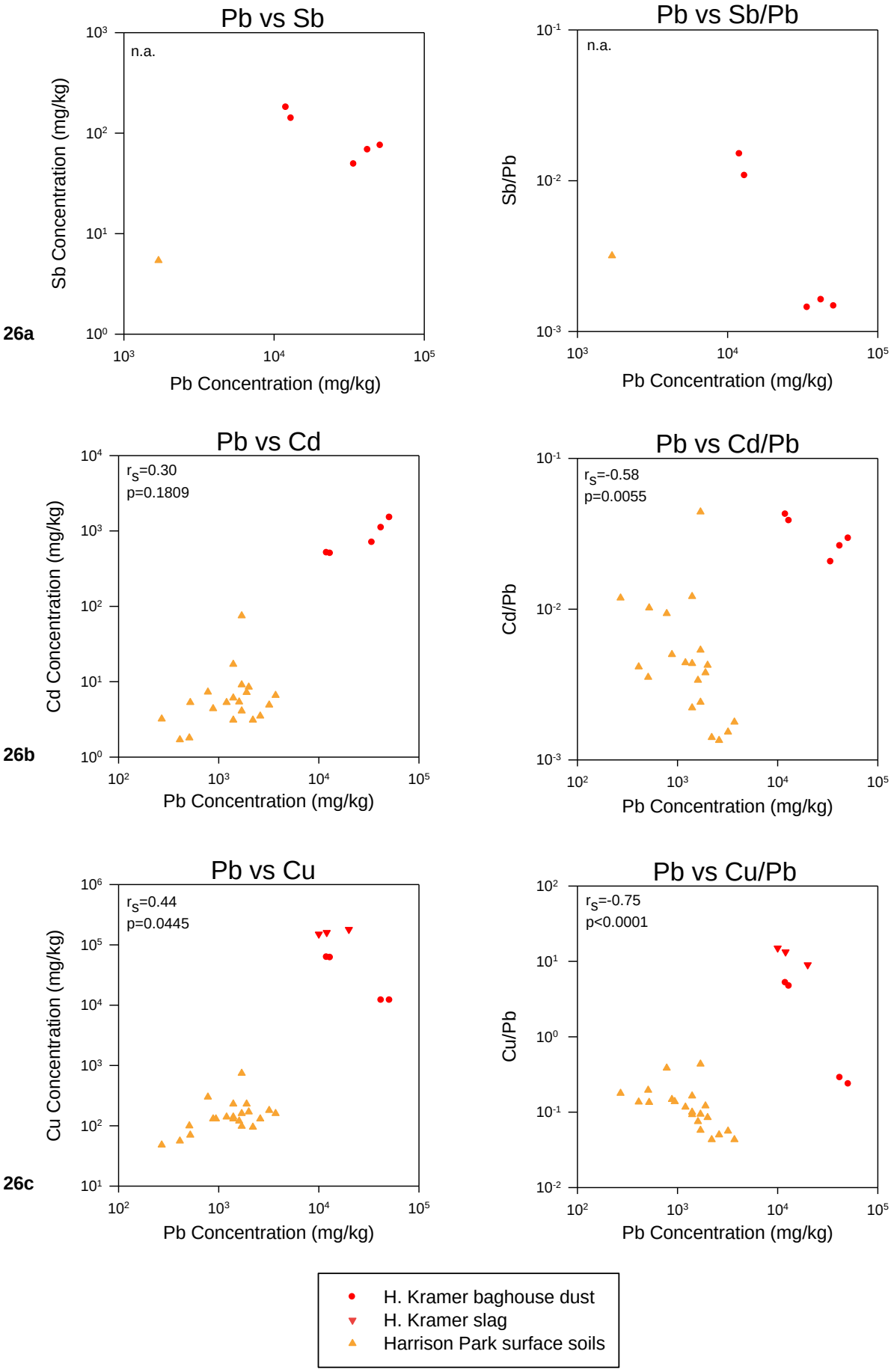

Figures 26a-c. Harrison Park reference area surface soils (0–6 inches). Slag composition (H. Kramer, 2014a).

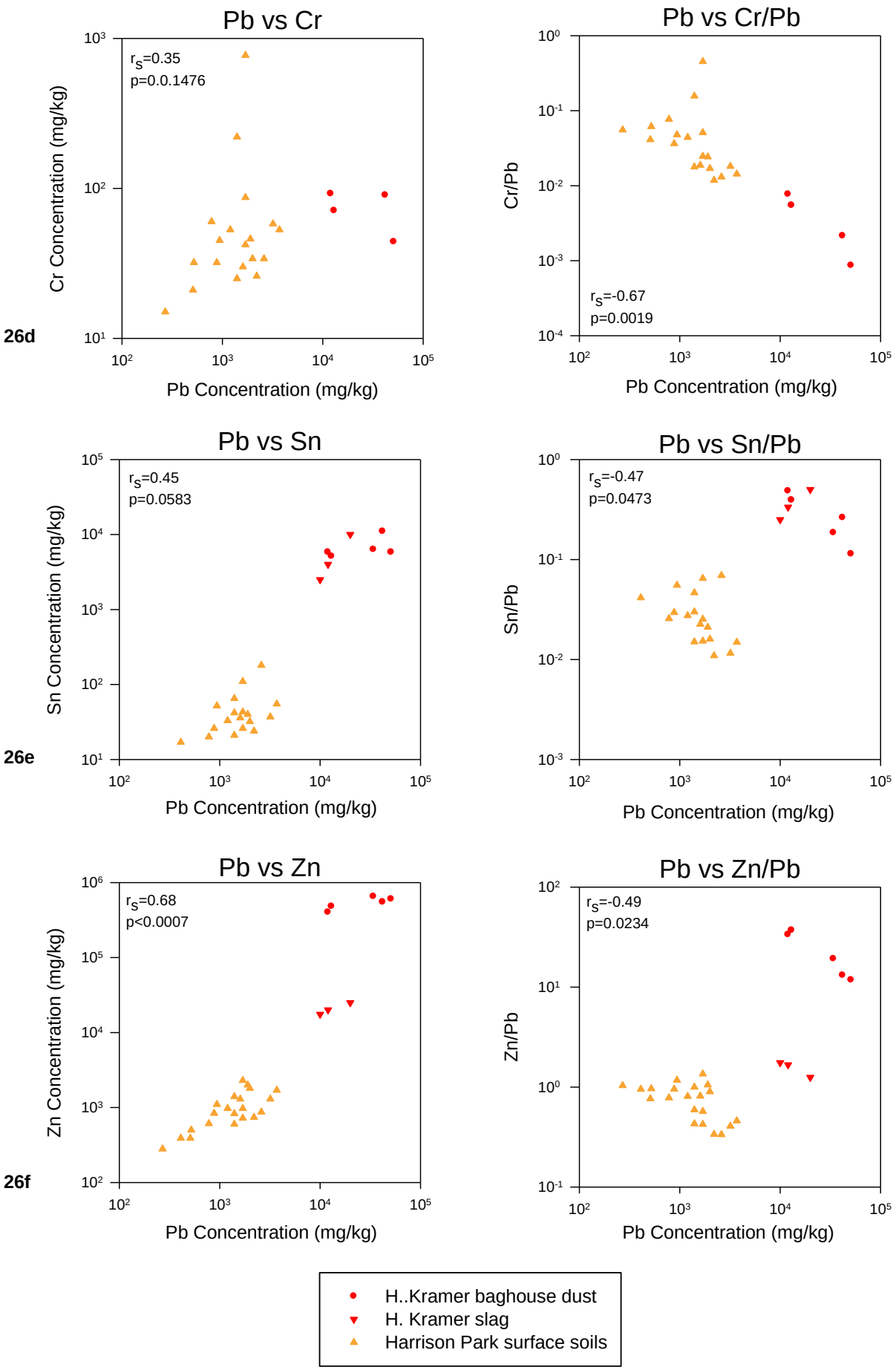

Figures 26d-f. Harrison Park reference area surface soils (0–6 inches). Slag composition (H. Kramer, 2014a).

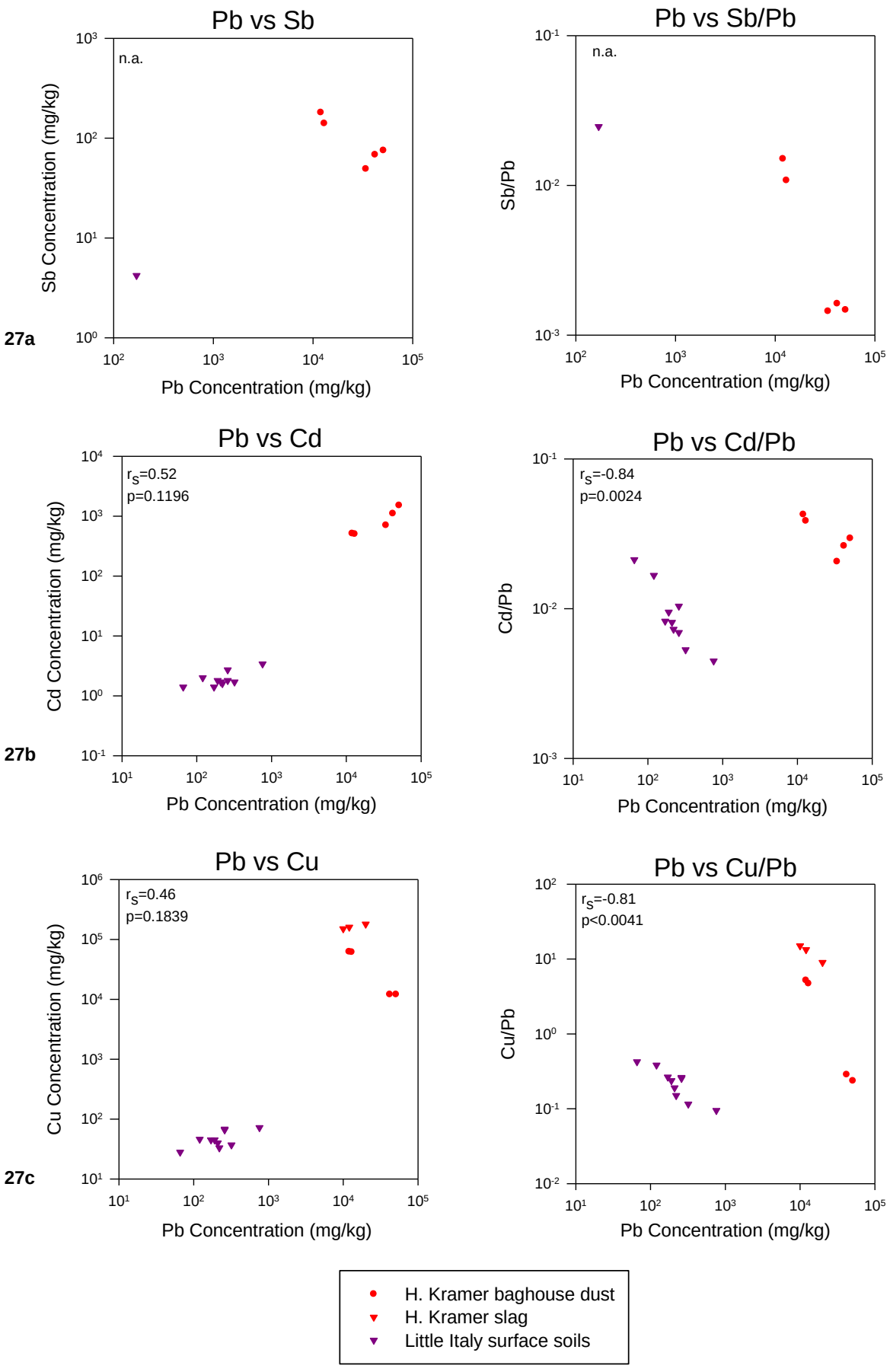

Figures 27a-c. Little Italy reference area surface soils (0–6 inches). Slag composition (H. Kramer, 2014a).

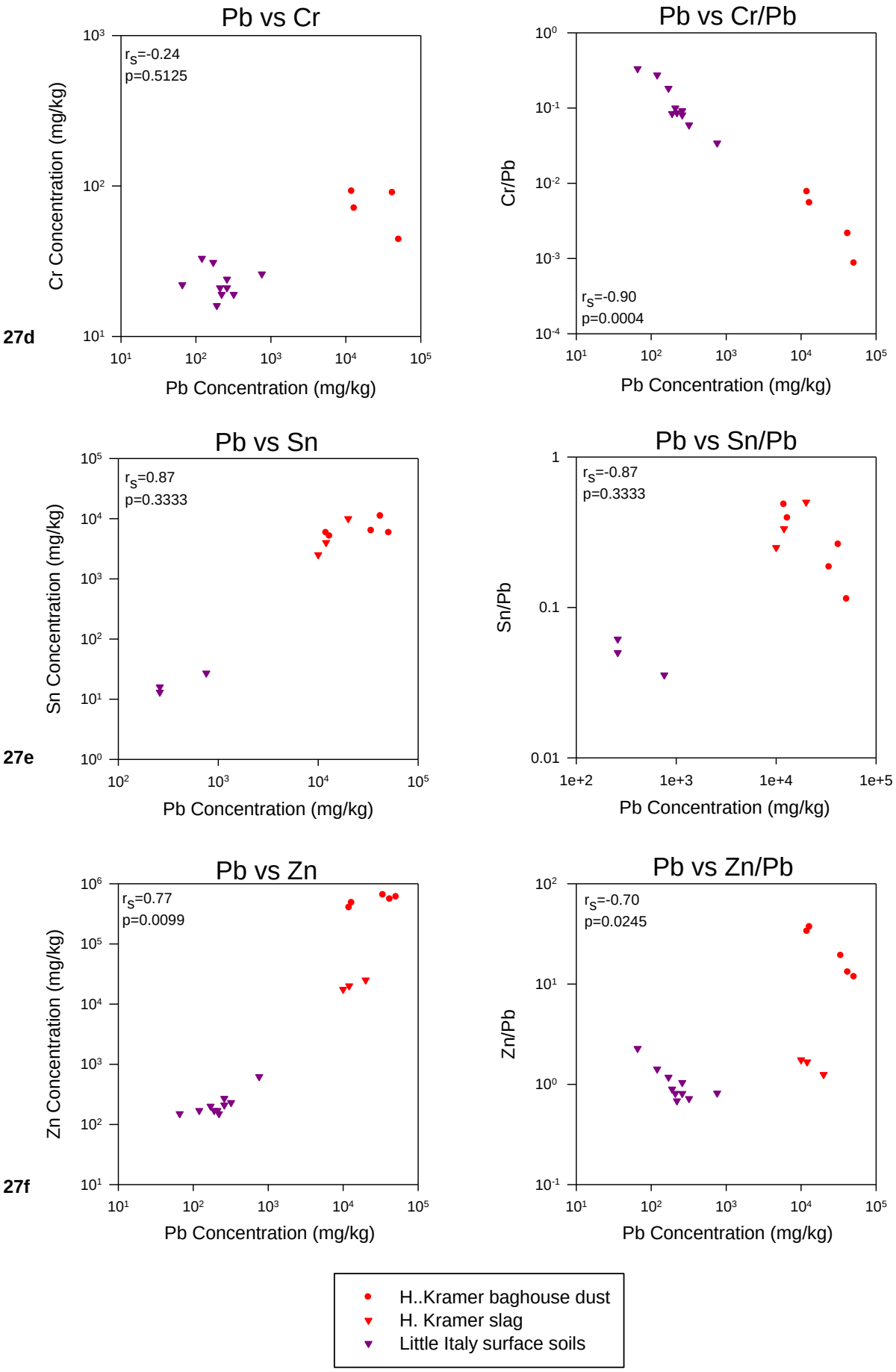

Figures 27d-f. Little Italy reference area surface soils (0–6 inches). Slag composition (H. Kramer, 2014a).

Correlation Analysis and Scatterplot Results by Soil Sampling Area

Alley Surface Soils

Spearman rank correlation coefficients, r_s, (**Table 6a**) indicated at the 95% confidence level (p-value < 0.05) strong positive correlations ($|r_s| > 0.7$) of Pb with Cd, Cu, Sn, and Zn in alley surface soils (0–6 inches). The Spearman rank correlation coefficent for Pb with Cr indicated a moderate correlation ($0.3 < |r_s| < 0.7$) at the 90% confidence level (p-value < 0.10). There were few soils (n=5) from the alley with Sb concentrations above the reporting limit; those soils did not present a clear pattern, and relationships between Sb and Pb were not statistically significant (p-value > 0.10) at the 90% confidence level. These correlation coefficients suggested that Pb was most strongly associated with Cd, Cu, Sn, and Zn; less strongly associated with Cr; and probably not associated with Sb.

The scatterplots (**Figures 21a-f**) illustrate relationships suggested by the correlation coefficients. Concentrations of Pb, Cd, Cu, Sn, and Zn in alley surface soils were less than concentrations observed in H. Kramer baghouse dust and slag. Higher concentrations of Pb generally corresponded to higher concentrations of Cd, Cu, Sn, and Zn and plotted in alignment with H. Kramer slag and/or baghouse dust, suggesting a major source of Pb in the alley was associated with Cd, Cu, Sn, and Zn. In particular, Pb and Zn in alley surface soils aligned well with H. Kramer slag (**Figure 21f**). Concentrations of Sb and Cr in many alley surface soils were similar to or exceeded concentrations found in H. Kramer baghouse dust, suggesting H. Kramer emissions were probably not the primary source of Sb or Cr in the alley surface soils.

Scatterplots of Pb vs. (X)/Pb for alley surface soils are shown in **Figures 21a-f**. Scatterplots of alley surface soil for Pb vs. (X)/Pb, where (X) = Cd, Cu, Sn, or Zn, did not appear to correlate with Pb concentration and, for Cd/Pb and Zn/Pb, exhibited a relatively flat trend. These patterns, along with r_s and p-values ($|r_s| < 0.4$ and p-values > 0.2) indicating low confidence in any correlation but strong positive correlations of Pb with Cd, Cu, Sn, and Zn, were consistent with a major source of Pb in the alley being associated with Cd, Cu, Sn, and Zn. Furthermore, Cu/Pb, Sn/Pb, and Zn/Pb in alley surface soils were almost entirely within the range found in H. Kramer baghouse dust and slag. In particular, the ratios of Zn/Pb in alley surface soils aligned near Zn/Pb ratios in H. Kramer slag (**Figure 21f**). The scatterplot of Pb vs Cr/Pb revealed two distinct trends with negative slopes, suggesting Cr was not associated with the predominant source of Pb in the alley surface soils.

Consideration of scatterplots and Spearman rank correlation coefficients indicated the main source of Pb in the alley surface soils was strongly associated with Cd, Cu, Sn, and Zn. Pb, Cd, Cu, Sn, and Zn are components used in the production of brass and bronze and were found in H. Kramer baghouse dust and slag (H. Kramer, 2012 and 2014b; Morris, 2004). Because Pb, Cd, Cu, Sn, and Zn concentrations in alley surface soils were lower than, and aligned with,

concentrations in H. Kramer baghouse dust and slag, these elemental data were consistent with Pb-bearing material originating from H. Kramer being mixed and diluted with area soil. Because Pb, Cd, Cu, Sn, and Zn collectively are not characteristic of Pb-based paint, leaded gasoline, automobile battery lead, or tire dust (Friedlander, 1973; Hurst et al., 1996; Calvert, 2004; Lee and von Lehmden, 2012; Kaster, 2014), these potential sources of lead were not dominant in alley surface soils.

Railroad Surface Soils

Spearman rank correlation coefficients, r_s, (**Table 6a**) indicated at the 95% confidence level (p-value < 0.05) strong positive correlations ($|r_s| > 0.7$) of Pb with Cd, Cu, Sn, and Zn in railroad surface soils (0–6 inches). Relationships between Pb and Sb or Cr were not statistically significant (p-value > 0.10) at the 90% confidence level. These correlation coefficients suggested that Pb was most strongly associated with Cd, Cu, Sn, and Zn.

The scatterplots (**Figures 22a-f**) show relationships suggested by their correlation coefficients. Concentrations of Pb, Cd, Cu, Sn, and Zn in railroad surface soils were less than concentrations observed in H. Kramer baghouse dust and slag. Higher concentrations of Pb generally corresponded to higher concentrations of Cd, Cu, Sn, and Zn and plotted in alignment with H. Kramer slag and/or baghouse dust, suggesting a major source of Pb in the railroad soil was associated with Cd, Cu, Sn, and Zn.

Scatterplots of railroad surface soils for Pb vs. (X)/Pb, where X = Cd, Cu, Sn, and Zn, did not appear to vary with Pb concentration. These patterns, along with no indication of correlation for Pb with Cd/Pb, Cu/Pb, and Sn/Pb (**Table 6b**) with a high degree of confidence (p-values > 0.15) but strong positive correlations of Pb with Cd, Cu, Sn, and Zn, were consistent with a major source of Pb in the alley being associated with Cd, Cu, Sn, and Zn. Furthermore, Cu/Pb, Sn/Pb, and Zn/Pb in railroad soil were within or close to the range found in H. Kramer baghouse dust and slag. The scatterplot of Pb vs Cr/Pb revealed a weak pattern, and the associated Spearman rank correlation coefficient indicated a strong negative correlation at the 95% confidence level ($|r_s| = -0.94$, p-value < 0.05), suggesting Cr was not associated with the predominant source of Pb in railroad surface soils. Although a generally negative slope was shown in the scatterplot for Pb vs. Sb/Pb, the associated Spearman rank correlation coefficient was not statistically significant at the 90% confidence level.

Consideration of scatterplots and Spearman rank correlation coefficients indicated the main source of Pb in the railroad surface soils was strongly associated with Cd, Cu, Sn, and Zn. Pb, Cd, Cu, Sn, and Zn are components used in the production of brass and bronze and were found in H. Kramer baghouse dust and slag (H. Kramer, 2012 and 2014b; Morris, 2004). Because Pb, Cd, Cu, Sn, and Zn concentrations in railroad surface soils were lower than, and aligned with, concentrations in H. Kramer baghouse dust and slag, these elemental data were consistent with Pb-bearing material originating from H. Kramer being mixed and diluted with

area soil. Because Pb, Cd, Cu, Sn, and Zn collectively are not characteristic of Pb-based paint, leaded gasoline, automobile battery lead, or tire dust (Friedlander, 1973; Hurst et al., 1996; Calvert, 2004; Lee and von Lehmden, 2012; Kaster, 2014), these potential sources of lead were not dominant in alley surface soils.

Res 1 Surface Soils

Spearman rank correlation coefficients, r_s, (**Table 6a**) indicated strong positive correlations of Pb with Cu, Sn, and Zn and a moderately strong positive correlation with Cd in Res 1 surface soils (0–6 inches) at the 95% confidence level (p-value < 0.05). The Spearman rank correlation coefficents for Pb with Cr and Sb were not statistically significant at the 90% confidence level (p-value > 0.10). These correlation coefficients suggested that Pb was most strongly associated with Cd, Cu, Sn, and Zn.

The scatterplots (**Figures 23a-f**) illustrate relationships suggested by their correlation coefficients. Concentrations in Res 1 surface soils for Pb, Cd, Cu, Sn, and Zn were less than concentrations observed in H. Kramer baghouse dust and slag. Higher concentrations of Pb in Res 1 soils generally corresponded to higher concentrations of Cd, Cu, Sn, and Zn and plotted in alignment with H. Kramer slag and/or baghouse dust, suggesting a major source of Pb in Res 1 soils was associated with Cd, Cu, Sn, and Zn.

Scatterplots of Res 1 surface soils for Pb vs. (X)/Pb, where X = Cd, Cu, Sn, and Zn, did not appear to vary with Pb concentration and, for Cu/Pb and Zn/Pb, exhibited generally flat trends. These patterns, along with no indication of correlation for Pb with Cd/Pb, Cu/Pb, Sn/Pb, and Zn/Pb (**Table 6b**) with a high degree of confidence (p-values > 0.2) but moderately strong to strong positive correlations of Pb with Cd, Cu, Sn, and Zn, were consistent with a major source of Pb in Res 1 soils being associated with Cd, Cu, Sn, and Zn. Furthermore, Cu/Pb and Zn/Pb in Res 1 soils were within or close to the range found in H. Kramer baghouse dust and slag. In particular, the ratios of Zn/Pb in Res 1 surface soils aligned near Zn/Pb ratios in H. Kramer slag (**Figure 23f**). The Pb vs Cr/Pb and Pb vs Sb/Pb scatterplots of Res 1 soils revealed negatively sloped patterns. In addition, the Spearman rank correlation coefficient for Pb with Cr/Pb in Res 1 soils indicated a strong negative correlation at the 95% confidence level, suggesting Cr was not associated with the predominant source of Pb in Res 1 soils.

Consideration of scatterplots and Spearman rank correlation coefficients indicated the main source of Pb in Res 1 surface soils was strongly associated with Cd, Cu, Sn, and Zn. Res 1 surface soil scatterplots and Spearman correlation coefficients were similar to those for alley and railroad surface soils, although concentrations and ratios were generally shifted lower. Pb, Cd, Cu, Sn, and Zn are components in brass and bronze and were found in H. Kramer baghouse dust and slag (H. Kramer, 2012 and 2014b; Morris, 2004). Because Pb, Cd, Cu, Sn, and Zn concentrations in Res 1 surface soils were lower than, and aligned with, concentrations in H. Kramer baghouse dust and slag, these elemental data were consistent with Pb-bearing material

originating from H. Kramer being mixed and diluted with area soil. Because Pb, Cd, Cu, Sn, and Zn collectively are not characteristic of Pb-based paint, leaded gasoline, automobile battery lead, or tire dust (Friedlander, 1973; Hurst et al., 1996; Calvert, 2004; Lee and von Lehmden, 2012; Kaster, 2014), these potential sources of lead were not dominant in alley surface soils.

Res 2 Surface Soils

Spearman rank correlation coefficients, r_s, (**Table 6a**) indicated strong positive correlations of Pb with Cd, Cu, Cr, and Zn in Res 2 surface soils (0–6 inches) at the 95% confidence level (p-value < 0.05). The Spearman rank correlation coefficient for Pb with Sn was moderate at the 95% confidence level. The Spearman rank correlation coefficent for Pb with Sb was not statistically significant at the 90% confidence level (p-value > 0.10). These correlation coefficients suggested that Pb was most strongly associated with Cd, Cu, Cr, Sn, and Zn.

The scatterplots (**Figures 24a-f**) illustrate relationships suggested by their correlation coefficients. Concentrations in Res 2 surface soils for Pb, Cd, Cu, Sn, and Zn were much less than concentrations observed in H. Kramer baghouse dust and slag. Higher Pb concentrations in Res 2 soil generally corresponded to higher concentrations of Cd, Cu, and Zn, and, to a lesser extent, Sn. Scatterplots of Res 2 soil of Pb with Cd, Cu, and Zn, and, to a lesser extent, Sn, aligned with H. Kramer baghouse dust and/or slag, suggesting a major source of Pb in Res 2 soils was associated with Cd, Cu, Sn, and Zn.

Scatterplots of Res 2 surface soils for Pb vs. (X)/Pb, where X = Cd, Cu, and Zn, did not appear to vary with Pb concentration and, for Cu/Pb and Zn/Pb, exhibited generally flat trends. These patterns, along with no indication of correlation for Pb with Cd/Pb, Cu/Pb, and Zn/Pb (**Table 6b**) with a high degree of confidence (p-values > 0.4) but strong positive correlations of Pb with Cd, Cu, and Zn, were consistent with a major source of Pb in Res 2 soils being associated with Cd, Cu, and Zn. Furthermore, Cu/Pb and Zn/Pb in Res 2 soils were within or close to the range found in H. Kramer baghouse dust and slag. In particular, the ratios of Zn/Pb in Res 2 surface soils aligned near Zn/Pb ratios in H. Kramer slag (**Figure 24f**). The Pb vs Cr/Pb scatterplot of Res 2 soils revealed a negatively sloped pattern, and the Spearman rank correlation coefficient for Pb with Cr/Pb indicated a strong negative correlation at the 95% confidence level, suggesting Cr was not associated with the predominant source of Pb in Res 2 soils. Furthermore, Cr concentrations in Res 2 soils were similar to Cr concentrations in reference area soils (Harrison Park and Little Italy).

Consideration of scatterplots and Spearman rank correlation coefficients indicated the sources of Pb in Res 2 surface soils were strongly associated with Cd, Cu, and Zn and moderately associated with Sn. A minor secondary source of Pb associated with Cr but not Cu and Zn was indicated in Res 2 soils, which was not consistent with H. Kramer baghouse dust. Res 2 surface soil scatterplots and Spearman correlation coefficients for Pb with Cd, Cu, Sn, and Zn were similar to those for alley, railroad, and Res 1 surface soils, although concentrations and

ratios were generally shifted lower. Pb, Cd, Cu, Sn, and Zn are components in brass and bronze and were found in H. Kramer baghouse dust and slag (H. Kramer, 2012 and 2014b; Morris, 2004). Because Pb, Cd, Cu, Sn, and Zn concentrations in Res 2 surface soils were lower than, and aligned with, concentrations in H. Kramer baghouse dust and slag, these elemental data were consistent with the predominant source of Pb-bearing material originating from H. Kramer being mixed and diluted with area soil. Because Pb, Cd, Cu, Sn, and Zn collectively are not characteristic of Pb-based paint, leaded gasoline, automobile battery lead, or tire dust (Friedlander, 1973; Hurst et al., 1996; Calvert, 2004; Lee and von Lehmden, 2012; Kaster, 2014), these potential sources of lead were not dominant in alley surface soils.

Res 3 Surface Soils

Spearman rank correlation coefficients, r_s, (**Table 6a**) indicated strong positive correlations of Pb with Sn and Zn and moderate correlations with Cd and Cu in Res 3 surface soils (0–6 inches) at the 95% confidence level (p-value < 0.05). The Spearman rank correlation coefficient for Pb with Cr was not statistically significant at the 90% confidence level (p-value > 0.10). These correlation coefficients suggested that Pb was strongly associated with Sn and Zn and moderately associated with Cd and Cu. Correlation coefficients for Pb with Cd, Cu, Sn, and Zn were generally weaker in Res 3 soils than in alley, railroad, Res 1, and Res 2 soils.

The scatterplots (**Figures 25a-f**) illustrate relationships suggested by their correlation coefficients. Concentrations of Pb, Cd, Cu, Sn, and Zn in Res 3 surface soils were much less than concentrations observed in H. Kramer baghouse dust and slag. Higher Pb concentrations in Res 3 soils generally corresponded to higher concentrations of Cd, Cu, Sn, and Zn. Scatterplots of Res 3 soils of Pb with Cd, Cu, Sn, and Zn aligned with H. Kramer baghouse dust and/or slag, suggesting a source of Pb in Res 3 soil was associated with Cd, Cu, Sn, and Zn.

Scatterplots of Res 3 surface soils for Pb vs. (X)/Pb (where X = Cd, Cu, Cr, Sn, and Zn) exhibited negatively sloped patterns. Pb vs Zn/Pb plots, for example, clearly illustrate the change in Zn/Pb ratio with increasing Pb concentration. Negatively sloped strongly correlated data indicate an increase in Pb concentration without a corresponding increase in Zn. **Table 6b** shows no correlation of statistical significance (p-value <0.05) for Pb with Cd/Pb, Cu/Pb, Sn/Pb (exception Res 2), and Zn/Pb (exception railroad) in alley, railroad, Res 1, and Res 2 soils. However, Pb versus Cd/Pb, Cu/Pb, Sn/Pb and Zn/Pb in Res 3 were strongly correlated and negatively sloped, suggesting a different predominant source of Pb from that observed in alley, railroad, Res 1, and Res 2 areas. Furthermore, Zn concentrations and Sn/Pb and Zn/Pb ratios in Res 3 soils were shifted lower than in alley, railroad, Res 1, and Res 2 surface soils.

The negatively sloped pattern of the Pb vs Cr/Pb scatterplot of Res 3 soils and the Spearman rank correlation coefficient for Pb with Cr/Pb indicating a strong negative correlation at the 95% confidence level also suggested Cr was not associated with the predominant source of Pb in Res 3 soils.

Scatterplots and Spearman rank correlation coefficients indicated the source of Pb in Res 3 surface soils associated with Cd, Cu, Sn, and Zn was much less dominant in Res 3 soils compared to alley, railroad, Res 1, and Res 2 soils. Although Pb-bearing material associated with Cd, Cu, Sn, and Zn impacted Res 3 soil, additional significant Pb-bearing source(s) with considerably less associated Cd, Cu, Sn, and Zn were present in Res 3 soils. Because Pb, Cd, Cu, Sn, and Zn concentrations in Res 3 soils were comparable to concentrations in Harrison Park, the predominant source of Pb-bearing material was not likely from H. Kramer.

Harrison Park Surface Soils

Spearman rank correlation coefficients, r_s, (**Table 6a**) indicated moderate positive correlation of Pb with Zn and Cu in Harrison Park surface soils (0–6 inches) at the 95% confidence level (p-value < 0.05). The Spearman rank correlation coefficient for Pb with Sn indicated a moderate positive correlation of Pb with Sn at the 90% confidence level (p-value < 0.10). The Spearman rank correlation coefficients for Cd and Cr were not statistically significant at the 90% confidence level (p-value > 0.10). These correlation coefficients suggested Pb was moderately associated with Zn, Cu, and Sn in the Harrison Park surface soils, notably weaker relationships than in alley, railroad, Res 1, Res 2, and Res 3 soils.

The scatterplots (**Figures 26a-f**) illustrate relationships suggested by their correlation coefficients. Higher Pb concentrations in Harrison Park soils generally corresponded to higher concentrations of Cu, Sn, and Zn. Scatterplots of Harrison Park surface soils for Pb vs. (X)/Pb, where X = Cd, Cu, Cr, and Sn exhibited generally negatively sloped patterns. These patterns, along with moderate to strong negative correlations (**Table 6b**) for Pb with Cd/Pb, Cu/Pb, Cr/Pb, Sn/Pb, and Zn/Pb at the 95% confidence level (p-values < 0.05) and moderate positive correlations of Pb with Cu, Sn, and Zn, indicated any Pb associated with Cd, Cu, Cr, Sn, and Zn was less dominant and/or more variable in Harrison Park soils compared to alley, railroad, Res 1, and Res 2 surface soils. These relationships agreed with Harrison Park soil sample locations being spread over a much larger area than any of the other areas and with a variety of industries having operated there. Furthermore, because concentrations of Cu, Pb, and Zn were mostly greater than in Little Italy soils, additional significant sources of Pb associated with Cu and Zn were suggested in Harrison Park soils. The negatively sloped pattern of the Pb vs Cr/Pb scatterplot of Harrison Park soils and the Spearman rank correlation coefficient for Pb with Cr/Pb indicating a moderate negative correlation suggested Cr was not associated with a dominant source of Pb in Harrison Park soils.

Little Italy Surface Soils

Spearman rank correlation coefficients, r_s, (**Table 6a**) indicated strong positive correlation of Pb with Zn in Little Italy surface soils (0–6 inches) at the 95% confidence level (p-value < 0.05). The Spearman rank correlation coefficients for Cd, Cu, Cr, and Sn were not statistically significant at the 90% confidence level (p-value > 0.10). These correlation

coefficients suggested, except for Pb with Zn, notably weaker relationships than in alley, railroad, Res 1, Res 2, and Res 3 soils. Scatterplots (**Figures 27a-f**) illustrate the relationships of Pb with Sb, Cd, Cu, Cr, Sn, and Zn.

Scatterplots of Little Italy surface soils for Pb vs. (X)/Pb, where X = Cd, Cu, Cr, and Zn, exhibited generally negatively sloped patterns. These patterns, along with strong negative correlations (**Table 6b**) for Pb with Cd/Pb, Cu/Pb, Cr/Pb, and Zn/Pb at the 95% confidence level (p-values < 0.05) indicated a source of Pb associated with Cd, Cu, and Zn was not dominant in Little Italy soils. The negatively sloped pattern of the Pb vs Cr/Pb scatterplot of Little Italy soils and the Spearman rank correlation coefficient for Pb with Cr/Pb indicating a strong negative correlation at the 95% confidence level also suggested Cr was not associated with the predominant source of Pb in Little Italy soils.

DISCUSSION

Results for alley, railroad, Res 1, and Res 2 soils were consistent with materials originating from brass and bronze production (H. Kramer, 2012 and 2014b; Morris, 2004), as observed in the previous study (NEIC, 2012), where Pb was associated with Cd, Cu, Sn, and Zn. Furthermore, the high correlation between these metals suggested they were added to the soils largely from the same or similar material or process rather than as independently distributed constituents, similar to findings for Pb and Zn in Chicago soils by the USGS (2003). These strong to moderate correlations suggested Cd, Cu, Sn, and Zn were co-contaminants in Pb-contaminated soils from a source with a relatively consistent Pb composition.

In contrast, the correlations of these metals were not consistent with Pb-based paint, leaded gasoline emissions, tire dust, or battery lead as significant sources of Pb in alley, railroad, Res 1, Res 2, or Res 3 soils. Although the composition of coal fly ash varies depending on the composition of the coal burned (Valentim et al., 2009), a previous study showed that Pb was approximately three orders of magnitude lower (1000x) in Fisk coal fly ash than in H. Kramer baghouse dust and contributed minimal lead to the ambient air (NEIC, 2012). Because of this and because a unique particle type of amorphous, alumino-silicate spheres exhibited by coal fly ash (Kutchko and Kim, 2006) was not observed by SEM in any of the soil areas, coal fly ash was not a dominant source of Pb in the Pilsen area. The PRP producing coal fly ash was Fisk.

Metals most associated with Pb-based paint included Cr (Novotny et al., 1998). Strong associations of Pb with Cr were only observed in Res 2 soils, and Cr concentrations were comparable to reference soil concentrations. Strong to moderate correlations of Pb with Cd, Cu, Sn, and Zn suggested any contributions of leaded paint with associated Cr were not dominant in alley, railroad, and residential soils. Because associations of Cd, Cu, and Sn in paint are rare, non-industrial Pb from leaded paints historically used on homes and buildings in the Pilsen area were not dominant sources of Pb in alley, railroad, residential, and Harrison Park soils. Non-

industrial Pb-based paint exhibits a unique layered morphology (Union Pacific, 2008), and Pb-based paint particle types were not observed by SEM in any soil areas.

Metals associated with leaded gasoline emissions include Pb, Zn, Cu, and Cd in decreasing abundance (Ter Haar et al., 1972; Lee and von Lehmden, 2012), and Sn was not typically associated. Although correlations of Pb with Zn, Cu, and Cd were strong in alley, railroad, Res 1, and Res 2 soils, correlations of Pb with Sn were also mostly strong (moderate in Res 2). Furthermore, concentrations of Zn were generally greater relative to those of Pb (Zn/Pb>1), in contrast to their relative abundances in leaded gasoline emissions. In Res 3 soils, Pb also correlated strongly with Sn. These correlations and relative concentrations of metals, in addition to strong to moderate correlations of Pb with Sn, suggested vehicle exhaust from the historical use of leaded gasoline was not a dominant source of Pb in alley, railroad, and residential soils. Following emissions from combustion of leaded fuel, Pb is found primarily in the atmosphere in the form of Pb halide salts (Van Borm et al., 1990; Liu et al., 1995). Pb sulfates are subsequently formed from reaction of the halide salts with sulfate present in the urban atmosphere. $PbBr_2$ salts typically occur as agglomerates of fine particles with diameters ranging 100s of nanometers (Biswas et al., 2003). Leaded fuel combustion particles types were not observed by SEM.

Tire manufacturers use metal oxides as activators during vulcanization. Although Pb-oxide was used historically, Zn-oxide is now used exclusively (Friedlander, 1973; Kaster, 2014; State of California, 1996). Zn is often associated with dust from tires and in considerably greater abundances than other metals, including Pb. Sn and Cu have not been associated with tire manufacturing. Significant correlations between Cu, Sn, Pb, and Zn in alley, railroad, and residential soils suggested tire dust was not a dominant source of Pb (or Zn) in these soils. The PRP associated with tires was Tire Grading.

Sb concentrations were typically very low, often not detectable in any of the soil areas, and Sb correlations with Pb were not observed. Low Sb concentrations and lack of correlation with Pb were not consistent with babbit (Sn with Cu, Sb, and Pb), antimonial Pb, and battery Pb manufacturing (Prengaman, 1995; Calvert, 2004; ASTM, 2014) as dominant sources of Pb in the soil areas studied. The PRPs that manufactured these products included Century, Loewenthal, and NL.

Scatterplots of Cd, Cu, Pb, Sn, and Zn concentrations in alley and railroad surface soils (**Figures 21 and 22**) showed significant relationships between these metals, as was also indicated by their correlation coefficients that revealed mostly strong to moderate, positive correlations (**Table 6a**). Significant relationships between Cd, Cu, Sn, Pb, and Zn suggested these metals had been contributed to the alley and railroad surface soils largely from the same or similar material or process rather than distributed independently from a variety of sources. Such a finding was also made for Pb and Zn in Chicago soils by the USGS (2003). These results were also consistent with H. Kramer processes as observed in the earlier study (NEIC, 2012). Cu, Pb,

Sn, and Zn are associated with copper-alloy production at H. Kramer, and Cd, often associated with Zn, is commonly liberated during metal recovery from scrap metal processing as conducted at H. Kramer (Morris, 2004; Manahan, 2005; Omenazu, 2011; H. Kramer, 2012 and 2014b). Cd is also commonly associated with zincite (Mindat, 2011; Webmineral, 2011) which was present in railroad soil (**Figure 6b**). The relative concentrations of Cd, Cu, Pb, Sn, and Zn were consistent with baghouse dust and slag from H. Kramer. Furthermore, decreasing concentration trends of these elements in alley, railroad, Res 1, Res 2, and Res 3 soils with distance of the soil area from H. Kramer and alignment with H. Kramer baghouse dust and/or slag (in particular, Pb and Zn in alley surface soil aligned with H. Kramer slag) were consistent with dilution and mixing in these soils by materials produced at H. Kramer. These results for the alley and railroad soils were in agreement with the Pb isotope ratio results.

Scatterplots of Pb concentration (mg/kg) versus Cd/Pb, Cu/Pb, Sn/Pb, and Zn/Pb (**Figures 21 and 22**) allow comparisons between elemental ratios in alley and railroad surface soils and in H. Kramer baghouse dust and slag. The range of Cu/Pb ratios in alley and railroad surface soils corresponded well with the range of Cu/Pb ratios in baghouse dust and slag. Furthermore, Sn/Pb ratios largely corresponded with the range of Sn/Pb ratios in baghouse dust and slag. Although Zn/Pb and Cd/Pb ratios in alley and railroad surface soils were markedly lower than those observed in baghouse dust, Zn/Pb ratios were more similar to slag ratios for the alley and railroad surface soils.

While the Zn/Pb and Cd/Pb ratios in alley and railroad soils appeared to be inconsistent with Cu/Pb and Sn/Pb ratios and the Pb isotope ratio measurements, this apparent discrepancy may be explained by differences in the processes of elemental and isotopic fractionation. An important property of Pb is that its isotopes do not fractionate during natural or anthropogenic (smelting) processes (Doe, 1970; Bollhöfer and Rosman, 2001; Shiel et al., 2010). Because of this and the consistency in the primary raw material used for Pb alloying (H. Kramer, 2011; Omenazu, 2011), the Pb isotope signature of H. Kramer slag would be consistent with that of H. Kramer baghouse dust. Therefore, slag and fume emissions (baghouse dust is largely condensed fume, and fume is the process exit gas) from the same melt would have indistinguishable Pb isotope ratios. Slag from H. Kramer would have Pb isotope ratios similar to those observed in the baghouse dust. In contrast to Pb isotope behavior during smelting, fractionation of elements during smelting occurs with the more volatile elements (with lower boiling points) enriched in furnace emissions compared to slag waste (DHEW, 1969; Ketterer, 2006; H. Kramer, 2014b). Greater differences between the boiling points of elements result in greater fractionation of those elements during smelting (**Table 7**). With much lower boiling points and greater volatility, Zn and Cd would enrich fume emissions (and baghouse dust) relative to Cu, Pb, and Sn compared to the slag waste left behind in the melt (DHEW, 1969; EPA 1977). Thus, slag from H. Kramer likely contained lower abundances of Zn and Cd relative to Pb than those found in baghouse dust. However, because Pb/Cu and Pb/Sn ratios in alley and railroad soils were mostly

consistent with those in baghouse dust and because Cd and Zn were both low boiling point metals relative to Pb, elemental fractionation was the most probable explanation.

Table 7. BOILING POINTS OF METALS
Additional Characterization of Lead in Soils
Pilsen Neighborhood, Chicago, Illinois

Metal	Boiling Point (°C)[a]
Cd	765
Zn	907
Pb	1740
Sb	1750
Sn	2270
Cu	2567
Cr	2672

[a] CRC (2013).

Furthermore, smelting-related elemental fractionation was well supported by the SEM observations of an abundance of Pb-bearing particles consistent with the composition of brass and bronze foundry slag in alley, railroad, and residential soils. Multi-phase, angular particles, micrometer-scale and greater, are characteristic of slag material (CLEMEX, 2008; Pistorius and Kotzé, 2009; Perederly et al., 2012; Bernal et al., 2014; Piatak et al., 2014). The composition of non-ferrous slag is dominated by Fe and Si with lesser amounts of Al and Ca (Piatak et al., 2014). Slag from a brass and bronze foundry contains high Cu and Zn relative to Pb (EPA, 1995; Shen and Forssberg, 2003). Pb-bearing particles of slag with relative responses for Cu, Pb, and Zn were consistent with the composition of slag from brass and bronze foundry. While slag produced at H. Kramer would have Pb isotope ratios similar to those in baghouse dust, soil containing slag from H. Kramer may exhibit Pb isotope ratios along a mixing line with Pb isotope ratios of baghouse dust at one end. Pb isotope ratios of the railroad soils in which slag was observed at the time of sampling (EPA, 2014a) plotted along such a line (**Figure 20**).

SEM results also indicated micrometer-scale Zn-oxide particles in railroad soil similar to baghouse dust particles. In particular, railroad soil collected near the brick furnace building with historical cracks in the walls and roof that may have allowed release of furnace emissions dust (Omenazu, 2011). The absence of SEM observations of micrometer-scale Zn-oxide particles in residential soils may have been due to the occurrence of dissolution over time (Cernik et al., 1995; Wilcke and Kaupenjohann, 1998; Manceau et al., 2000; Voegelin et al., 2005). Dissolution textures and lack of crystallite morphology associated with micrometer-scale Zn-oxide particles in railroad soil was indicative of dissolution weathering resulting from exposure to moisture. Micrometer-scale Zn-oxide particles with greater solubility and greater surface area to volume (based on smaller particle size, 1s–10s µm) would solubilize much more readily than silica-rich slag particles (1s–100s µm), with significantly less surface area to volume ratios

(Alexander, 1957). Zn/Pb ratios in residential soils were considerably more consistent with slag than baghouse dust.

Comparison of Soil Areas

Comparison of the Res 1, Res 2, and Res 3 soils was facilitated by including the alley, railroad, Harrison Park, and Little Italy data sets together in a series of plots with the Res 1, Res 2, and Res 3 data sets superimposed in those plots separately (**Figures 28–32**). A brief summary is provided for the following sets of plots showing Res 1, Res 2, and Res 3 soils data in series with increasing distance by soil area from H. Kramer and in relationship to the alley, railroad, and reference area soils:

Figures 28a-b. Cd and Pb concentrations and Pb concentrations and Cd/Pb ratios in surface soils of the Res 1, Res 2, and Res 3 areas compared to surface soils of the alley, railroad, Harrison Park, and Little Italy, and H. Kramer baghouse dust and H. Kramer slag.

Figures 29a-b. Cu and Pb concentrations and Pb concentrations and Cu/Pb ratios in surface soils of the Res 1, Res 2, and Res 3 areas compared to surface soils of the alley, railroad, Harrison Park, and Little Italy, and H. Kramer baghouse dust and H. Kramer slag.

Figures 30a-b. Sn and Pb concentrations and Pb concentrations and Sn/Pb ratios in surface soils of the Res 1, Res 2, and Res 3 areas compared to surface soils of the alley, railroad, Harrison Park, and Little Italy, and H. Kramer baghouse dust and H. Kramer slag.

Figures 31a-b. Zn and Pb concentrations and Pb concentrations and Zn/Pb ratios in surface soils of the Res 1, Res 2, and Res 3 areas compared to surface soils of the alley, railroad, Harrison Park, and Little Italy, and H. Kramer baghouse dust and H. Kramer slag.

Figures 32a-b. Cr and Pb concentrations and Pb concentrations and Cr/Pb ratios in surface soils of the Res 1, Res 2, and Res 3 areas compared to surface soils of the alley, railroad, Harrison Park, and Little Italy, and H. Kramer baghouse dust and H. Kramer slag.

Figure 33. Comparison of Pb isotope composition in alley, railroad, Res 1, Res 2, Res 3, Harrison Park, and Little Italy soils.

Figures 34a-f. Comparison of high energy portion of EDS spectra (7.5 to 15.5 keV) collected from typical Pb-bearing, multi-phase particles in soil from the alley, railroad, Res 1, Res 2, Res 3, and Harrison Park.

Figure 35. Comparison of Zn and Pb concentrations in Res 1, Res 2, and Res 3 surface soils relative to H. Kramer baghouse dust and slag (simplified from **Figure 31a**).

For concentrations of Pb vs. Cd, Cu, Sn, and Zn, railroad surface soils aligned well with alley surface soils. Three railroad surface soils with the highest Pb and Zn concentrations aligned with H. Kramer baghouse dust, suggesting the presence of abundant baghouse dust in those soils. Those soils were collected near reported baghouse dust storage/transport stations,

and one of them contained Zn-oxide particles consistent with baghouse dust as observed under the SEM.

In Pb vs. Cd, Cu, Sn, and Zn concentration scatterplots, Res 1 surface soils also aligned with and overlapped alley and railroad surface soils, except for a general offset to the right and lower right, with little overlap of Harrison Park soils (**Figures 28a-31a**). In the Pb vs. (X)/Pb plots (where X = Cd, Cu, Sn, and Zn), Res 1 soil (X)/Pb ratios coincided with those of the alley and railroad soils, ranging down to the lower ratios in the Harrison Park soils. Res 1 soil (X)/Pb ratios did not correlate with increasing Pb concentrations (**Figures 28b-31b**).

Although Res 2 surface soils aligned with alley and railroad surface soils in Pb vs. Cd, Cu, Sn, and Zn concentrations plots, they only overlapped alley and railroad soils slightly in the center of the plot. In contrast to Res 1 soils, however, a much greater offset to the right and lower right existed, with significant overlap of Harrison Park soils and an extension of Res 2 soils to the lower left, overlapping with Little Italy soils. In the Pb vs. (X)/Pb plots, Res 2 soil (X)/Pb ratios ranged from the lower ratios of the alley and railroad soils and ranged down to the middle ratios in the Harrison Park soils. The ratios did not correlate with increasing Pb concentrations.

Although Res 3 surface soils also aligned with alley and railroad surface soils in Pb vs. Cd, Cu, Sn, and Zn concentration scatterplots, in contrast to Res 2 soils, the alignment was offset and Res 3 soils did not overlap alley and railroad soils. Furthermore, Res 3 soils nearly entirely overlapped Harrison Park and Little Italy soils and did not extend toward alley and railroad soils. In the Pb vs. (X)/Pb plots, Res 3 soil (X)/Pb ratios coincided with those of the Little Italy and Harrison Park soils and decreased with increasing Pb concentrations.

In contrast, Pb versus Cr scatterplots (**Figures 32a-b**) for alley, railroad, Res 1, Res 2, and Res 3 soils overlapped Harrison Park and Little Italy soils. Pb versus Cr/Pb plots also overlapped Harrison Park and Little Italy soils. Correlations of Pb and Cr in all but Res 2 soils were not statistically significant, and all Pb versus Cr/Pb plots were strongly correlated and negatively sloping, suggesting Pb contamination was not associated with Cr in the alley, railroad, Res 1, Res 2 and Res 3 soils.

Canar et al. (2014) performed basic statistics, conducted ANOVA (analysis of variance), and evaluated ranked means of Cd, Cu, Pb and Zn to compare alley, railroad, Res 1, Res 2, and Res 3 soils. These findings were in agreement with Pb versus elemental ratio [(X)/Pb] plot observations in that Pb contamination in Res 3 soils differed from that in alley, railroad, Res 1, and Res 2 soils but was not differentiated from Little Italy soils.

These data patterns suggested a general shift to lower Cd, Cu, Sn, and Zn concentrations and lower (X)/Pb ratios with increased distance from H. Kramer. These findings were corroborated by similar trends of shifting Pb isotopic compositions with increased distance from H. Kramer observed in the Res 1, Res 2, and Res 3 soils.

Figure 33 shows the offset in Pb isotope ratios in the Res 3 soils relative to alley and railroad soils and H Kramer material compositions. These shifts with increased distance from H. Kramer in the isotopic and elemental composition of the alley, railroad, Res 1, Res 2, and Res 3 area soils were strong indicators that these soil areas were impacted by Pb from H. Kramer, and that the Pb impact diminished with distance from the facility.

Shifts in elemental concentrations and Pb isotope ratios in the alley, railroad, Res 1, Res 2, and Res 3 soil areas with increased distance from H. Kramer indicated a diminishing impact to these soil areas by Pb with distance from a location coinciding with that of H. Kramer and Century. Other studies have documented similar patterns of decreasing metals with distance from a smelter (Manceau et al., 2000; Glass, 2003). As distance from H. Kramer increased (from alley to railroad, Res 1, Res 2, and Res 3) the elemental relationships generally weakened as indicated by Spearman correlations coefficients of Pb with Cd, Cu, Sn, and Zn (**Table 6a**) and as exhibited by scatterplot patterns. This pattern was in agreement with plots presented by Canar et al. (2014) in which Cd, Cu, Sn, Pb, and Zn concentrations decreased as a function of distance from H. Kramer. This weakening elemental relationship was accompanied by a gradual shift from the Pb isotope mixing line with increased distance from H. Kramer in the predominant downwind direction to the northeast. In addition, SEM data revealed a subtle change in Pb-bearing particle composition. Soils from the alley, railroad, Res 1, and Res 2 generally exhibited Pb-bearing particle composition consistent with slag and in which Zn typically exhibited a much greater spectral response than Pb. In contrast, Res 3 and Harrison Park soils exhibited Pb-bearing particles consistent with slag in which Pb typically exhibited a much greater spectral response than Zn and Cu. **Figures 34a–f** show comparison of relative spectral responses of Cu, Pb, and Zn in typical Pb-bearing, multi-phase particles in soils from the alley, railroad, Res 1, Res 2, Res 3, and Harrison Park areas. The difference in Pb-bearing particle composition in these soil areas was related to an increased distance from H. Kramer and was consistent with the shift in Zn/Pb soil ratios with distance from H. Kramer in the predominant downwind direction.

Figure 35 is a simplified version of the series of plots in **Figure 31a** comparing Zn and Pb in Res 1, Res 2, and Res 3 soils to each other and to H. Kramer baghouse dust and slag data. In the lower left of the plot, Res 3 soils, which are farthest in distance from H. Kramer, plot at the lower concentrations of Pb and Zn. In the center of the plot, Res 1 soils, which are closest in distance from H. Kramer, plot at the higher concentrations of Pb and Zn. Res 2 soils, which are intermediate in distance from H. Kramer, generally plot at slightly lower concentrations of Pb and Zn than Res 1 and also include some lower concentrations of Pb and Zn similar to Res 3. Ranked means of Pb and Zn in Res 1, Res 2, and Res 3 soils (Canar et al., 2014) were in agreement with Pb contamination in Res 3 soils differing from that in Res 1 and Res 2 soils. This plot shows a strong relationship between Pb and Zn and distance from H. Kramer, a strong indicator that these soil areas were impacted by Pb from H. Kramer. In this case, distance from H. Kramer in the predominant downwind direction was a unique discriminator differentiating H. Kramer from several other PRPs, in particular, Loewenthal and NL (**Figure 1**).

The overall pattern for the three sets of data displayed in **Figure 35** is the reverse of that required for Loewenthal and NL to be implicated as predominant sources of Pb in Res 1 and Res 2 soils. In addition, comparisons of alley and railroad soil data patterns with Res 1, Res 2, and Res 3 soil data patterns in **Figures 28-31** also indicated the opposite of that required for Loewenthal and NL to be implicated as predominant sources of Pb in alley and railroad soils. Because Century and H. Kramer were located next to each other, distance from H. Kramer was not a discriminator for these two PRPs. However, low Sb concentrations in area soils and poor correlations between Sb and Pb eliminated Century babbit manufacturing as a dominant source of Pb in area soils because Sb was a major component of babbit material (EPA, 2014a). Furthermore, strong correlations between Zn and Pb in alley, railroad, Res 1, and Res 2 soils excluded Century's small-scale solder manufacturing as a dominant source of Pb in area soils because Zn was not a significant component of most solders (King et al., 2005).

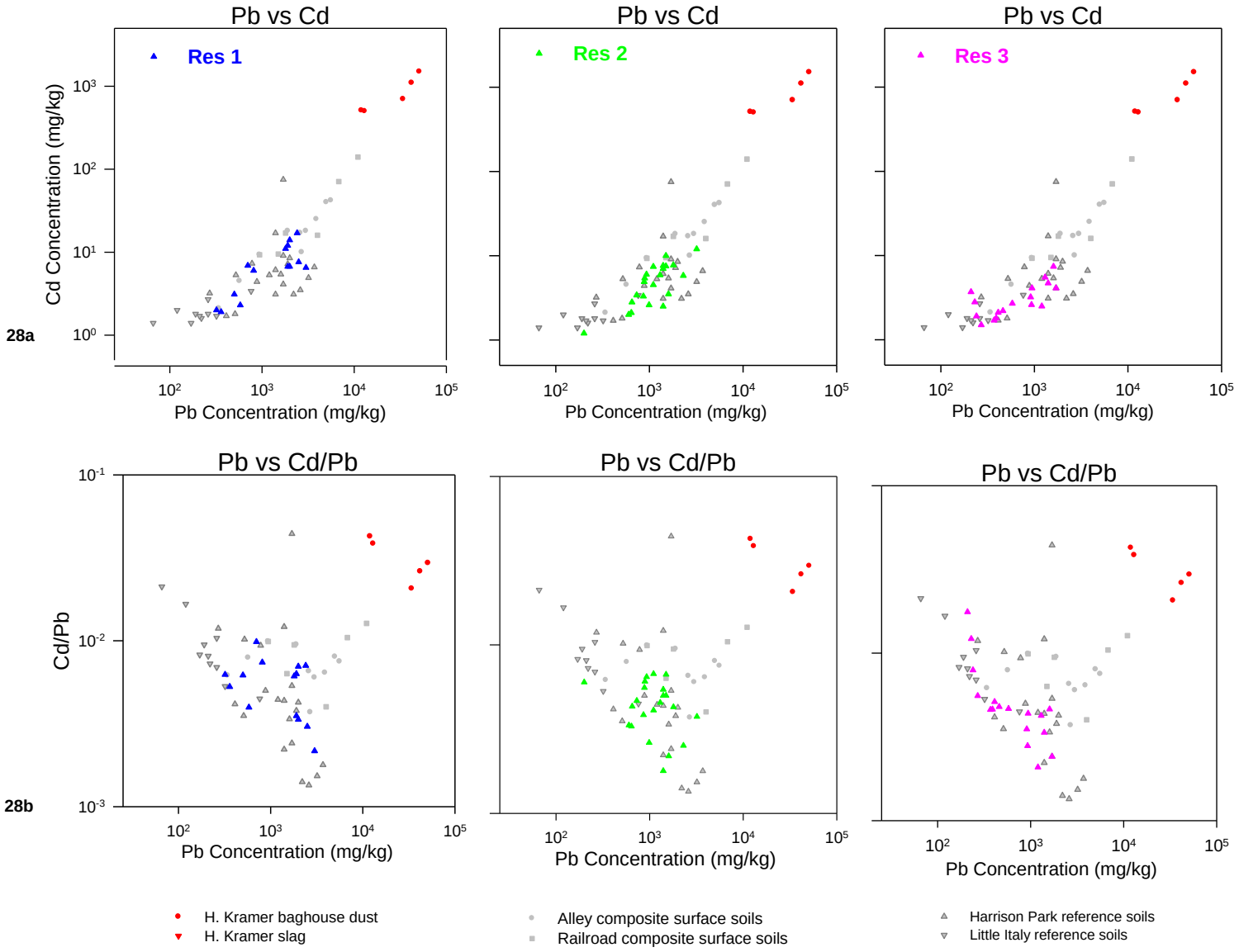

Figures 28a-b. Comparison of Cd and Pb in alley, railroad, Res 1, Res 2, Res 3, Harrison Park, and Little Italy surface soils. Note progressive general shift (left to right) of Res 1, Res 2, and Res 3 soils from alley and railroad soils to Harrison Park and Little Italy soils.

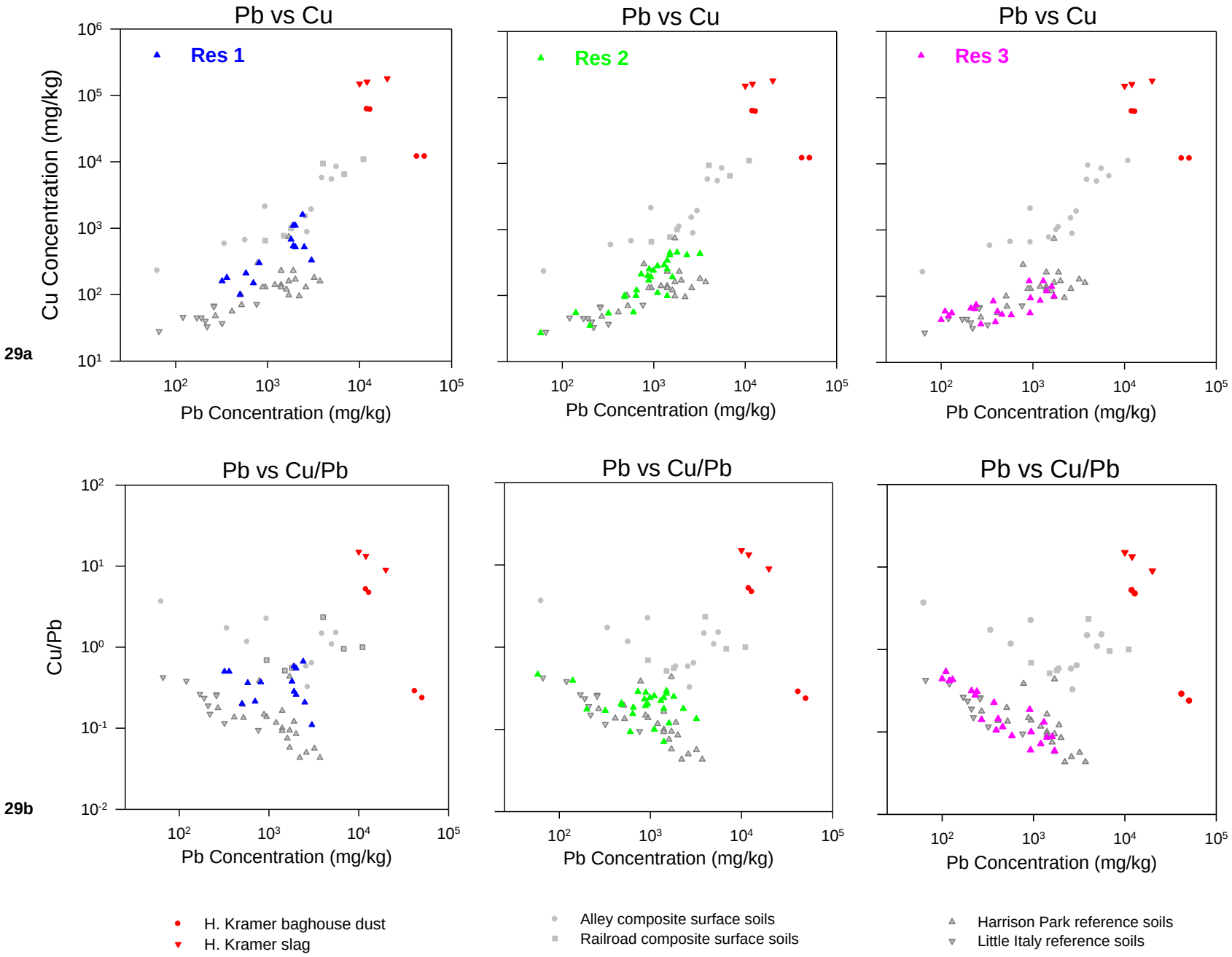

Figures 29a-b. Comparison of Cu and Pb in alley, railroad, Res 1, Res 2, Res 3, Harrison Park, and Little Italy surface soils. Note progressive general shift (left to right) of Res 1, Res 2, and Res 3 soils from alley and railroad soils to Harrison Park and Little Italy soils. Slag composition (H. Kramer, 2014a).

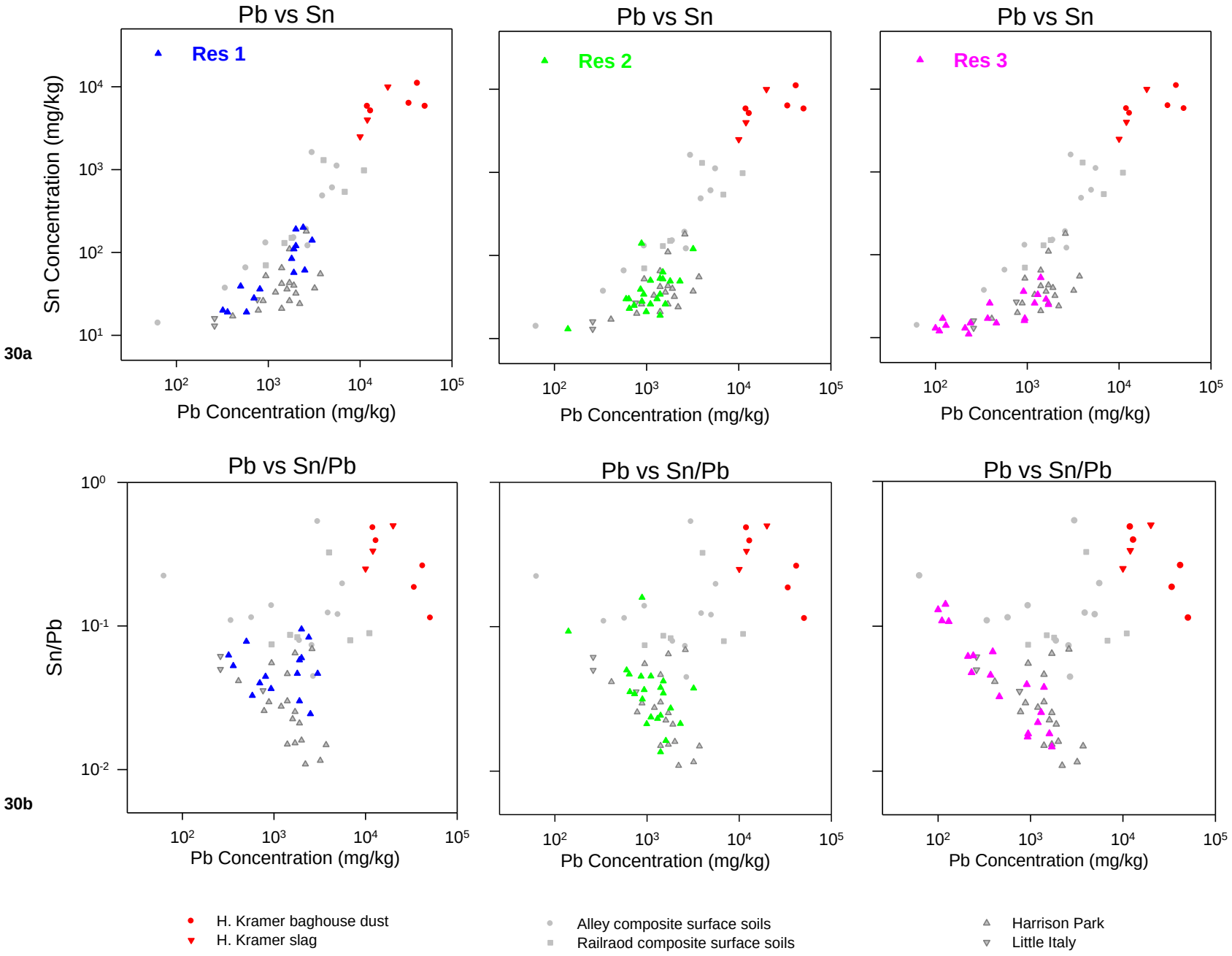

Figure 30a-b. Comparison of Sn and Pb in alley, railroad, Res 1, Res 2, Res 3, Harrison Park, and Little Italy surface soils. Note progressive general shift (left to right) of Res 1, Res 2, and Res 3 soils from alley and railroad soils to Harrison Park and Little Italy soils. Slag composition (H. Kramer, 2014a).

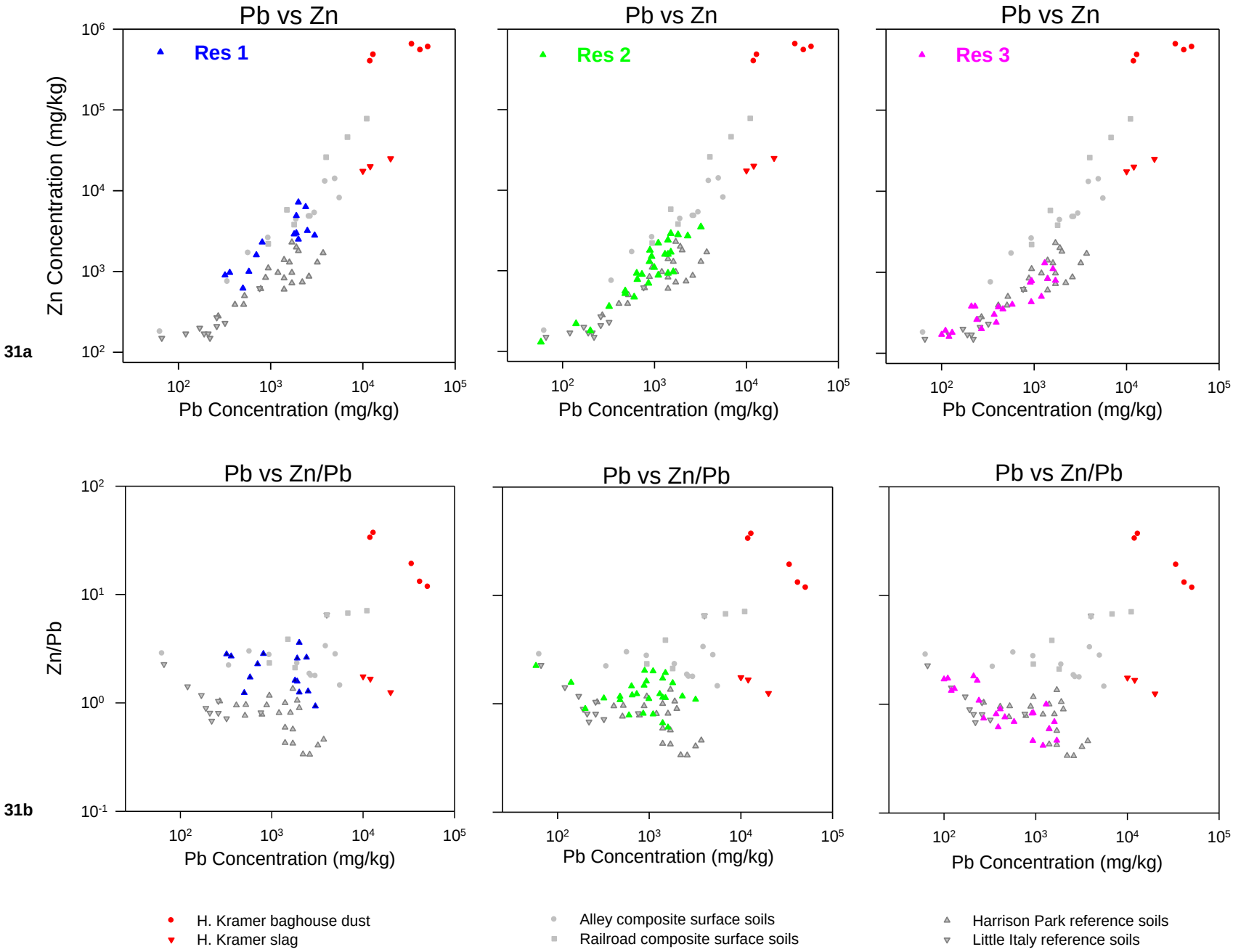

Figure 31a-b. Comparison of Zn and Pb in alley, railroad, Res 1, Res 2, Res 3, Harrison Park, and Little Italy surface soils. Note progressive general shift (left to right) of Res 1, Res 2, and Res 3 soils from alley and railroad soils to Harrison Park and Little Italy soils. Slag composition (H. Kramer, 2014a).

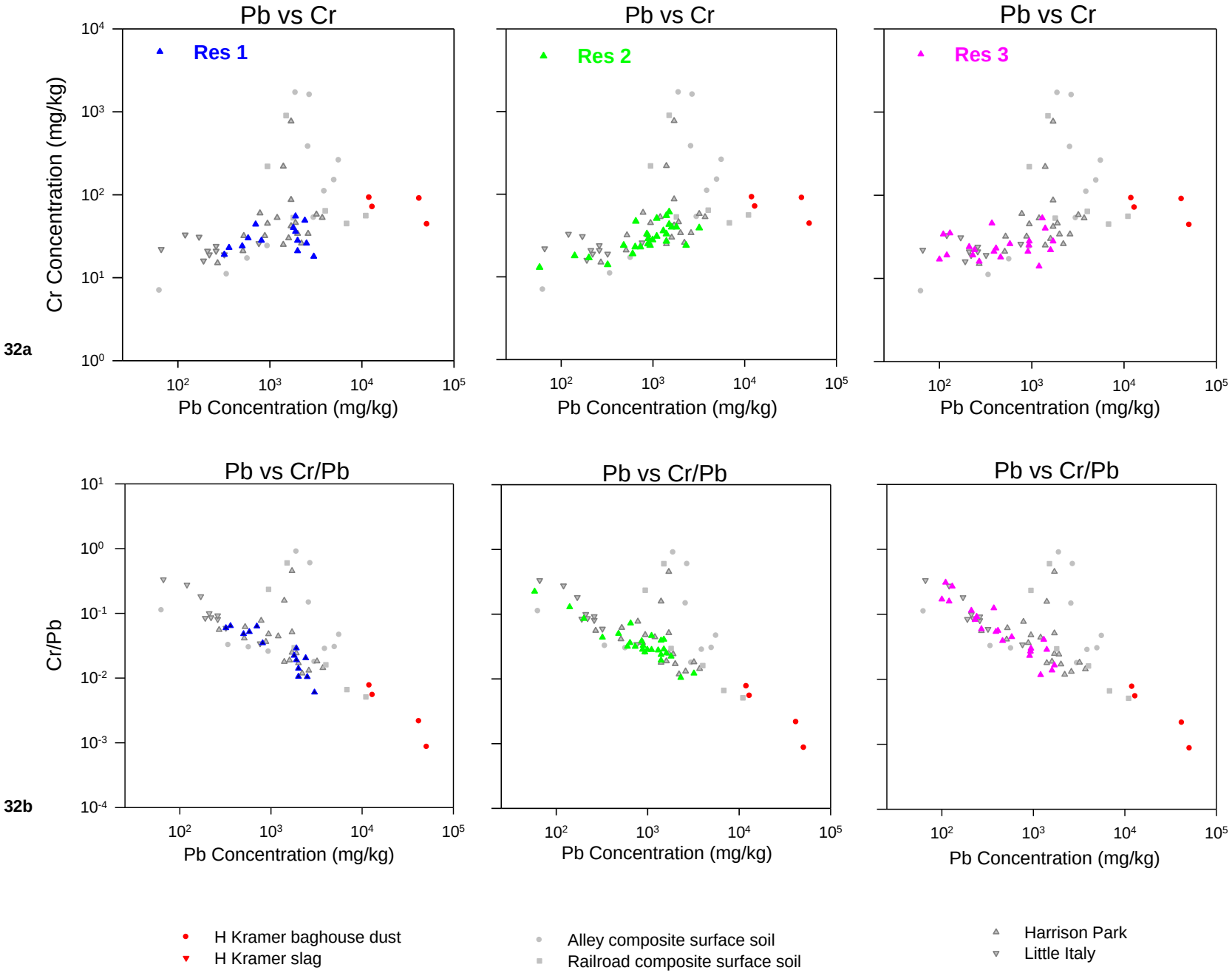

Figures 32a-b. Comparison of Cr and Pb in alley, railroad, Res 1, Res 2, Res 3, Harrison Park, and Little Italy surface soils. In contrast to Cd, Cu, Sn, and Zn with Pb in Figures 28-31, note the relative consistency of Res 1, Res 2, and Res 3 soils (left to right) with Harrison Park and Little Italy soils.

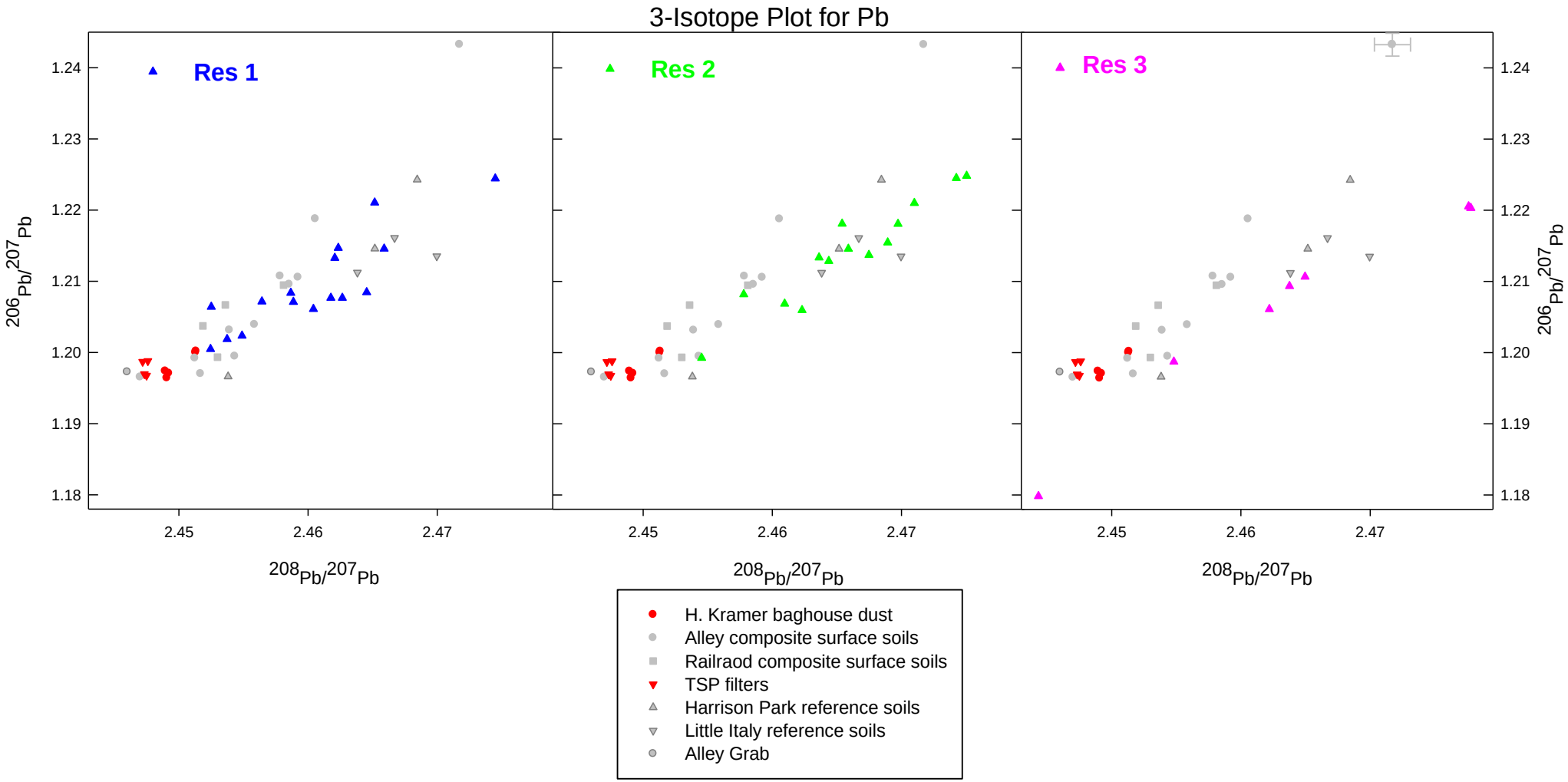

Figure 33. Comparison of Pb isotope composition in alley, railroad, Res 1, Res 2, Res 3, Harrison Park, and Little Italy soils. Note progressive general shift (left to right) of Res 1, Res 2, and Res 3 soils from alley and railroad soils to Harrison Park and Little Italy soils.

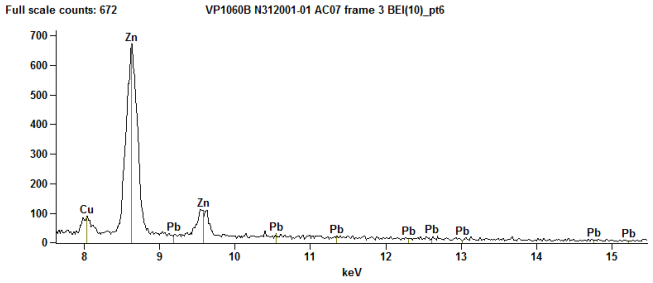

34a) **Alley** Cu>Pb and Zn>>Pb

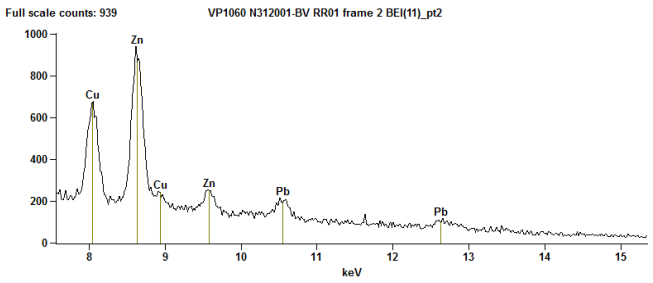

34b) **Railroad** Cu>Pb and Zn>>Pb

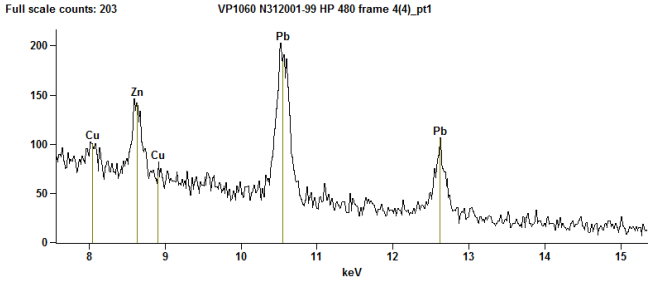

34c) **Harrison Park** Pb>>Cu and Pb>Zn

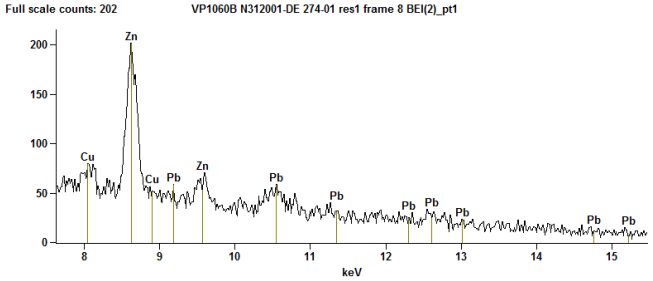

34d) **Res 1** Zn>>Pb

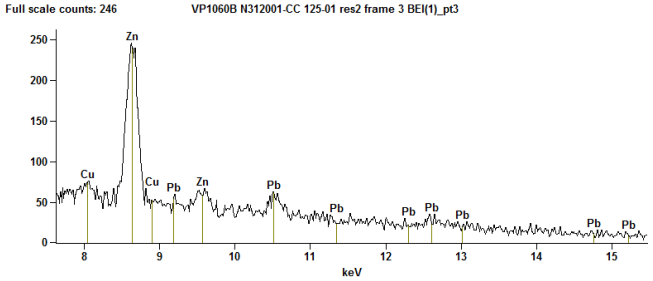

34e) **Res 2** Zn>>Pb

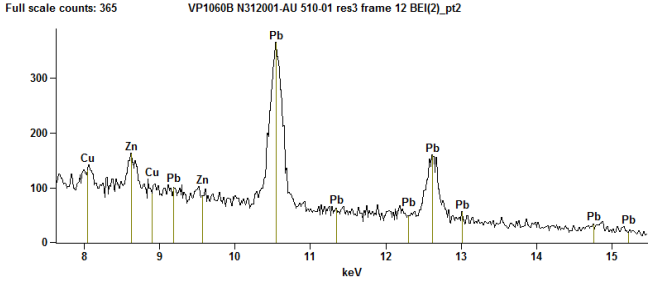

34f) **Res 3** Pb>>Cu, Zn

Figure 34a. High-energy portion of an EDS spectrum (7.5 to 15.5 keV) collected from a Si-oxide phase in a typical angular Pb-bearing, multi-phase particle in soil from the alley (N312001-01). Relative spectral responses where Cu>Pb and Zn>>Pb were consistent with composition of slag from brass and bronze foundry (EPA, 1995; Shen and Forssberg, 2003).

Figure 34b. High-energy portion of an EDS spectrum (7.5 to 15.5 keV) collected from an Fe-oxide phase in a typical angular Pb-bearing, multi-phase particle in soil from the railroad (N312001-BV). Relative spectral responses where Cu>Pb and Zn>>Pb were consistent with composition of slag from brass and bronze foundry.

Figure 34c. High-energy portion of an EDS spectrum (7.5 to 15.5 keV) collected from a typical angular Pb-bearing, Si-oxide particle in soil from the Harrison Park area (N312001-99). Relative spectral responses where Pb>>Cu and Pb>Zn were not characteristic of slag composition from brass and bronze foundry.

Figure 34d. High-energy portion of an EDS spectrum (7.5 to 15.5 keV) collected from a typical angular Pb-bearing, multi-phase particle in Res 1 soil (N312001-DE). Relative spectral responses where Zn>>Pb were consistent with composition of slag from brass and bronze foundry.

Figure 34e. High-energy portion of an EDS spectrum (7.5 to 15.5 keV) collected from a typical angular Pb-bearing, multi-phase particle in Res 2 soil (N312001-CC). Relative spectral responses where Zn>>Pb were consistent with composition of slag from brass and bronze foundry.

Figure 34f. High-energy portion of an EDS spectrum (7.5 to 15.5 keV) collected from a typical sub-angular Pb-bearing, multi-phase particle in Res 3 soil (N312001-AU). Relative spectral responses where Pb>>Cu, Zn were not characteristic of slag composition from brass and bronze foundry.

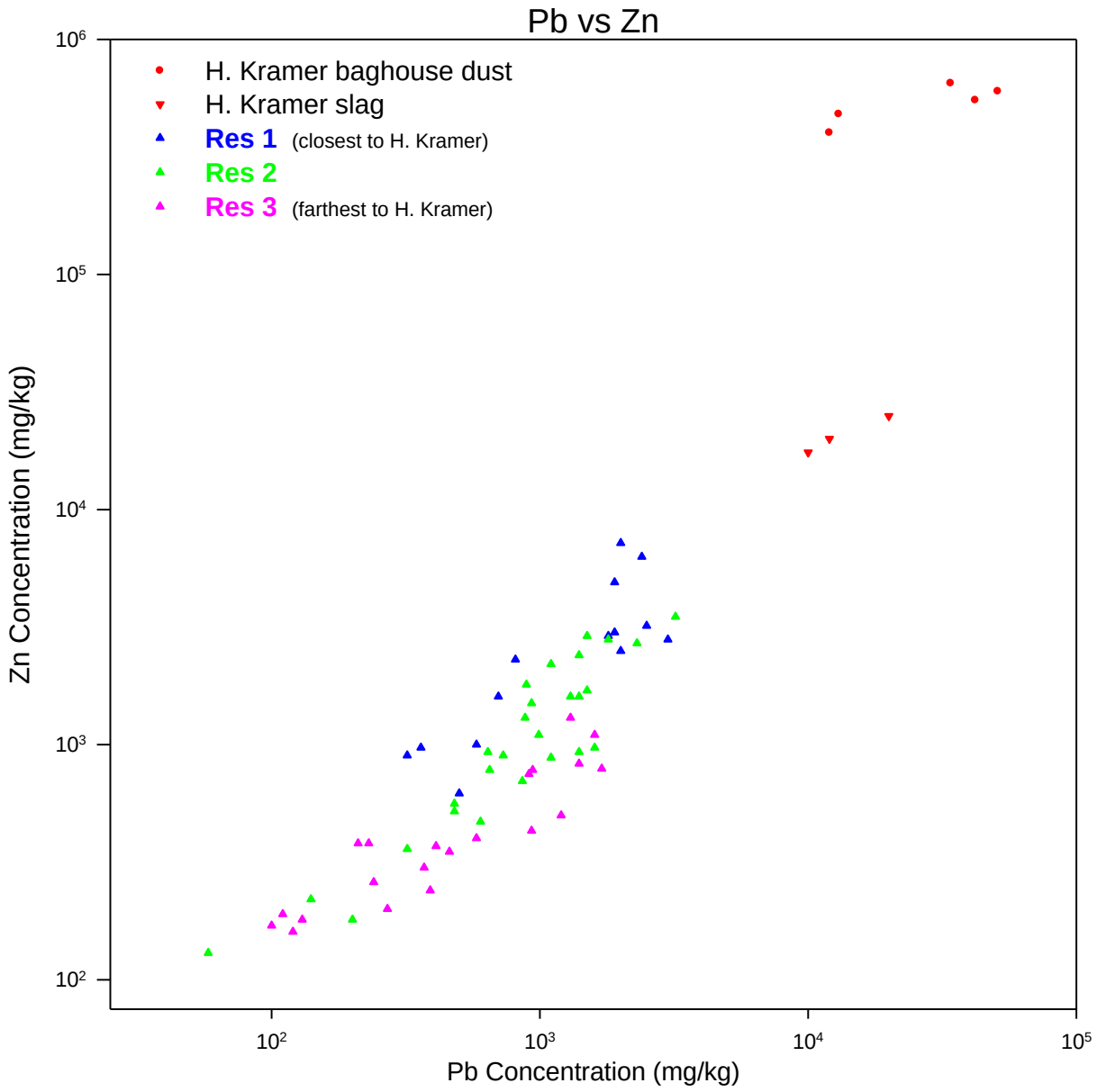

Figure 35. Comparison of Zn and Pb concentrations in Res 1, Res 2, and Res 3 surface soils relative to H. Kramer baghouse dust and slag (simplified from Figure 31a). Note the lower concentrations of Pb and Zn to the lower left in Res 3 soils which are farthest in distance from H. Kramer and the higher concentrations of Pb and Zn to the upper right closest in distance to H. Kramer. Slag composition (H. Kramer, 2014a).

SUMMARY AND CONCLUSIONS

Analytical results of alley, railroad, residential, and reference soils from the Pilsen neighborhood were compared to results of TSP filters, H. Kramer baghouse dust, and H. Kramer slag data, and to distance from H. Kramer in the predominant downwind direction. These comparisons allowed potential sources of Pb in these soils to be included or excluded.

Results were ***consistent with*** brass and bronze foundry materials (emissions dust or slag) as predominant sources of Pb in alley, railroad, Res 1, and Res 2 soils because of the following:

1) Micrometer-scale (1–10 μm) Zn-oxide particles found in railroad soil were similar to micrometer-scale Zn-oxide particles observed in baghouse dust from H. Kramer.

2) Relative elemental concentrations indicated similar relative abundances of Cu, Pb, and Sn in H. Kramer baghouse dust and in alley and railroad soils near H. Kramer.

3) Correlation analysis and scatterplots indicated cadmium (Cd), Cu, Sn, and Zn were co-contaminants with a predominant source of Pb in alley, railroad, Res 1, and Res 2 soil. Cu, Pb, Sn, and Zn are associated with brass and bronze production, and Cd is a common contaminant associated with Zn recovery from scrap metal.

4) The predominant morphology (angular), size (1s–100s μm), and composition of Pb-bearing particles (iron [Fe]- and silicon [Si]-oxides, multi-phase particles) in alley, railroad, Res 1, and Res 2 soils were consistent with slag material from industrial processes such as smelting.

5) The predominant relative spectral responses of Cu, Pb, and Zn (Cu, Zn > Pb) in these slag particles and the presence of Pb-bearing Cu-oxide, Sn-oxide, and Zn-oxide particles were consistent with compositions of brass and bronze foundry slag and in agreement with Zn/Pb ratios in alley, Res 1, and Res 2 soils being similar to H. Kramer slag composition.

6) Lead isotope ratios measured in particulate matter collected on TSP filters were isotopically similar to Pb isotope ratios measured in H. Kramer baghouse dust. In addition, four alley soil samples exhibited Pb isotopic compositions consistent with the TSP filters and H. Kramer baghouse dust.

7) Pb isotope ratios in alley, railroad, Res 1, and 2 soils exhibited a broad range and linear trend, suggesting mixing of a source of Pb isotopically consistent with the TSP filters and H. Kramer baghouse dust with soil containing a historical baseline Pb isotope signature. Res 1 and 2 soils generally exhibited a greater contribution from the baseline Pb isotope signature with increasing distance from the H. Kramer facility.

8) A general shift to higher $^{208}Pb/^{207}Pb$ ratios; lower Cd, Cu, Sn, and Zn concentrations; and lower (X)/Pb ratios with increased distance from H. Kramer was indicated by the relative compositions of Res 1, Res 2, and Res 3 soils. Shifts in these data with increased distance from H. Kramer were strong indicators that these soil areas were impacted by Pb from H. Kramer with diminishing Pb impact with distance from the facility.

Results were ***not consistent with*** the following as predominant sources of Pb in alley, railroad, Res 1, Res 2, Res 3, and Harrison Park soils because of the following:

9) Although correlation analysis and scatterplots indicated Res 3 soil was impacted by Pb associated with Cd, Cu, Sn, and Zn, the predominant source of Pb was ***not*** consistent with H. Kramer materials.

10) Because of minimal Pb from fly ash in ambient air dust and because a unique particle type of amorphous, alumino-silicate spheres exhibited by coal fly ash was ***not*** observed by SEM in any of the soil areas, the only PRP producing coal fly ash, Fisk, was eliminated as a dominant source of Pb in the soils.

11) Pb, Cd, Cu, Sn, and Zn collectively are ***not*** characteristic of tire dust, suggesting tire dust was ***not*** a dominant source of Pb (or Zn) in these soils. As the only PRP associated with tires, Tire Grading was eliminated as a dominant source of Pb in the soils.

12) Associations of Cd, Cu, and Sn in leaded paint are rare, and Pb-based paint particle types were ***not*** observed by SEM in any of the soil areas. Thus, non-industrial Pb from leaded paint historically used on homes and buildings in the Pilsen area was ***not*** a dominant source of Pb in alley, railroad, residential, and Harrison Park soils.

13) Pb, Cd, Cu, Sn, and Zn collectively are ***not*** characteristic of leaded gasoline emissions, and leaded fuel combustion particles types were ***not*** observed by SEM in any of the soil areas. Thus, vehicle exhaust from the historical use of leaded gasoline was ***not*** a dominant source of Pb in alley, railroad, residential soils, and Harrison Park soils.

14) Babbit, solder, antimonial Pb, and battery lead manufacturing by Century, Loewenthal, or NL were excluded as dominant sources of Pb in the soils because Sb soil concentrations were low; correlations between Sb and Pb were lacking; Sb-bearing particle types were ***not*** observed by SEM in any of the soil areas; and Pb, Cd, Cu, Sn, and Zn collectively are ***not*** characteristic of babbit, solder, antimonial Pb, or battery lead materials.

15) Loewenthal and NL were differentiated from H. Kramer as potential sources of Pb by the pattern of Pb, Cd, Cu, Sn, and Zn soil concentrations relative to distance from H. Kramer. This pattern was ***not*** consistent with Loewenthal and NL as predominant sources of Pb in alley, railroad, Res 1 and Res 2 soils.

16) The predominant morphology (angular), size (1s–100s μm), and composition of Pb-bearing (Fe- and Si-oxides, multi-phase particles) particles in Res 3 and Harrison Park

soils were consistent with slag material from an industrial source (not leaded gasoline emissions or leaded paint). The predominant relative spectral responses of Cu, Pb, and Zn (Pb > Cu, Zn) in these Pb-bearing particles were ***not*** characteristic of brass and bronze foundry slag compositions. The Pb isotope ratios in two Res 3 soils suggested significant Pb in those samples was ***not*** consistent with material from H. Kramer.

REFERENCES

Alexander, G.B. 1957. The effect of particle size on the solubility of amorphous silica in water. *Journal of Physical Chemistry*, 61, 1563–1564.

ASTM. 2014. ASTM B-23. http://www.astm.org/Standards/B23.htm, accessed December 30, 2014.

Bernal, S.A., Rose, V., and Provis, J.L. 2014. The fate of iron in blast furnace slag particles during alkali-activation. *Materials Chemistry and Physics*, 146, 1–5.

Biswas, S.K., Tarafdar, S.A., Islam, A., Khaliquzzaman, M., Tervahattu, H., and Kupiainen, K. 2003. Impact of unleaded gasoline introduction on the concentration of lead in the air of Dhaka, Bangladesh. *Journal of the Air and Waste Management Association*, 53, 1355–1362.

Bollhöfer, A., and Rosman, K. J. R. 2001. Isotopic source signatures for atmospheric lead: the northern hemisphere. *Geochimica et Cosmochimica Acta*., 65, 1727–1740.

Buckle, E. R., and Pointon, K.C. 1976. Condensation of aerosols in metallic fume. *Faraday Discussions of the Chemical Society*, 61, 92–99.

Calvert, J. B. 2004. Lead. https://mysite.du.edu/~jcalvert/phys/lead.htm, accessed August 27, 2014.

Canar, J., Jacobson, L., and Roth, C. 2014. U.S. EPA Region 5 Report for the Statistical Analysis of Cadmium, Copper, Lead, Tin, and Zinc found in Soil at and near the H. Kramer facility, Chicago, IL. U.S. EPA, Region 5, October 27, 2014.

Cernik, M., Federer, P., Borkovec, M., and Sticher, M. 1995. Calculation of zinc transport in a soil contaminated by a brass foundry. Groundwater Quality: Remediation and Protection, Proceedings of the Prague Conference, May 1995, IAHS Publ. no. 225, 239–246.

CLEMEX. 2008. Slag Particles, Image Analysis by Microscopy. Clemex Application Note. http://www.clemex.com/clemex/media/assets/pdf/Applications/Image-Analysis-Reports/327_SlagParticles_Phases.pdf, accessed December 5, 2014.

CRC. 2013. *CRC Handbook of Chemistry and Physics*, 94th Edition, William M. Haynes, June 17, 2013, by CRC Press.

Davison, R.L., Natusch, D.F., and Wallace, J.R. 1974. Trace elements in fly ash dependence of concentration on particle size. *Environmental Science and Technology*, 8, 1107–1112.

DHEW. 1969. Air pollution aspects of brass and bronze smelting and refining industry. U.S. Department of Health, Education, and Welfare, Public Health Service, Consumer Protection and Environmental Health Service, National Air Pollution Control Administration, Brass and Bronze Ingot Institute; Raleigh, North Carolina, November 1969.

Doe, B.R. 1970. *Lead Isotopes.* Springer-Verlag, New York, 136p.

EPA. 1977. Emission Factors and Emission Source Information for Primary and Secondary Copper Smelters. U.S. Department of Commerce, National Technical Information Service, PB-280 377; U.S. Environmental Protection Agency, Research Triangle Park, December 1977.

EPA. 1995. EPA Office of Compliance Sector Notebook Project: *Profile of the Nonferrous Metals Industry*. U.S. Environmental Protection Agency.

EPA. 1996. Method 3050B, Acid Digestions of Sludges, Sediments, and Soils. http://www.epa.gov/wastes/hazard/testmethods/sw846/pdfs/3050b.pdf, accessed February 24, 2014.

EPA. 1998. Locating and Estimating Air Emissions from Sources of Lead and Lead Compounds. Office of Air Quality, Planning, and Standards, Office of Air and Radiation, U.S. Environmental Protection Agency, Research Triangle Park, NC 27711, May 1998, EPA-454-98-006.

EPA. 2007. Method 6020A, Inductively Coupled Plasma Mass Spectrometry. http://www.epa.gov/wastes/hazard/testmethods/sw846/pdfs/6020a.pdf, accessed February 24, 2014.

EPA. 2011. U.S. Environmental Protection Agency. http://www.epa.gov/ttn/airs/airsaqs/detaildata/downloadaqsdata.htm, accessed August 29, 2011.

EPA. 2013. United States of America and the State of Illinois vs. H. Kramer and Co. Consent Decree, Civil Action No. 13 CV 0771. http://www.epa.gov/reg5oair/enforce/pilsen/pdf/hkramer-consentdecree.pdf, accessed February 19, 2014.

EPA. 2014a. Site Assessment Report for Pilsen Area Soil Site: Railroad/Alley Chicago, Cook County, Illinois. Prepared by Weston Solutions, Inc. for the Emergency Response Branch, Region 5, U.S. Environmental Protection Agency, April 2, 2014.

EPA. 2014b. Removal Site Evaluation for Pilsen Soil Assessment Area: Residential; Chicago, Cook County, Illinois. Prepared by Weston Solutions, Inc. for the Emergency Response Branch, Region 5, U.S. Environmental Protection Agency, November 17, 2014.

Erel, Y., Veron, A., and Halicz, L. 1997. Tracing the transport of anthropogenic lead in the atmosphere and in soils using isotopic ratios. *Geochimica et Cosmochimica Acta*, 61, 4495–4505.

Ewing, S., Christensen, J.N., Brown, S., Vancuren, R.A., Cliff, S.S., and DePaolo, D.J. 2010. Pb isotopes as an indicator of the Asian contribution to particulate air pollution in urban California. *Environmental Science & Technology*, 44, 8911–8916.

Flegal, A.R., Nriagu, J.O., Niemeyer, S., and Coale, K.H. 1989. Isotopic tracers of lead contamination in the Great Lakes. *Nature*, 339, 455–458.

Friedlander, S.K. 1973. Chemical element balances of air pollution sources. *Environmental Science and Technology*, 7, 235–240.

Gale, N.H. 1996. A new method for extracting and purifying lead from difficult matrices for isotopic analysis. *Analytica Chimica Acta*, 332, 15–21.

Gerstman, B.B. 2013. http://www.sjsu.edu/faculty/gerstman/StatPrimer/correlation.pdf, accessed September 21, 2013.

Glass, G.L. 2003. Trace Element Analysis for Selected Soil Samples, Vashon-Maury Island and King County Mainland, Tacoma Smelter Plume Site. Tacoma-Pierce County Health Department and Washington State Department of Ecology, April 2003.

Good, P.I., and Hardin, J.W. 2003. *Common Errors in Statistics (and How to Avoid Them),* 1st Edition. John Wiley & Sons, Inc., Hoboken, New Jersey, 100–107.

Gulson, B.L., Tiller, K.G., Mizon, K.J., and Merry, R.H. 1981. Use of lead isotopes in soils to identify the source of lead contamination near Adelaide, South Australia. *Environmental Science and Technology*, 15, 691–696.

H. Kramer. 2011. http://www.hkramer.com/, accessed August 4, 2011.

H. Kramer. 2012. http://hkramer.com/HKramer-Nominal-Compositions.pdf, accessed May 10, 2012.

H. Kramer. 2014a. Follow-up Questions and Requests to U.S. EPA, May 2014.

H. Kramer. 2014b. http://www.hkramer.com/KramerTechReferenceManual.pdf, accessed February 12, 2014.

Hamelin, B., Ferrand, J.L., Alleman, L., Nicolas, E., and Veron, A. 1997. Isotopic evidence of pollutant lead transport from North America to the subtropical North Atlantic gyre. *Geochimica et Cosmochimica Acta*, 61, 4423–4428.

Heasman, I., and Watt, J. 1989. Particulate pollution case studies which illustrate uses of individual particle analysis by scanning electron microscopy. *Environmental Geochemistry and Health*, 11, 157–162.

Hopper, J.F., Ross, H.B., Sturges, W.T., and Barrie, L.A. 1991. Regional source discrimination of atmospheric aerosols in Europe using the isotopic composition of lead. *Tellus*, 43B, 45–60.

Hunt, A., Johnson, D.L., Watt, J.M., and Thornton, I. 1992. Characterizing the sources of particulate lead in house dust by automated scanning electron microscopy. *Environmental Science and Technology*, 26, 1513–1523.

Hurst, R.W., Davis, T.E., and Chinn, B.D. 1996. The lead fingerprints of gasoline contamination. *Environmental Science & Technology*, 30, 304–307.

Jochum, P.K., Nohl, U., Herwig, K., Lammel, E., Stoll, B., and Hofmann, A.W. 2005. GeoRem: A new Geochemical Database for Reference Materials and Isotopic Standards. *Geostandards and Geoanalytical Research*.

Kaster. 2014. Tire Manufacturing Processes. Kaster & Lynch, PA. http://tirefailures.com/PDF_vf/whitepaper.pdf, accessed August 27, 2014.

Ketterer, M.E. 2006. The ASARCO El Paso smelter: A source of local contamination of soils in El Paso (Texas), Ciudad Juarez (Chihuahua, Mexico), and Anapra (New Mexico). Summary Report prepared for The Sierra Club, January 27, 2006.

King, M., Ramachandran, V., Prengaman, R.D., DeVito, S.C., and Breen, J. 2005. Lead and Lead Alloys. In: *Kirk-Othmer Encyclopedia of Chemical Technology*, 5th edition. John Wiley & Sons, New York, 14, 727–782.

Kutchko, B.G, and Kim, A.G. 2006. Fly ash characterization by SEM-EDS. *Fuel*, 85, 2537–2544.

Kylander, M.E., Klaminder, J., Bindler, R., and Weiss, D.J. 2010. Natural lead variations in the atmosphere. Earth and Planetary Science Letters, 290, 44–53.

Laerd. 2013. https://statistics.laerd.com/statistical-guides/pearson-correlation-coefficient-statistical-guide-2.php, accessed September 6, 2013.

Lee, R.E. Jr., and von Lehmden, D. J. 2012. Trace metal pollution in the environment, *Journal of the Air and Pollution Control Association*, 23, 853–857.

Linton, R.W., Natusch, D.F., Solomon, R.L., and Evans, C.A. 1980. Physiochemical characterization of lead in urban dusts. A microanalytical approach to lead tracing. *Environmental Science and Technology*, 14, 150–155.

Liu, X., Hopke, P.K., Cohen, D., and Bailey, G. 1995. Sources of fine particle lead, bromine, and elemental carbon in southeastern Australia. *Science in the Total Environment*, 175, 65–79.

Machemer, S.D. 2004. Characterization of airborne and bulk particulate from iron and steel manufacturing facilities. *Environmental Science and Technology*, v 38, 381–389.

Machemer, S.D., Hosick, T.J., Ingamells, R.L. 2007. Source identification of lead contamination in residential and undisturbed soil adjacent to a battery manufacturing facility (Part I). *Environmental Forensics*, 8, 77–95.

Maddaloni, M., Lolacono, N., Manton, W., Blum, Conrad, C., Drexler, J., and Graziano, J. 1998. Bioavailability of soilborne lead in adults, by stable isotope dilution. *Environmental Health Perspectives*, 106, 1589–1594.

Mahaffy, P.G., Martin, N.I., Newman, K.E., Hohn, B., Mikula, R.J., and Munoz, V.A. 1998. Laundry dryer lint: A novel matrix for nonintrusive environmental lead screening. *Environmental Science and Technology***, 32,** 2467–2473.

Manahan, S.E. 2005. *Environmental Chemistry*. CRC Press, Boca Raton, Florida, 785 pp.

Manceau, A., Lanson, B., Schlegel, M.L., Hargé, J.C., Musso, M., Eybert-Bérard, L., Hazemann, J., Chateigner, D., and Lamble, G.M. 2000. Quantitative Zn speciation in smelter-contaminated soils by EXAFS spectroscopy. *American Journal of Science*, 300, 289–343.

Mattigod, S.V. 2003. Characterization of fly ash particles. *Scanning Electron Microscopy*, 11, 611–617.

Miller, J.C., and Miller, J.N. 1993. *Statistics for Analytical Chemistry*, 3rd Edition. Eds. Masson, M., Tyson, J., and Stockwell, P., PTR Prentice Hall Analytical Chemistry Series; Ellis Horwood Limited, West Sussex, England, 158–159.

Mindat. 2011. http://www.mindat.org, accessed August 4, 2011.

Morris, T.K. 2004. Cadmium exposures at three nonferrous foundries: An unexpected trace source. *Journal of Occupational and Environmental Hygiene*, 1, 39–44.

Mukai, H., Furuta, N., Fujii, T., Ambe, Y., Sakamoto, K., and Hashimoto, Y. 1993. Characterization of sources of lead in the urban air of Asia using ratios of stable lead isotopes. *Environmental Science and Technology*, 27, 1347–1356.

Mukai, H., Tanaka, A., and Fujii, T. 1994. Lead isotope ratios of airborne particulate matter as tracers of long-range transport of air pollutants around Japan. *Journal of Geophysical Research*, 99, D2, 3717–3726.

Myers, J., and Thorbjornsen, K. 2004. Identifying metals contamination in soil: A geochemical approach. *Soil & Sediment Contamination: An International Journal*, 13, 1–16.

NEIC. 2010. Speciated Chromium Analysis, Scanning Electron Microscopy, and X-Ray Diffractometry of Glass Fiber Filters Collected at Two Locations in the East Liverpool, Ohio, Area from January 2006 to August 2007. U.S. EPA, National Enforcement Investigations Center, Technical Report NEICVP0856E01, January 2010, Machemer, S., and Hosick, T.

NEIC. 2011a. Characterization of Lead-Bearing Particulate Matter, Pilsen Neighborhood, Chicago, Illinois. U.S. EPA, National Enforcement Investigations Center, Technical Report NEICVP0948E01, August 2011, Machemer, S., and Hosick, T.

NEIC. 2011b. Marietta, Ohio, Source-Receptor Study: Results and Interpretation. U.S. EPA, National Enforcement Investigations Center, Technical Report NEICVP0591E07, April 2011, Machemer, S., and Hosick, T.

NEIC. 2012. Additional Characterization of Lead-Bearing Particulate Matter, Pilsen Neighborhood, Chicago, Illinois. U.S. EPA, National Enforcement Investigations Center, Technical Report NEICVP0965E01, August 2013, Machemer, S., and Hosick, T.

NEIC. 2014. Characterization of Lead in Soils, Pilsen Neighborhood, Chicago, Illinois. U.S. EPA, National Enforcement Investigations Center, Interim Technical Report NEICVP1060E01, March 2014, Machemer, S., Hosick, T., and Pribil, M.

Neymark, L.A., Kwak, L.M., and Peterman, Z.E. 2008. Lead isotopes and trace metals in dust at Yucca Mountain. 12th International High-Level Radioactive Waste Management Conference, Las Vegas, NV, September 7–11.

Novotny, M., Solc, Z., and Trojan, M. 1998. Pigments (inorganic). In: *Kirk-Othmer Encyclopedia of Chemical Technology*, 4th edition. John Wiley & Sons, New York, 19, 1–40.

Omenazu, O.T.W. 2011. Regarding: H. Kramer and Company. City of Chicago, Department of Environment. http://www.pilsenperro.org/0705reports/CDOE_070105.pdf, accessed August 4, 2011.

Perederly, I., Papangelakis, V.G., and Mihaylov, I. 2012. Nickel smelter slag microstructure and its effect on slag leachability. Proceedings of T.T. Chen Honorary Symposium on Hydrometallurgy, Electrometallurgy, and Materials Characterization. The Minerals, Metals & Materials Society Annual Meeting, Orlando, Florida, March 11-15, p.225–237.

Piatak, N.M., Parsons, M.B., and Seal, R.R. 2014. Characteristics and environmental aspects of slag: A review. *Applied Geochemistry*, in press, available on line, http://www.sciencedirect.com/science/article/pii/S0883292714000821, accessed December 31, 2014.

Pistorius, P. C., and Kotzé, H. 2009. Role of silicate phases during comminution of titania slag. *Minerals Engineering*, 22, 182–189.

Post, J.E., and Buseck, P.R. 1984. Characterization of individual particles in the Phoenix urban aerosol using electron-beam instruments. *Environmental Science and Technology*, 18, 35–42.

Prengaman, R.D. 1995. Lead Alloys. In: Kirk-Othmer Encyclopedia of Chemical Technology, 4th edition. John Wiley & Sons, New York, v. 15, 113-132.

Pribil, M.J., Maddaloni, M.A., Staiger, K., Wilson, E., Magriples, N., Mustafa, A., and Santella, D. 2014. Investigation of off-site airborne transport of lead from a superfund removal action site using lead isotope ratios and concentrations. *Applied Geochemistry*, 41, 89–94.

Rabinowitz, M.B. 1988. Stable isotope ratios of lead contaminants in soil. In: *Lead in Soil: Issues and Guidelines*, Davies, B.E., and Wixson, B.G., eds., Whistable Litho Printers Ltd., Whistable, Kent, U.K., 131–141.

Ridley, W.I. 2005. Plumbo-Isotopy: The measurement of lead isotopes by multi-collector inductively coupled mass spectrometry. U.S. Geological Survey Open File Report 2005-1393.

Schiff, K., and Weisberg, S.B. 1999. Iron as a reference element for determining trace metal enrichment in California coastal shelf sediments. *Marine Environmental Research*, 48, 161–176.

Schwartz, H.E., H. Kramer, Kallan, L.E., and Stein, A. 1955. Controlling atmospheric contaminants in the smelting and refining of copper-base alloys. *Journal of the Air Pollution Control Association*, 5, 5–26.

Seeley, J.L., Dick, D., Arvik, J.H., Zimdahl, R.L., and Skogerboe, R.K. 1972. Determination of lead in soil. *Applied Spectroscopy*, 26, 456–460.

Shen, H., and Forssberg, E. 2003. An overview of recovery of metals from slags. *Waste Management*, 23, 933–949.

Shiel, A.E., Weiss, D., and Orians, K.J. 2010. Evaluation of zinc, cadmium and lead isotope fractionation during smelting and refining. *Science of the Total Environment*, 408, 2357–2368.

Sobanska, S., Ricq, N., Laboudigue, A., Guillermo, R., Bremard, C., Laureyns, J., Merlin, J.C., and Wignacourt, J.P. 1999. Microchemical investigations of dust emitted by a lead smelter. *Environmental Science and Technology*, 33, 1334–1339.

State of California. 1996. Effects of Waste Tires, Waste Tire Facilities, and Waste Tire Projects on the Environment. Lawrence Livermore National Laboratory. California Integrated Waste Management Board, Publication # 432-96-029.

Sterling, D.A., Johnson, D.L., Murgueytio, A.M., and Evans, R.G. 1998. Source contribution of lead in house dust from a lead mining waste superfund site. *Journal of Exposure Analysis and Environmental Epidemiology*, 8, 359–373.

Takaoka, M., Yoshinaga, J., and Tanaka, A. 2006. Influence of paint chips on lead concentration on the soil of public playgrounds in Tokyo. *Journal of Environmental Monitoring*, 8, 393–398.

Ter Haar, G.L., Lenane, D.L., Hu, J.N., and Brandt, M. 1972. Composition, size, and control of automobile exhaust particulates. *Journal of the Air Pollution Control Association*, 22, 39–46.

Thorbjornsen, K., and Myers, J. 2006. A geochemical evaluation technique for identifying metals in groundwater. In: *Proceedings of the Fifth International Conference on Remediation of Chlorinated and Recalcitrant Compounds*, Monterey Bay, CA., May 2006, Paper H-26.

Thorbjornsen, K., and Myers, J. 2007a. Identifying metals contamination in groundwater using geochemical correlation evaluation. *Environmental Forensics*, 8, 25–35.

Thorbjornsen, K., and Myers, J. 2007b. Identification of metals contamination in firing-range soil using geochemical correlation evaluation. *Soil & Sediment Contamination*, 16, 337–349.

Union Pacific. 2008. Forms of Lead in Residential Soil and Parks, Soil Samples from the Omaha Lead Site. Prepared by Newfields for the Union Pacific Railroad Company. https://www.uprr.com/newsinfo/attachments/media_kit/epa/attachment_5.pdf, accessed January 25, 2015.

USGS. 2003. Concentrations of polynuclear aromatic hydrocarbons and inorganic constituents in ambient surface soils, Chicago, Illinois: 2001-02. U.S. Geological Survey, Water-Resources Investigations Report 03-4105. http://il.water.usgs.gov/pubs/wrir03_4105.pdf, accessed March 7, 2014.

Valentim, B., Guedes, A., Flores, D., Ward, C.R., and Hower, J.C. 2009. Variations in fly ash compositions with sampling location: case study from a Portuguese power plant. *Coal Combustion and Gasification Products*, 1, 14–24.

Van Borm, W., Wouters, L., Van Grieken, R., and Adams, F. 1989. Lead particles in an urban atmosphere: an individual particle approach. *The Science of the Total Environment*, 90, 55–66.

van Oss, H.G. 2003. Slag–Iron and Steel. U.S. Geological Survey, Minerals Yearbook–2003. http://minerals.usgs.gov/minerals/pubs/commodity/iron_&_steel_slag/islagmyb03.pdf, accessed December 5, 2014.

Veron, A.J., and Church, T.M. 1997. Use of stable lead isotopes and trace metals to characterize air mass sources into the eastern North Atlantic. *Journal of Geophysical Research*, 102, 2849–2858.

Voegelin, A., Pfister, S., Scheinost, A.C., Marcus, M.A., and Kretzschmar, R. 2005. Changes in zinc speciation in field soil after contamination with zinc oxide. *Environmental Science and Technology*, 39, 6616–6623.

Webmineral. 2011. http://www.mindat.org, accessed August 4, 2011.

Wilcke, W., and Kaupenjohann, M. 1998. Heavy metal distribution between soil aggregate core and surface fractions along gradients of deposition from the atmosphere. *Geoderma*, 83, 55–66.

Woodhead, J. 2002. A simple method for obtaining highly accurate Pb isotope data by MC-ICP-MS. JAAS. 17, 1381–1385.